


In presenting the dissertation as a partial fulfillment of the requirements for an advanced degree from the Georgia Institute of Technology, I agree that the Library of the Institution shall make it available for inspection and circulation in accordance with its regulations governing materials of this type. I agree that permission to copy from, or to publish from, this dissertation may be granted by the professor under whose direction it was written, or, in his absence, by the dean of the Graduate Division when such copying or publication is solely for scholarly purposes and does not involve potential financial gain. It is understood that any copying from, or publication of, this dissertation which involves potential financial gain will not be allowed without written permission.



FREQUENCY TRANSIENTS IN A SINUSOIDAL OSCILLATOR
SYNCHRONIZED BY A SINUSOIDAL SIGNAL OF
ARBITRARY INITIAL PHASE

A THESIS

Presented to
the Faculty of the Graduate Division

By

Thomas Mitchell White, Jr.

In Partial Fulfillment
of the Requirements for the Degree
Doctor of Philosophy in the School
of Electrical Engineering

Georgia Institute of Technology

June, 1963

42
12-R

FREQUENCY TRANSIENTS IN A SINUSOIDAL OSCILLATOR
SYNCHRONIZED BY A SINUSOIDAL SIGNAL OF
ARBITRARY INITIAL PHASE

Approved:

h

W. T. S.

Date Approved by Chairman: 9 May 1963

ACKNOWLEDGMENTS

I wish to thank my thesis advisor, Dr. W. B. Jones, Jr., for his encouragement and advice during this investigation. I also wish to express my appreciation for the suggestions given by Professor Howard L. McKinley during the experimental work and by Dr. J. L. Hammond during the manuscript preparation.

TABLE OF CONTENTS

	Page
ACKNOWLEDGMENTS	ii
LIST OF ILLUSTRATIONS	v
LIST OF SYMBOLS	ix
SUMMARY	xi
CHAPTER	
I. INTRODUCTION	1
II. REVIEW OF BASIC OSCILLATOR THEORY	4
Sinusoidal Oscillators	
Van der Pol Analysis of Sinusoidal Oscillators	
III. SYNCHRONIZATION OF SINUSOIDAL OSCILLATORS BY SINUSOIDAL SIGNALS	10
Development of the Synchronization Equation	
Solutions of the Nonlinear Differential Equation of Synchronization	
Synchronization by Phase Control	
Other Approaches to Synchronization	
IV. SYNCHRONIZATION FREQUENCY TRANSIENTS AS A FUNCTION OF INITIAL PHASE DIFFERENCE	21
Mathematical Development	
Development of Universal Curves	
V. MEASUREMENT OF SYNCHRONIZATION FREQUENCY TRANSIENTS . . .	65
General Description of the Equipment	
Use of the Equipment and Calibration Procedures	
Equipment Details	
VI. APPLICATIONS	87
Interrupted Synchronizing Signals	
Synchronization by Sidebands	
Minimizing the Frequency Transient	

CHAPTER	Page
VII. SUMMARY AND CONCLUSIONS	106
APPENDIX	110
BIBLIOGRAPHY	118
VITA	119

LIST OF ILLUSTRATIONS

Figure	Page
1. Approximate Representation of an Oscillator	5
2. Typical Nonlinear Characteristic	7
3. Oscillator Representation	11
4. Relationship Among Oscillator and Synchronizing Voltage Phasors	11
5. Frequency Spectrum Relating Terms of Synchronization Equation	13
6. Block Diagram of a Phase-Locked Oscillator	16
7. Oscillator Frequency as a Function of Reactance Tube Control Voltage	17
8. Phasor Diagram Showing Oscillator Conditions During Synchronization	22
9. Plot of $d\theta/dt = \omega_s - \omega_c \sin \theta$ for $\omega_s < \omega_c$	25
10. Diagram Defining θ_f	28
11. Sketch of Instantaneous Phase Angle as a Function of Time	31
12. Instantaneous Phase Angle as a Function of Time for $\theta_f = 11.53^\circ$, $\theta_f = 30^\circ$, and $\theta_f = 74.2^\circ$	33
13. Instantaneous Phase Angle as a Function of Time for $\omega_s = 2\pi(500)$, $\omega_c = 2\pi(1000)$, and $\theta_o = -150^\circ$	34
14. Instantaneous Phase Angle and Instantaneous Frequency as a Function of Time for $\omega_s = 2\pi(500)$, $\omega_c = 2\pi(1000)$, and $\theta_f = 30^\circ$	36
15. Instantaneous Frequency as a Function of Time for $\omega_s = 2\pi(200)$, $\omega_c = 2\pi(400)$, $\theta_f = 30^\circ$, and $\theta_o = -200^\circ$	38
16. Theoretical Family of Frequency Transients for $\omega_s = 2\pi(200)$, $\omega_c = 2\pi(400)$, and $\theta_f = 30^\circ$	39
17. Experimental Family of Frequency Transients for $\omega_s = 2\pi(200)$, $\omega_c = 2\pi(400)$, and $\theta_f = 30^\circ$	40

Figure		Page
18.	Family of Instantaneous Phase Angle and Frequency Curves for $\theta_f = 11.53^\circ$, $\theta_f = 30^\circ$, and $\theta_f = 74.2^\circ$	42
19.	Family of Experimentally Observed Frequency Transients	44
20.	Plot of $d\theta/dt = \omega_s - \omega_c \sin \theta$ for $\omega_s > \omega_c$	45
21.	(a) Instantaneous Phase Angle for $\omega_s > \omega_c$ (b) Instantaneous Frequency for $\omega_s > \omega_c$	48
22.	Instantaneous Frequency for $\omega_s > \omega_c$	50
23.	Oscillator Frequency Behavior for $\omega_s = 2\pi(1000)$, $\omega_c = 2\pi(900)$	50
24.	Plot of $d\theta/dt = \omega_s - \omega_c \sin \theta$ for $\omega_s = \omega_c$	52
25.	Plot of Instantaneous Phase Angle and Oscillator Frequency for $\theta_f = 90^\circ$	54
26.	Several Oscillator Frequency Transients for $\omega_s = \omega_c = 2\pi(300)$ and $\theta_f = 90^\circ$	56
27.	Family of Frequency Transients for $\omega_s = \omega_c = 2\pi(200)$	57
28.	Family of Experimentally Observed Frequency Transients. The effect of bandwidth on the transient amplitude and the transient duration is clearly shown	58
29.	(a) Family of Instantaneous Phase Angle Curves. (b) Family of Instantaneous Frequency Curves (Normalized)	60
30.	(a) Instantaneous Phase Angle as a Function of Time (b) Instantaneous Frequency as a Function of Time	63
31.	Block Diagram of Experimental Equipment for Observing Oscillator Synchronization Frequency Transients	67
32.	Oscilloscope Trace Showing Discriminator Output	70
33.	Typical Trace on Dual Trace Oscilloscope	71
34.	Synchronization Bandwidth as a Function of Signal Source Voltage	73
35.	Calibration Curves Relating Instantaneous Output Voltage Amplitude to Instantaneous Phase Between Two Mixer Input Signals. The Curves are for the Ideal Case	76

Figure	Page
36. Calibration Curves Relating Mixer Instantaneous Output Voltage Amplitude to Instantaneous Phase Between Two Input Signals. These are the Actual Curves Used	78
37. Linearity of Discriminator in Range of Instantaneous Observed Values	79
38. Experimentally Observed Frequency Transient	80
39. Test Oscillator	81
40. Symmetry of Synchronization Bandwidth about ω_c	81
41. Monostable Multivibrator	82
42. Gate Circuit	83
43. Phase Shifter and Amplifier	83
44. Limiter and Discriminator	84
45. Discriminator Characteristic	86
46. Synchronizing Signal Used by Fraser	87
47. Illustration of Change of Phase Angle During One Period of Gate Signal	88
48. Change in Oscillator Phase Angle During One Period of Gating Function when Oscillator is Synchronized by Interrupted Synchronizing Signal for $\omega_s = 2\pi(80)$, $\omega_c = 2\pi(400)$, $T = 1.59$ milliseconds, and $\theta_f = 11.53^\circ$. . .	90
49. Alternate Solution to First Example of Synchronization by Interrupted Signals	92
50. Synchronization by an Interrupted Synchronizing Signal when $\omega_s = 2\pi(200)$, $\omega_c = 2\pi(400)$, $\omega_m = 2\pi(675)$, $K = 0.75$, and $\theta_f = 30^\circ$	93
51. Instantaneous Oscillator Phase Angle and Frequency for $\omega_s = 2\pi(200)$, $\omega_c = 2\pi(400)$, $\theta_f = 30^\circ$, $\omega_m = 2\pi(675)$, and $K = 0.75$	95
52. Synchronization by a Synchronizing Signal Interrupted by a Rectangular Gating Function	96

Figure	Page
53. Modulation Frequencies Required for Synchronization . . .	99
54. Determination of Minimum Gate Function Frequency	100
55. Synchronization by the First Lower Sideband for $\omega = 2\pi(200)$, $\omega_c = 2\pi(400)$, $\omega_m = 2\pi(263)$, $K = 0.417$, and $\theta_f = 30^\circ$. . .	102
56. Block Diagram of Circuit for Minimizing Frequency Transient	103
57. (a) Instantaneous Phase Angle as a Function of Time (b) Instantaneous Frequency as a Function of Time	107
58. Instantaneous Phase Angle and Instantaneous Frequency Curves for $\theta_f = 0^\circ$	112
59. Instantaneous Phase Angle and Instantaneous Frequency Curves for $\theta_f = 11.55^\circ$	113
60. Instantaneous Phase Angle and Instantaneous Frequency Curves for $\theta_f = 30^\circ$	114
61. Instantaneous Phase Angle and Instantaneous Frequency Curves for $\theta_f = 53.1^\circ$	115
62. Instantaneous Phase Angle and Instantaneous Frequency Curves for $\theta_f = 60^\circ$	116
63. Instantaneous Phase Angle and Instantaneous Frequency Curves for $\theta_f = 90^\circ$	117

LIST OF SYMBOLS

Symbol	Definition
C	Capacitance.
L	Inductance.
G	Conductance.
G_n	Negative conductance.
s	Complex frequency.
v	Instantaneous voltage variable.
$A(t)$	Slowly varying amplitude.
ω_o	Radian frequency of free-running oscillator, $\omega_o = 2\pi f_o$.
V_1	Injected synchronizing signal voltage.
V_r	Voltage returned from feedback network.
V_g	Input voltage to the active element.
θ	Instantaneous phase angle between oscillator and synchronizing signal voltages.
θ_o	Initial value of θ .
θ_f	Terminal value of θ .
ω	Instantaneous radian frequency of oscillator, $\omega = 2\pi f$.
ω_1	Radian frequency of synchronizing signal, $\omega_1 = 2\pi f_1$.
$d\theta/dt$	Instantaneous radian frequency deviation, $d\theta/dt = \omega_1 - \omega$.
β	Phase angle introduced by feedback network.
Q	Quality factor.
ω_s	Radian difference frequency, $\omega_s = \omega_1 - \omega_o$.
ω_c	Half-width of radian frequency synchronization band, $\omega_c = \frac{\omega_o V_1}{2QV_g}.$

Symbol	Definition
ω_u	Half-width of radian frequency synchronization band in phase-locked oscillator, $\omega_u = \text{SU}$.
u	Instantaneous reactance tube control voltage.
U	Maximum value of u .
Z	Impedance.
R	Resistance.
X	Reactance.
V	Voltage.
F	Frequency.
A_R, F_R, A_X, F_X	Compliance Coefficients.
B	Radian frequency, $B = \sqrt{\omega_c^2 - \omega_s^2}$
k	$\tan(\theta_p/2)$.
ϕ	Phase angle, $\phi = \tan^{-1} (\omega_c / \sqrt{\omega_s^2 - \omega_c^2})$ for case $\omega_s > \omega_c$.
x	Instantaneous angle, $x = \frac{\sqrt{\omega_s^2 - \omega_c^2}}{2} (t + t_0)$ for case $\omega_s > \omega_c$.
V_o	Output voltage.
K	Duty cycle of gating function, $K = \text{"on time"}/\text{period}$.
θ_1, θ_2	Limits of θ when synchronization is achieved by interrupted synchronizing signal.
$a, b, c, D,$ $S, \gamma, \delta, k_1,$ K_1	Constants.

SUMMARY

The phenomenon of synchronization has been observed in mechanical and electrical systems for many years. Synchronization of sinusoidal oscillators by sinusoidal synchronizing signals has been the subject of many papers in the literature. Analytical and graphical methods used by several authors lead to essentially the same conclusions although the methods of attack are varied. The synchronization behavior of the oscillator is explained by these authors in terms of the instantaneous phase angle existing between the oscillator voltage and the signal voltage.

There is a unique relationship existing between the instantaneous phase angle of an oscillator being synchronized and the instantaneous frequency of the oscillator. The mathematical analysis in this investigation utilizes that relationship to extend the results of other authors to a more general study of instantaneous frequency as well as instantaneous phase. Of particular interest in this investigation is the effect of circuit parameters and initial phase angle on the frequency transient during synchronization.

A nonlinear differential equation, called Adler's (6) equation in the development, gives the starting point for the mathematical analysis. This equation is solved for the instantaneous phase angle by a procedure similar to that used by Labin (7). The solutions of this equation are presented in analytic and graphical form for three cases which occur when the synchronizing signal lies within, outside, or on the boundary of the bandwidth of synchronization of the oscillator.

The expressions for the instantaneous phase angle are differentiated to give instantaneous frequency deviation expressions which are combined with the frequency of the synchronizing signal to give equations describing the instantaneous frequency behavior of the oscillator. The same three cases considered in the study of the instantaneous phase angle are considered in the study of the instantaneous frequency. Complete results of the phase angle and frequency investigation are given as a set of universal curves. Parameters determined by the signal frequency, the oscillator frequency, and the synchronization bandwidth of the oscillator fix the choice of the particular curves of the set to be used in a given transient study.

Effects of initial phase angles on the instantaneous frequency behavior of the oscillator are available when the proper curves, determined by the parameters mentioned above, are selected from the instantaneous phase angle and instantaneous frequency set of curves. A given initial phase angle, when its value is located on the instantaneous phase angle curve, establishes a time reference on the instantaneous frequency curve. The instantaneous frequency curve then gives the frequency transient from this reference time out to infinite time.

A unique experimental set-up allows the observation of frequency transients in an oscillator affected in a manner described in the mathematical analysis. The equipment offers the following features:

- (1) A control circuit to inject the synchronizing signal when the proper phase relationship exists between the oscillator and synchronizing source voltages;

- (2) A circuit for measuring and controlling the phase angle between the oscillator and source voltages;
- (3) A circuit for observing and measuring the actual frequency transient;
- (4) A delay circuit for ensuring that one transient has completely died out after observation and that the oscillator has returned to the normal free-running condition before the synchronizing signal is injected again; and
- (5) A circuit for careful measurement of the reference frequencies involved.

Photographs of the experimentally observed transients verify with good accuracy the results predicted by the mathematical analysis. These photographs are presented in several places with the corresponding theoretical curves.

The following conclusions can be considered the principal results of the investigation:

- (1) The possible frequency transients that can occur in a given oscillator being synchronized by a given synchronizing source are determined by the half synchronization bandwidth of the oscillator and the difference between the synchronizing frequency and the frequency of the free-running oscillator; the exact transient that does occur is determined by the phase angle between the oscillator voltage and the synchronizing voltage at the time the signal is injected.
- (2) The maximum departure of the instantaneous oscillator frequency from the free-running frequency of the oscillator is equal to the half synchronization bandwidth of the oscillator.

(3) The maximum theoretical duration of an oscillator synchronization frequency transient is infinite; practically, however, when the instantaneous frequency of the oscillator approaches within a certain degree of proximity to the synchronizing frequency, synchronization can be said to have occurred; if the degree of proximity is defined as being ten per cent of the half synchronization bandwidth, the maximum transient duration is given empirically by the half synchronization radian bandwidth divided into ten.

(4) If a frequency transient during synchronization is to be minimized, the synchronizing signal must be injected into the oscillator at such a time that the instantaneous phase angle between the oscillator voltage and the synchronizing voltage is equal to the final angle normally reached after the synchronization transient.

(5) Oscillators with a large synchronization bandwidth are subject to greater frequency fluctuations during synchronization but the duration of the transient is inversely proportional to the maximum amplitude of the fluctuation.

(6) Synchronization frequency transients are independent of the actual values of the free-running frequency of the oscillator and the frequency of the synchronizing source; it is the difference between the two that is of importance.

(7) An inversion of the resultant curves makes the entire mathematical analysis valid when the synchronizing frequency is less than the free-running frequency of the oscillator.

(8) The period of the difference frequency between the free-running frequency of the oscillator and the synchronizing frequency is

of the order of, or greater than the duration of the synchronization frequency transient.

The graphical procedure developed in this investigation gives an alternate way of solving a synchronization problem proposed and investigated by Fraser (8). Fraser investigated the effect of gating a sinusoidal synchronizing signal with a rectangular gate voltage. Many of his results are compared with data obtained by the alternate method and the comparison shows that both methods of attack lead to the same results. Synchronization is interpreted in terms of the fundamental signal frequency and in terms of the sideband frequencies.

An application of interest in the event that a synchronization frequency transient is undesirable involves the use of an outgrowth of the experimental equipment to automatically inject the synchronizing signal at such a time that the frequency transient is minimized. The equipment is discussed in block diagram form. It has the shortcoming that a delay greater than the duration of the synchronization transient is introduced by the system.

CHAPTER I

INTRODUCTION

The phenomenon of synchronization has been observed for many years in electrical and mechanical systems. Huygens, who discovered that clocks hanging on the same wall tend to synchronize, was probably the first to note this phenomenon. Electrical oscillators, discussed in such references as Edson (1), van der Pol (2), and Gillies (3), are subject to synchronization effects.

Electrical oscillators can be broadly classified as sinusoidal or non-sinusoidal. These oscillators can be synchronized by signals which are usually either of sinusoidal form or of fixed-interval pulse form. Mathematical attention has been given to all combinations of oscillators and synchronizing sources, i.e., non-sinusoidal oscillator -- sinusoidal source, non-sinusoidal oscillator -- non-sinusoidal source, sinusoidal oscillator -- non-sinusoidal source, and sinusoidal oscillator -- sinusoidal source. The literature concerning the analysis of the synchronization of a sinusoidal oscillator by a sinusoidal synchronizing source is of the most importance to the discussion in the following chapters. Some of the most important papers on this subject are by Appleton (4), Huntoon and Weiss (5), Adler (6), and Labin (7).

When a sinusoidal oscillator with a free-running frequency ω_0 is synchronized by a small-amplitude synchronizing signal of frequency ω_1 there is a time interval when the actual frequency of the oscillator is

changing from ω_0 to ω_1 and the frequency differs from both ω_0 and ω_1 . Several important papers, mentioned previously, study the behavior of the instantaneous phase angle between the oscillator voltage and the synchronizing source voltage during this time interval, but the treatment stops short of the instantaneous frequency behavior of the oscillator.

The subject of the investigation in the following chapters is the instantaneous frequency behavior of a sinusoidal oscillator which is being synchronized by a small amplitude sinusoidal synchronizing signal. In particular the effects of different initial conditions and circuit parameters on the actual frequency transient are considered. The investigation is both mathematical and experimental.

Chapter II reviews some basic oscillator theory which is helpful in introducing the idea of synchronization of oscillators.

Chapter III reviews several papers on the synchronization of sinusoidal oscillators by sinusoidal synchronizing signals. Two major references (6,7) are developed in sufficient detail that their results form the basis for the mathematical development of the problem.

The problem is analyzed mathematically in Chapter IV. The synchronization of the oscillator by the synchronizing source is described by a nonlinear differential equation. Solutions to this equation are fully developed analytically and a family of curves plotted from this analytic solution gives the possible frequency transients during synchronization. A graphical procedure is developed to allow initial condition effects to be considered.

The experimental procedure is described in Chapter V. The test

oscillator, the synchronizing source, the control equipment, and the measurement equipment are described in enough detail that duplication of the equipment is possible. Calibration procedures are given with a discussion of the use of the equipment.

Chapter VI demonstrates how the results of the development can be utilized in an alternate approach to a problem analyzed by Fraser (8) and it considers a possible application of the results to the problem of avoiding or at least minimizing the frequency transient that occurs during synchronization. A block diagram description of a circuit for accomplishing the minimization is included.

Chapter VII reviews the results of the development and it summarizes the conclusions reached concerning the problem.

CHAPTER II

REVIEW OF BASIC OSCILLATOR THEORY

An oscillator can be defined as a device for transforming d-c energy into a-c energy. It can be classified in many ways, some of which are: feedback or negative resistance; sinusoidal or non-sinusoidal; stable or unstable; and synchronized or free-running. It can be classified according to the active element used as vacuum tube, transistor, or tunnel diode. It can be classified according to the name of the individual circuit used as Hartley, Colpitts, or tuned collector, etc. There is no need here for a complete treatment of all these subjects; this chapter briefly reviews only those oscillator principles which are helpful in understanding the following work.

Sinusoidal Oscillators

True sinusoidal oscillators do not exist but in many cases the harmonic content of the oscillator output can be minimized. Only these so-called sinusoidal oscillators are considered throughout this development. Approximate mathematical analyses of many sinusoidal oscillators are possible while mathematical analyses of many non-sinusoidal oscillators are almost impossible.

Many oscillators, no matter whether they are feedback or negative resistance oscillators, can be reasonably approximated by a tuned circuit in parallel with a negative conductance. Figure 1 represents one equivalent circuit. Describing the behavior of the negative conductance

and its effect on the circuit is a complicated procedure in most cases and comprises the most difficult part of the analysis.

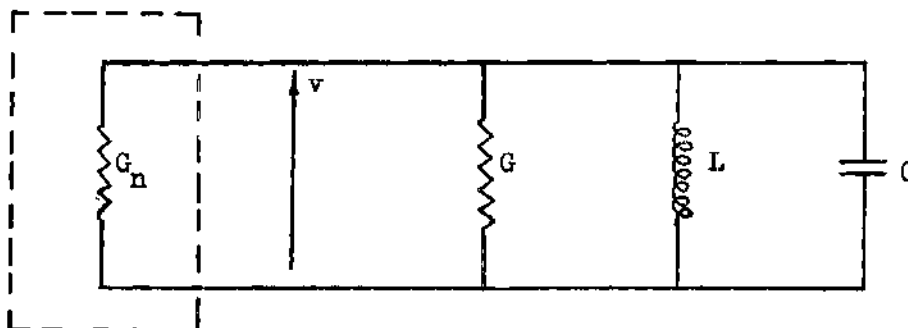


Figure 1. Approximate Representation of an Oscillator.

As a first approach to the problem consider the node differential equation for Figure 1:

$$C \frac{dv}{dt} + (G_n + G)v + \frac{1}{L} \int v dt = 0. \quad (1)$$

If initial conditions are neglected, the Laplace transform of equation (1) gives

$$Cs V(s) + (G_n + G) V(s) + \left(\frac{1}{Ls}\right) V(s) = 0. \quad (2)$$

If oscillations are to exist the system determinant must equal zero, i.e.,

$$s^2 + \frac{G_n + G}{C} s + \frac{1}{LC} = 0. \quad (3)$$

The roots of equation (3) are given as

$$s = -\frac{G_n + G}{2C} \pm \sqrt{\left(\frac{G_n + G}{2C}\right)^2 - \frac{1}{LC}} \quad (4)$$

Since G_n is a negative quantity, these roots are imaginary for the case $|G_n| = |G|$. In this case any disturbance in the system produces sustained oscillations which neither increase nor decrease unless some other disturbance occurs.

When $|G_n| < |G|$ the roots have negative real parts indicating the fact that any disturbance in the system produces decaying oscillations. For the case $|G_n| > |G|$ the roots have positive real parts indicating that any disturbance in the system produces increasing oscillations.

A practical oscillator is not composed of linear elements. If it were, a set of G_n values would have to be available for the system to function. Initially $|G_n|$ would have to be greater than $|G|$ so noise currents or fluctuations could establish the build up of oscillations in the circuit. After oscillation build-up $|G_n|$ would have to equal $|G|$ so that oscillations would be sustained at a fixed amplitude and, to afford a control action, $|G_n|$ would have to become greater than $|G|$ if any effects attempted to decrease oscillation amplitude and $|G_n|$ would have to become less than $|G|$ if any effects attempted to increase oscillation amplitude.

Van der Pol (2) Analysis of Sinusoidal Oscillators

As was stated previously, no practical oscillator can be truly linear and purely sinusoidal because it must somehow produce increasing oscillations until a desired amplitude is reached and it must regulate the amplitude of oscillation thereafter. No practical source of the negative conductance effect produces a linear negative conductance.

Instead, the characteristic curve of the device has an appearance somewhat like that of Figure 2. The operating point of the oscillator is

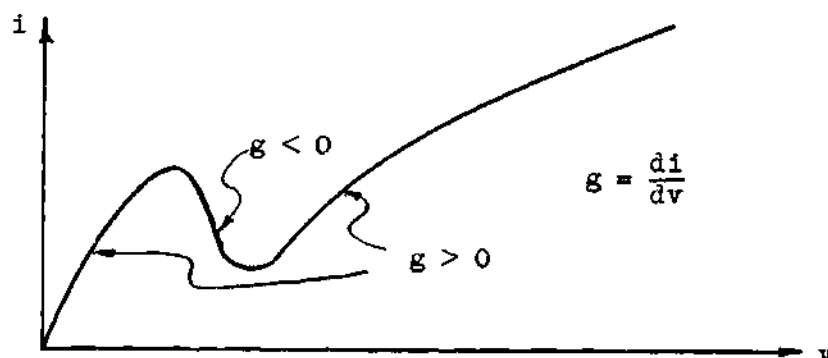


Figure 2. Typical Nonlinear Characteristic.

established approximately at the center of the negative conductance region. Any disturbance causes increasing oscillations until the net effective conductance of the system goes to zero whereupon oscillations are maintained. Regulation is automatically accomplished by the characteristic of the negative conductance element. The output of such an oscillator is sinusoidal if the tuned circuit in parallel with the nonlinear element is a high Q circuit so that it offers a high impedance to only one frequency component of the generated waveform. Figure 1 shows the general circuit configuration of a practical oscillator if the G_n of Figure 1 is furnished by an active element with a characteristic similar to the characteristic of Figure 2.

Van der Pol analyzed the system described in the above paragraph by approximating the negative conductance region of the characteristic curve of Figure 2 by a cubic equation of the form

$$i = F(v) = -av + bv^3. \quad (5)$$

With this approximation the differential equation

$$C \frac{dv}{dt} + (G_n + G) v + \frac{1}{L} \int v dt = 0 \quad (1)$$

becomes

$$C \frac{dv}{dt} + (-av + bv^3) + Gv + \frac{1}{L} \int v dt = 0. \quad (6)$$

Equation (6) is easily reduced to the form

$$\frac{d^2v}{dt^2} - \frac{d}{dt} (cv - Dv^3) + \omega_0^2 v = 0. \quad (7)$$

Equation (7) is referred to as the van der Pol (2) equation. This form of equation arises in many practical situations.

Since the present discussion is restricted to sinusoidal oscillators, the assumption is made that the first derivative term of equation (7) is small. Van der Pol (2) offered two methods for the solution of equation (7) under this condition. The two methods are referred to as the method of variation of parameters and the method of equivalent linearization. Since both of these methods lead to the same results, only the method of variation of parameters will be described briefly.

The analysis of equation (7) by the method of variation of parameters proceeds somewhat intuitively. The tuned circuit is a high Q circuit and the second term of equation (7) is considered to be small so the voltage across the tuned circuit may be closely approximated by

$$v = A(t) \cos \omega_0 t \quad (8)$$

where $A(t)$ is the slowly varying amplitude of the voltage. The first and second time derivatives of equation (8) yield several sine and cosine terms multiplied by $A(t)$ and its first and second derivatives. If equation (8) and the derivative terms obtained from it are substituted into equation (7) and the terms involving harmonics and the derivatives of $A(t)$ are neglected as being small, the resulting equation will have either a $\sin \omega_0 t$ or a $\cos \omega_0 t$ associated with each of its terms. This resultant equation, when separated into its sine and cosine components, yields two equations, one of which when solved gives the amplitude of the oscillation and the second of which when solved gives the frequency of the oscillation. The actual details involved are rather lengthy and can be found in many references.

The results of this procedure are:

for the amplitude

$$A = \sqrt{\frac{a - G}{\left(\frac{3}{4}\right) b}} \quad (9)$$

and for the frequency

$$\omega_0 = \sqrt{\frac{1}{LC}} \quad (10)$$

The analysis outlined in the preceding paragraphs has reviewed some simple oscillator theory and it has attempted to show some of the restrictions and limitations involved in the class of oscillators to be treated from a synchronization standpoint in the next chapters.

CHAPTER III

SYNCHRONIZATION OF SINUSOIDAL OSCILLATORS
BY SINUSOIDAL SIGNALS

This chapter reviews some of the more important papers on synchronization by sinusoidal signals. Two major references are summarized in sufficient detail to establish the basic equations from which the results of this investigation are developed. Other references are summarized briefly to show several approaches to the subject.

Development of the Synchronization Equation

Many oscillators which consist of an active element and a passive feedback network can be analyzed for phase transients by a method described by Adler (6). A physical line of reasoning leads to a differential equation which can be solved for the instantaneous phase difference between the oscillator voltage and the synchronizing signal voltage. This development is based on the assumption that time constants in the oscillator circuit are small compared to one period of the difference frequency.* Adler's equation is developed in considerable detail in the following paragraphs. Refer to Figure 3 for the oscillator configuration.

In Figure 3, V_1 is the phasor voltage representing the injected synchronizing signal, V_x is the phasor voltage representing the voltage returned from the feedback network, and V_g is the phasor voltage representing the voltage input to the active element. The relationship among

* A detailed discussion of the assumption is given by Adler (6).

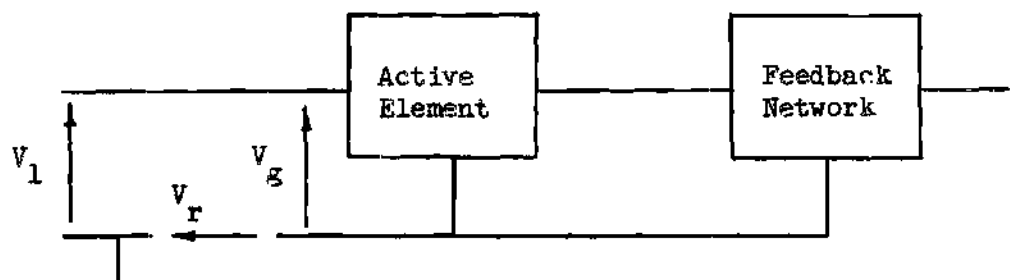


Figure 3. Oscillator Representation.

these voltages can be written

$$V_g = V_1 + V_r. \quad (11)$$

This relationship can be illustrated by the phasor diagram of Figure 4. V_1 has the angular velocity ω_1 of the synchronizing source, V_g has the angular velocity ω of the oscillator, and, if V_1 is small with respect to V_r , V_r has approximately angular velocity ω of the oscillator. Note that θ increases positively in the counterclockwise direction.

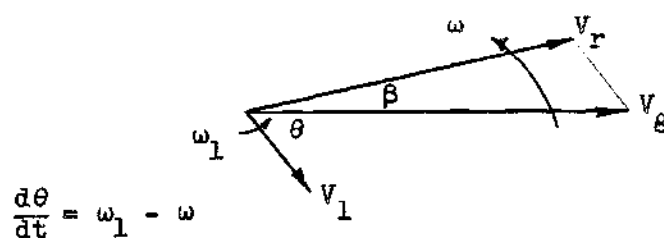


Figure 4. Relationship Among Oscillator and Synchronizing Voltage Phasors.

Examination of Figure 4 reveals that, for $V_1 \ll V_g$,

$$\beta \approx \tan^{-1} \frac{V_1 \sin \theta}{V_g} \approx \frac{V_1 \sin \theta}{V_g}. \quad (12)$$

The phase angle β between V_r and V_g is a function of frequency. Its behavior depends on the elements in the feedback network. For small deviations of frequency the relationship can be expressed

$$\beta = \frac{\partial \beta}{\partial \omega} (\omega - \omega_0) + \beta(\omega_0) \quad (13)$$

where $\frac{\partial \beta}{\partial \omega}$ is evaluated at $\omega = \omega_0$. For a simple tuned circuit $\frac{\partial \beta}{\partial \omega} = \frac{2Q}{\omega_0}$ and $\beta(\omega_0) = 0$ so equation (13) can be written

$$\beta = \frac{2Q}{\omega_0} (\omega - \omega_0) . \quad (14)$$

A combination of equations (12) and (14) yields

$$\omega - \omega_0 = \frac{\omega_0 V_1}{2QV_g} \sin \theta . \quad (15)$$

It is important to note that the phasor diagram of Figure 4 shows difference frequency and phase. The assumption that many high frequency oscillations occur during a small shift of the phasors allows the interpretation of $\frac{d\theta}{dt}$ as an instantaneous angular velocity. In other words ω changes slowly and the feedback network is able to respond to these changes.

Examination of Figure 4 suggests that θ changes at a rate determined by the difference between ω_1 and ω .

$$\frac{d\theta}{dt} = \omega_1 - \omega . \quad (16)$$

When the oscillator is synchronized, $\omega = \omega_1$ and $d\theta/dt = 0$. When $\omega \neq \omega_1$, then $d\theta/dt \neq 0$ and the oscillator is not synchronized. Equation (16) can be written

$$\frac{d\theta}{dt} = (\omega_1 - \omega_0) - (\omega - \omega_0) . \quad (17)$$

Substitution of equation (15) into equation (17) and defining

$$\omega_1 - \omega_0 = \omega_s \quad (18)$$

allow equation (17) to be written in the form

$$\frac{d\theta}{dt} = \omega_s - \omega_c \sin \theta \quad (19)$$

where

$$\omega_c = \frac{\omega_0 V_1}{2QV_g} . \quad (20)$$

Equation (19) is taken as the starting point for most of the development in the following chapters. A frequency spectrum shown in Figure 5 illustrates the relations between the terms of this equation.

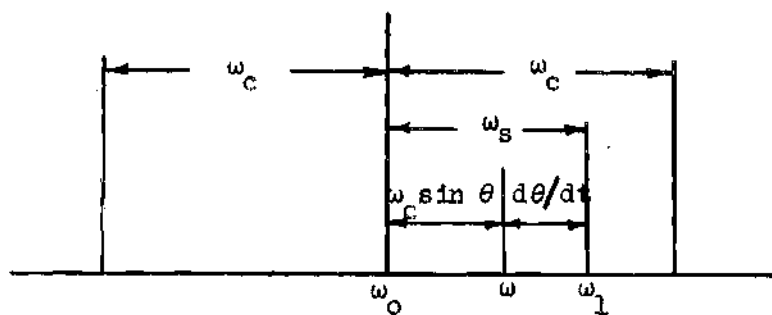


Figure 5. Frequency Spectrum Relating Terms of Synchronization Equation.

Since equation (19) is so important, the full significance of each of its terms must not be missed. An oscillator of free-running

frequency ω_0 is being synchronized by a signal of small amplitude V_1 and of frequency ω_1 . This establishes $\omega_s = \omega_1 - \omega_0$. The angle θ is the instantaneous phase angle between the phasor representing the active element voltage and the phasor representing the injected synchronizing signal voltage. The angle θ can assume any value between $-\pi$ and $+\pi$. The time derivative of θ , $d\theta/dt$, represents an instantaneous frequency whose value is the difference between the synchronizing source frequency and the instantaneous oscillator frequency. The difference between the instantaneous frequency of the oscillator and its free-running frequency is given by the term $\omega_c \sin\theta$. The development of this term is based on the assumption of small linear phase shifts due to the feedback network. The assumption is justifiable for small departures of ω from ω_0 .

Since θ can assume all values, $\sin\theta$ can assume all values between plus one and minus one. The terms of equation (19) are all frequency terms. Use of limiting values of $\sin\theta$ allows an interpretation of the frequency limits to be expected. Note that the condition $\omega_s \leq \omega_c$ allows synchronization since $d\theta/dt$ can be zero for this condition while $\omega_s > \omega_c$ does not allow synchronization since $d\theta/dt$ cannot be zero for this condition. The half-bandwidth of synchronization is equal to ω_c .

When synchronization occurs, $\omega = \omega_1$ and $d\theta/dt = 0$. Equation (19) gives the value of ω for this condition as

$$\theta_f = \sin^{-1} \omega_s / \omega_c . \quad (21)$$

The limiting value of θ_f , $\theta_f = \pm 90^\circ$, is the value obtained as ω_s is allowed to move to the boundary of the synchronization band.

Solutions of the Nonlinear Differential Equation of Synchronization

The nonlinear differential equation

$$\frac{d\theta}{dt} = \omega_s - \omega_c \sin\theta \quad (19)$$

can be solved by direct integration. Jones (9) has developed the results in the form

$$\theta = 2 \tan^{-1} \frac{1}{\omega_s} \left[\omega_s - \sqrt{\omega_c^2 - \omega_s^2} \tanh \frac{1}{2} \sqrt{\omega_c^2 - \omega_s^2} (t + t_0) \right] \quad (22)$$

where $\omega_s < \omega_c$ and t_0 is an integration constant. For the case $\omega_s > \omega_c$ the solution is

$$\theta = 2 \tan^{-1} \frac{1}{\omega_s} \left[\omega_c + \sqrt{\omega_s^2 - \omega_c^2} \tan \frac{1}{2} \sqrt{\omega_s^2 - \omega_c^2} (t + t_0) \right] \quad (23)$$

where t_0 is again an integration constant.

Equation (22) for the case $\omega_s < \omega_c$ leads to the result of equation (21) for the value of θ and to the result $d\theta/dt = 0$ as t goes to infinity. These results are true because the hyperbolic tangent term goes to unity in the limit. Therefore, synchronization occurs and the final value of θ , given by equation (21), can also be expressed as

$$\theta_f = 2 \tan^{-1} \frac{\omega_c - \sqrt{\omega_c^2 - \omega_s^2}}{\omega_s} \quad (24)$$

Equation (23) for the case $\omega_s > \omega_c$ leads to θ as a periodic function of time as t goes to infinity because the natural tangent varies periodically. In this case $d\theta/dt$ is never equal to zero and synchronization never occurs.

Synchronization by Phase Control

An alternate development of the synchronization equation is patterned after a treatment described by Labin (7). The result is Adler's equation although the two systems from which the results are derived are considerably different. The solutions offered by Labin are of interest because they, when modified, give another way of developing solutions of Adler's equation. This modification forms the basis for much of the work in Chapter IV.

Consider the system of Figure 6. The oscillator to be synchronized

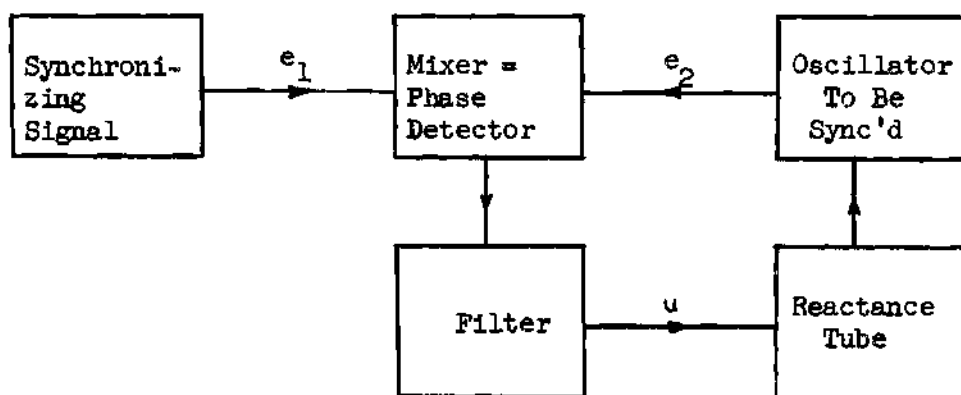


Figure 6. Block Diagram of Phase-Locked Oscillator.

is considered to have an instantaneous frequency ω . The synchronizing source has a fixed frequency ω_1 . The output e_2 of the oscillator to be synchronized is fed to the mixer along with the output e_1 of the synchronizing source. These two mixer inputs produce a mixer output unless the two inputs are at exactly the same frequency and phase angle. The mixer output in combination with the filter delivers a control voltage u to the reactance tube which adjusts the frequency (phase) of the oscillator to be synchronized.

The control of the frequency ω by the regulating voltage u is expressed by an equation of the type

$$\omega = \omega_0 + Su \quad (25)$$

for $|\omega - \omega_0|_{\max} = S|u|_{\max} \leq \gamma$ where ω_0 is the free-running frequency of the oscillator to be synchronized. As long as the error $|\omega - \omega_0|$ does not exceed the value γ , linear regulation of the oscillator frequency by the reactance tube is achieved. The assumption is made that a constant value $\omega = \omega_0 \pm \gamma$ is maintained for $\gamma/S < |u| < \delta/S$ and finally a forbidden region is assumed when $|u| > \delta/S$. Figure 7 shows a sketch of the instantaneous oscillator frequency ω versus the reactance tube control voltage u .

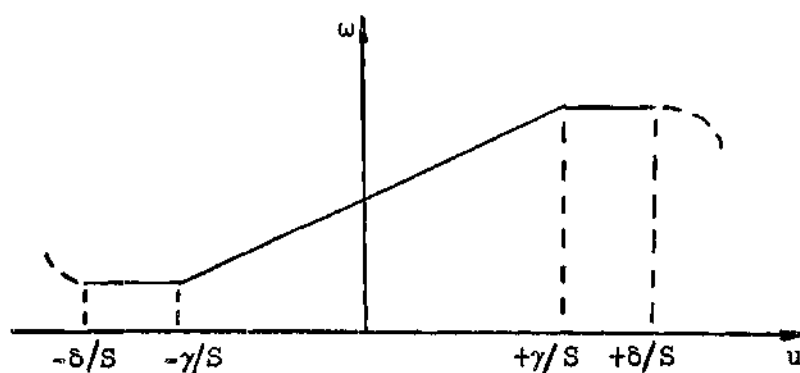


Figure 7. Oscillator Frequency as a Function of Reactance Tube Control Voltage.

Consider now the possibility that e_1 and e_2 are so near each other in frequency that the following equations can be written:

$$e_1 = E_1 \sin \omega_1 t \quad (26)$$

and

$$e_2 = E_2 \cos [\omega_1 t - \theta(t)] \quad (27)$$

where $d\theta(t)/dt$ is the frequency difference. Since $d\theta/dt$ is much less than ω_1 the filter can separate, from the mixer output, the frequency difference $d\theta/dt$ which arises, along with other frequencies, from the product of e_1 and e_2 in the mixer. The actual control voltage for the reactance tube is then written as

$$u = K_1 E_1 E_2 \sin \theta(t) = U \sin \theta \quad (28)$$

where $U = K_1 E_1 E_2$.

The frequency equation involved in the control loop is

$$\omega = \omega_1 - d\theta/dt = \omega_0 + Su \quad (29)$$

where $u = U \sin \theta$.

Allowing $\omega_1 - \omega_0 = +\omega_s$ and $SU = \omega_u$ in equation (29) leads to the final form

$$d\theta/dt = +\omega_s - \omega_u \sin \theta. \quad (30)$$

Equation (30) is identical in form to Adler's equation

$$d\theta/dt = +\omega_s - \omega_c \sin \theta. \quad (19)$$

It is important to note that the solutions of equations (19) and (30) are for the instantaneous phase angle as a function of time. Instantaneous frequency as a function of time can be found from these results.

The effect of different initial conditions on the frequency transient is also needed for a complete picture of the synchronization process.

Other Approaches to Synchronization

Huntton and Weiss (5) using a more general approach than Adler (6) used show that a synchronizing voltage in an oscillator can be replaced by a fictitious impedance $Z = R + jX$ through which a constant current is flowing to produce the same voltage effect. The output voltage V and the output frequency F of the oscillator are affected by this fictitious impedance according to a set of compliance coefficients defined as

$$\partial V / \partial R = A_R, \partial F / \partial R = F_R, -\partial V / \partial X = A_X, -\partial F / \partial X = F_X. \quad (31)$$

Manipulation of these compliance coefficients in complex form in connection with the fictitious impedance leads to a synchronization equation which can be reduced to Adler's equation.

Chapter II gives van der Pol's nonlinear differential equation representing the behavior of a free-running oscillator as

$$\frac{d^2 v}{dt^2} - \frac{d}{dt} (cv - Dv^3) + \omega_0^2 v = 0. \quad (7)$$

Van der Pol considered synchronization in terms of this equation with a driving voltage $E_1 \sin \omega_1 t$ added. The resulting equation for the driven oscillator is

$$\frac{d^2 v}{dt^2} - \frac{d}{dt} (cv - Dv^3) + \omega_0^2 v = \omega_1^2 E_1 \sin \omega_1 t. \quad (32)$$

Van der Pol's solutions for this equation describe the conditions for

synchronization but his method of attack doesn't lend itself to the study of frequency transients. With some simplifying assumptions, however, the equation can be reduced to a form similar to Adler's equation.

CHAPTER IV

SYNCHRONIZATION FREQUENCY TRANSIENTS AS A FUNCTION
OF INITIAL PHASE DIFFERENCE

Mathematical Development

The nonlinear differential equation governing the synchronization process of a sinusoidal oscillator synchronized by a sinusoidal synchronizing source of small amplitude has been presented in Chapter III in the form

$$d\theta/dt = \omega_s - \omega_c \sin \theta = \omega_1 - \omega \quad (33)$$

with

$$\omega_s = \omega_1 - \omega_0 \quad (34)$$

and

$$\omega - \omega_0 = \omega_c \sin \theta \quad (35)$$

where

$$\omega_c = \frac{\omega_0 V_1}{2Q V_g} \quad (36)$$

Figure 8 illustrates by means of a phasor diagram the conditions existing in the oscillator which is being affected by the synchronizing signal. V_1 is the phasor representing the synchronizing signal voltage of angular velocity ω_1 and V_g is the phasor representing the active

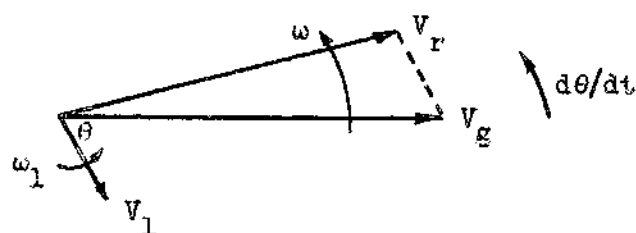


Figure 8. Phasor Diagram Showing Oscillator Conditions During Synchronization.

element input voltage of angular velocity ω . V_r is the phasor representing the voltage returned by means of the feedback network. The angular velocity of V_r is approximately ω because V_L is small in amplitude. Defining V_g as the reference phasor, the following interpretations can be made:

ω is the instantaneous angular velocity of the phasor which represents the oscillator voltage;

θ is the instantaneous phase angle existing between the phasors representing the oscillator and synchronizing source voltages;

θ_0 is the value of θ at the time the synchronizing signal is introduced or turned on. θ_0 can assume any value within a 360° interval; and

$d\theta/dt$ is an instantaneous angular velocity deviation which can be combined with ω_1 to give the instantaneous angular velocity ω of the oscillator.

Some preliminary interpretations of equation (33) are useful to indicate the manner in which the transient problem is approached. Note that the steady state is reached when $d\theta/dt = 0$. Then the relations

$$\omega = \omega_1$$

and

$$\omega_s = \omega_c \sin \theta$$

define the angular velocity $\omega = \omega_1$ and the phase angle $\theta = \sin^{-1} \omega_s / \omega_c$ which must exist when the oscillator is synchronized or in the steady state.

When steady state conditions are not satisfied,

$$d\theta/dt = \omega_s - \omega_c \sin \theta \neq 0 \quad (37)$$

and

$$\begin{aligned} \omega &= \omega_0 + \omega_c \sin \theta \\ &= \omega_0 + \omega_s - d\theta/dt \\ &= \omega_1 - d\theta/dt \end{aligned} \quad (38)$$

Equation (37) is a differential equation which can be solved for $\theta(t)$ and equation (38) gives the actual angular velocity ω as a function of θ or of $d\theta/dt$. An initial value of θ , θ_0 , at $t = 0$ leads to a unique value, at $t = 0$, of $d\theta/dt$ which establishes the starting point of the frequency (angular velocity) transient to be considered. A complete study of frequency transients must consider three cases:

Case I. $\omega_s < \omega_c$ with the synchronizing signal falling within the synchronization band;

Case II. $\omega_s > \omega_c$ with the synchronizing signal falling outside the synchronization band; and

Case III. $\omega_s = \omega_c$ with the synchronizing signal falling on the boundary of the synchronization band.

Equations (37) and (38) describe the phase transient $\theta(t)$ and the angular velocity transient $\omega(\theta)$ or $\omega(t)$. The solution of equation (37), in terms of an initial phase angle θ_0 , describes the behavior of $\theta(t)$ as this angle goes from $\theta = \theta_0$ to its steady state value $\theta = \sin^{-1} \omega_s / \omega_c$. Equation (38) then gives the angular velocity transient $\omega(t)$ corresponding to this phase transient. In cases I and III the transient will die out as the oscillator becomes synchronized. Case II is handled in a similar manner but no steady state condition is reached.

Development of Case I $\omega_s < \omega_c$

Equation (37) can be rewritten as

$$d\theta/dt = \omega_s - \omega_c \sin \theta \quad \omega_s < \omega_c \quad (39)$$

or as

$$\frac{d\theta}{\omega_s - \omega_c \sin \theta} = dt \quad \omega_s < \omega_c \quad (40)$$

A solution of equation (40) for $\theta(t)$ can be obtained and the derivative of $\theta(t)$ with respect to time can be used in equation (38) to give $\omega(t)$, the desired frequency transient. The initial phase angle, θ_0 , establishes a particular phase transient which in turn has associated with it a particular frequency transient for the given θ_0 .

A sketch of equation (39) in Figure 9 provides interesting information about some possible instantaneous angular velocities when it is used in conjunction with

$$\omega = \omega_1 - d\theta/dt. \quad (38)$$

Examination of the sketch and equation (38) shows the maximum instantaneous angular velocity deviation from ω_1 to be $\omega_s + \omega_c$ occurring for $\theta = -\pi/2$, the minimum instantaneous angular velocity deviation from ω_1

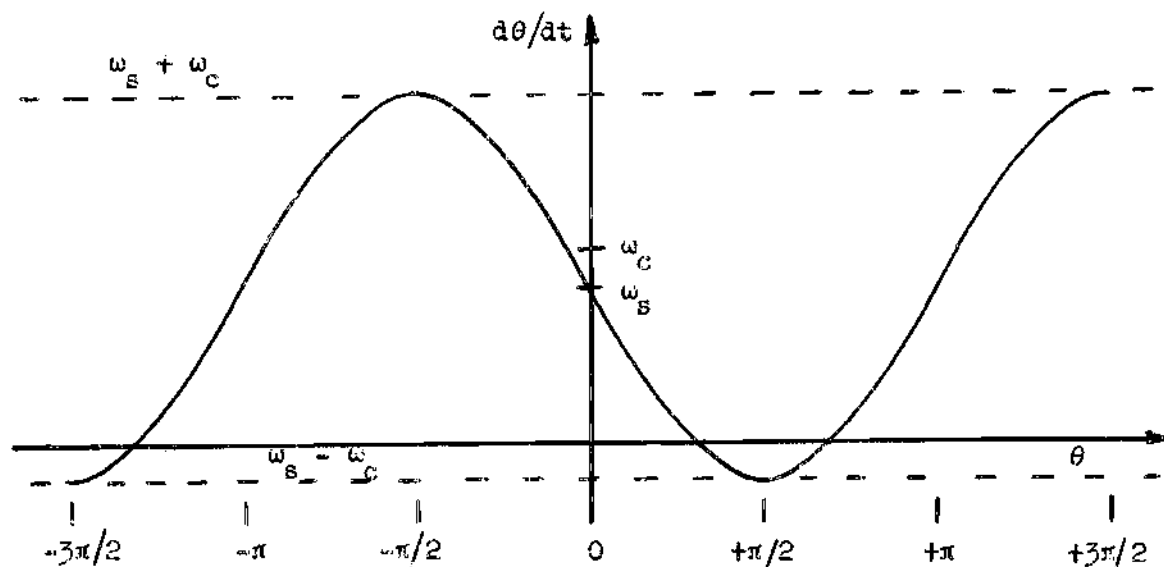


Figure 9. Plot of $d\theta/dt = \omega_s - \omega_c \sin \theta$ for $\omega_s < \omega_c$.

to be zero occurring for two values of $\theta = \sin^{-1} \omega_s/\omega_c$, and a smaller peak deviation to be $\omega_s - \omega_c$ occurring for $\theta = +\pi/2$. Note that one of the zero deviation points, where an increase in θ makes $d\theta/dt$ negative, is stable while the other point, where an increase in θ makes $d\theta/dt$ positive, is unstable. These observations yield some insight into the problem but they are short of the goal which is a solution for instantaneous frequency as a function of time.

Equation 436.00 in Dwight's Table of Integrals (10) gives the solution of

$$\frac{d\theta}{\omega_s - \omega_c \sin \theta} = dt \quad \omega_s < \omega_c \quad (40)$$

as

$$\frac{1}{\sqrt{\omega_c^2 - \omega_s^2}} \ln \left| \frac{\omega_s \tan(\theta/2) - \omega_c - \sqrt{\omega_c^2 - \omega_s^2}}{\omega_s \tan(\theta/2) - \omega_c + \sqrt{\omega_c^2 - \omega_s^2}} \right| = t + t_0 \quad (41)$$

where t_0 is a constant of integration. Letting $B = \sqrt{\omega_c^2 - \omega_s^2}$, equation (41) can be written

$$\frac{\omega_s \tan(\theta/2) - \omega_c - B}{\omega_s \tan(\theta/2) - \omega_c + B} = \pm e^{B(t + t_0)} \quad (42)$$

The \pm sign in equation (42) is necessary because $e^{B(t + t_0)}$ can not change sign, yet θ can have any value within a 360° interval which means that $\tan(\theta/2)$ can assume all values from minus infinity to plus infinity.

When

$$\tan(\theta/2) = \frac{\omega_c + B}{\omega_s} \quad (43)$$

the numerator of the left hand side of equation (42) equals zero. Values of θ above and below the value thus defined cause the numerator and, therefore, the ratio to change sign. Note that $e^{B(t + t_0)}$ equals zero at the value of θ defined by equation (43) and the value of $B(t + t_0)$ must equal minus infinity at this value of θ . A similar effect is noted in the denominator. When

$$\tan(\theta/2) = \frac{\omega_c - B}{\omega_s} \quad (44)$$

the denominator of the left hand side of equation (42) equals zero.

Values of θ above and below this value cause the denominator and, therefore, the ratio to change sign. At the value of θ defined by equation (44), $e^{B(t+t_0)}$ must equal infinity and this means that $B(t+t_0)$ must equal plus infinity at the same value of θ .

Considering first the plus sign, equation (42) becomes

$$\omega_s \tan(\theta/2) - \omega_c - B = \omega_s \tan(\theta/2) e^{B(t+t_0)} - \omega_c e^{B(t+t_0)} + B e^{B(t+t_0)} \quad (45)$$

or

$$\tan \frac{\theta}{2} = \frac{\omega_c}{\omega_s} - \frac{B}{\omega_s} \coth \frac{B(t+t_0)}{2} \quad (46)$$

In like manner the equation derived with the negative sign in equation (42) becomes

$$\tan \frac{\theta}{2} = \frac{\omega_c}{\omega_s} - \frac{B}{\omega_s} \tanh \frac{B(t+t_0)}{2} \quad (47)$$

Let $\sin \theta_f = \omega_s / \omega_c$ which leads to $\tan \theta_f = \omega_s / B$. Figure 10 illustrates this relationship. Equations (46) and (47) can be written in terms of θ_f as

$$\tan \frac{\theta}{2} = \frac{1}{\sin \theta_f} - \cot \theta_f \coth \frac{B(t+t_0)}{2} \quad (48)$$

and

$$\tan \frac{\theta}{2} = \frac{1}{\sin \theta_f} - \cot \theta_f \tanh \frac{B(t+t_0)}{2} \quad (49)$$

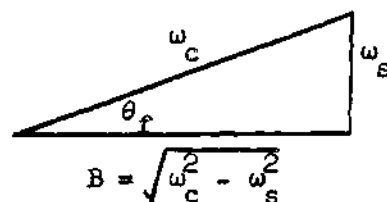


Figure 10. Diagram Defining θ_f .

Observe from equations (48) and (49) that allowing $B(t + t_0)$ to approach minus infinity (corresponding to the sign change condition of equation (43)) reduces both equations to

$$\tan \frac{\theta}{2} = \frac{1}{\sin \theta_f} + \cot \theta_f = \frac{1}{\tan \theta_f/2} \quad (50)$$

which leads to

$$\theta = \pi - \theta_f$$

or

$$\theta = -\pi - \theta_f$$

depending on which equation is used in the limiting process.

Allowing $B(t + t_0)$ to approach plus infinity (corresponding to the sign change condition of equation (44)) reduces equations (48) and (49) to

$$\tan \frac{\theta}{2} = \frac{1}{\sin \theta_f} - \cot \theta_f = \tan (\theta_f/2) \quad (51)$$

which leads to

$$\theta = \theta_f .$$

Equations (48) and (49) resulted from a sign choice in equation (42). The conclusion is now obvious, since $\coth \frac{B(t + t_0)}{2}$ can go to infinity and $\tanh \frac{B(t + t_0)}{2}$ cannot go to infinity, that the choice of the sign and, therefore, the choice between equations (48) and (49) depends on where the initial phase angle, θ_0 , appears. In summary use equation (49) for

$$\theta_f < \theta_0 < \pi - \theta_f$$

and use equation (48) for

$$-\pi - \theta_f < \theta_0 < \theta_f.$$

Note that

$$\coth y = \frac{e^y + e^{-y}}{e^y - e^{-y}} = 1 - \frac{2}{1 - e^{2y}} \quad (52)$$

and

$$\tanh y = \frac{e^y - e^{-y}}{e^y + e^{-y}} = 1 - \frac{2}{1 + e^{2y}}. \quad (53)$$

Use of the identities of equations (52) and (53) in equations (48) and (49) and the combination of equations (48) and (49) leads to the form

$$\tan \frac{\theta}{2} = \frac{1 - \cos \theta_f}{\sin \theta_f} + \frac{2 \cot \theta_f}{1 \pm e^{B(t + t_0)}}. \quad (54)$$

Use of

$$\frac{1 - \cos \theta_f}{\sin \theta_f} = \tan \frac{\theta_f}{2} \quad (55)$$

and

$$2 \cot \theta_f = \frac{1 - \tan^2 \theta_f/2}{\tan \theta_f/2} \quad (56)$$

changes equation (54) to

$$\tan \frac{\theta}{2} = \tan \frac{\theta_f}{2} + \frac{1 - \tan^2 \theta_f/2}{(\tan \theta_f/2) [1 \pm e^{B(t+t_0)}]}. \quad (57)$$

In a given case θ_f is constant, therefore, let $\tan(\theta_f/2) = k$ and rewrite equation (57) as

$$\tan \frac{\theta}{2} = k + \frac{1 - k^2}{k [1 \pm e^{B(t+t_0)}]}. \quad (58)$$

Use + in equations (57) and (58) for $\theta_f < \theta_0 < \pi - \theta_f$.

Use - in equations (57) and (58) for $-\pi - \theta_f < \theta_0 < \theta_f$.

In equation (58) the term $e^{B(t+t_0)}$ can be considered as $e^{Bt} e^{Bt_0}$.

If e^{Bt_0} is arbitrarily set equal to $1/k$, which amounts to choosing t_0

such that $\theta = \pm \pi/2$ at $t = 0$, equation (58) can be written as

$$\tan \frac{\theta}{2} = k + \frac{1 - k^2}{k [1 \pm (1/k) e^{Bt}]}. \quad (59)$$

or

$$\theta = 2 \tan^{-1} \left[k + \frac{1 - k^2}{k \pm e^{Bt}} \right]. \quad (60)$$

Use + in equations (59) and (60) for $\theta < \theta_0 < \pi - \theta_f$.

Use - in equations (59) and (60) for $-\pi - \theta_f < \theta_0 < \theta_f$.

Equation (60) is the general solution for the instantaneous phase angle as a function of time. A curve sketched from this solution appears in Figure 11. Note that θ always approaches θ_f asymptotically as synchronization occurs and note also that θ_f may be approached from above or below depending on θ_0 , the initial value of θ , when the synchronizing signal is introduced. The limiting value of θ above θ_f is $\pi - \theta_f$ and the limiting value below θ_f is $-\pi - \theta_f$. These limiting values are calculated by allowing t to approach minus infinity in equation (60). These are the same values predicted in the discussion immediately following equations (48) and (49) corresponding to sign change condition equation (43).

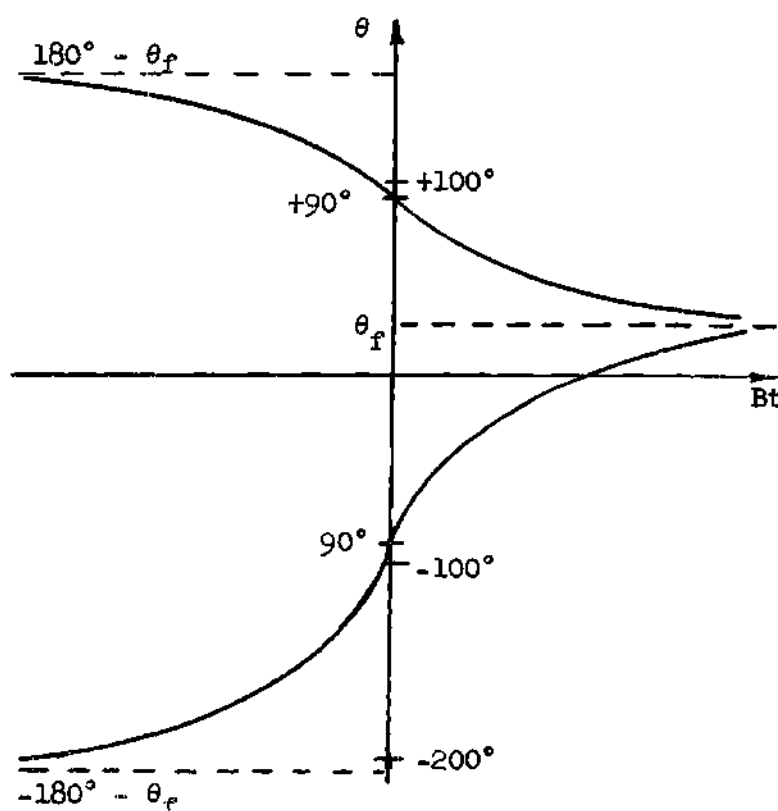


Figure 11. Sketch of Instantaneous Phase Angle as a Function of Time.

At this point in the development observe that no loss of generality occurred from setting $e^{Bt_0} = 1/k$ because it is a simple matter to go

to the curve in Figure 11 with an arbitrary initial phase angle, θ_0 . A shift of time scale places $t = 0$ at the proper θ_0 on the curve and the transient curve is available as θ progresses from θ_0 to θ_f while t goes from zero to infinity.

Figure 12 shows θ versus Bt for three different values of θ_f corresponding to $\sin \theta_f = 0.2$, $\sin \theta_f = 0.5$, and $\sin \theta_f = 0.964$. Use of these curves is illustrated by the following example.

Let $\omega_s = 2\pi (500)$ and $\omega_c = 2\pi (1000)$. This establishes values for $B = \sqrt{\omega_c^2 - \omega_s^2} = 2\pi (866)$ and $\sin \theta_f = \omega_s/\omega_c = 0.5$. If the initial phase difference between the synchronizing voltage and the oscillator voltage is -150° , the variation of θ with respect to time is obtained by entering the $\sin \theta_f = 0.5$ curve at $\theta = -150^\circ$, which is at the value $Bt = -0.72$, and following it to $Bt = \text{infinity}$. The Bt scale shifted 0.72 units and divided by B gives the proper time scale for the curve. See Figure 13 for the result.

Equation (60) gives instantaneous phase angle as a function of time. Equation (38) can now be used with the derivative of equation (60) to develop an expression for instantaneous frequency as a function of time. Repeated for convenient reference are

$$\theta = 2 \tan^{-1} \left[k + \frac{1 - k^2}{k \pm e^{Bt}} \right] \quad (60)$$

and

$$\omega = \omega_1 - d\theta/dt. \quad (38)$$

Differentiating equation (60) yields

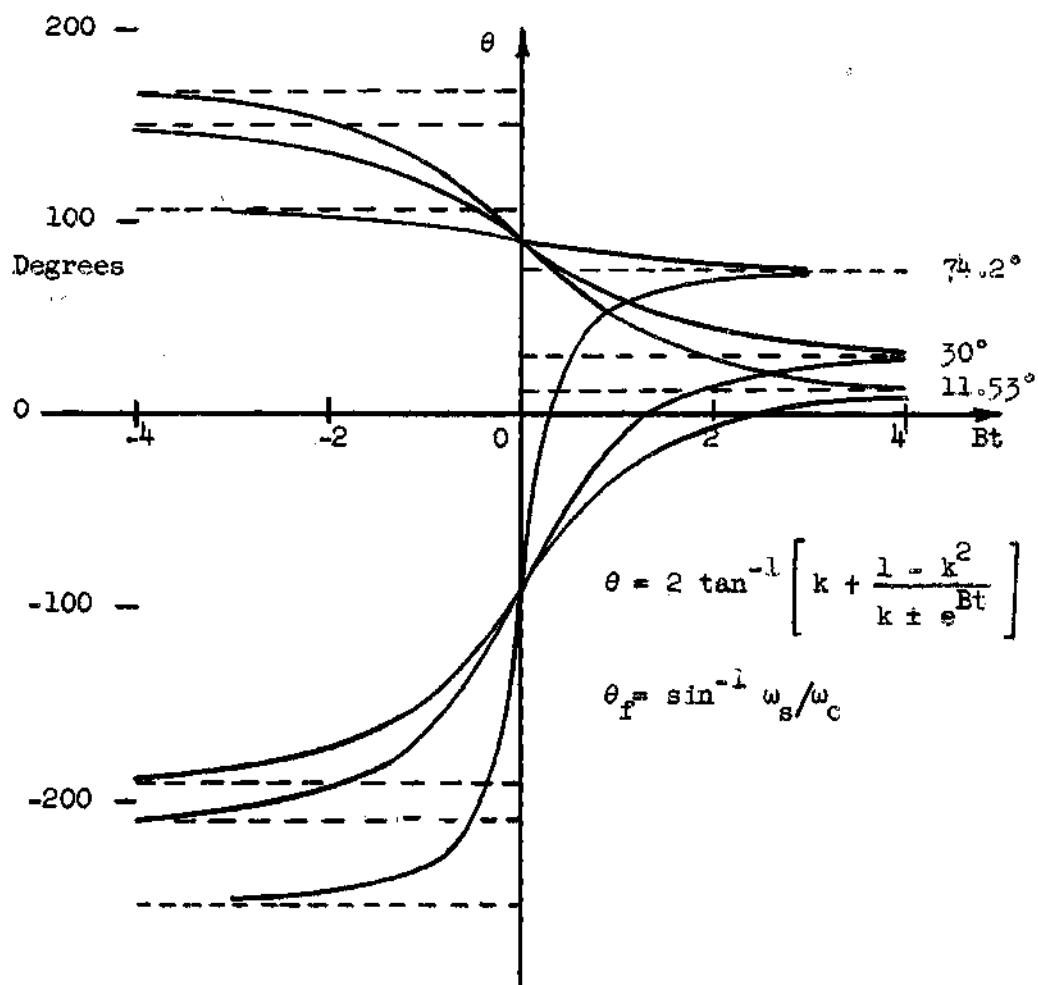


Figure 12. Instantaneous Phase Angle as a Function of Time for $\theta_f = 11.53^\circ$, $\theta_f = 30^\circ$, and $\theta_f = 74.2^\circ$.

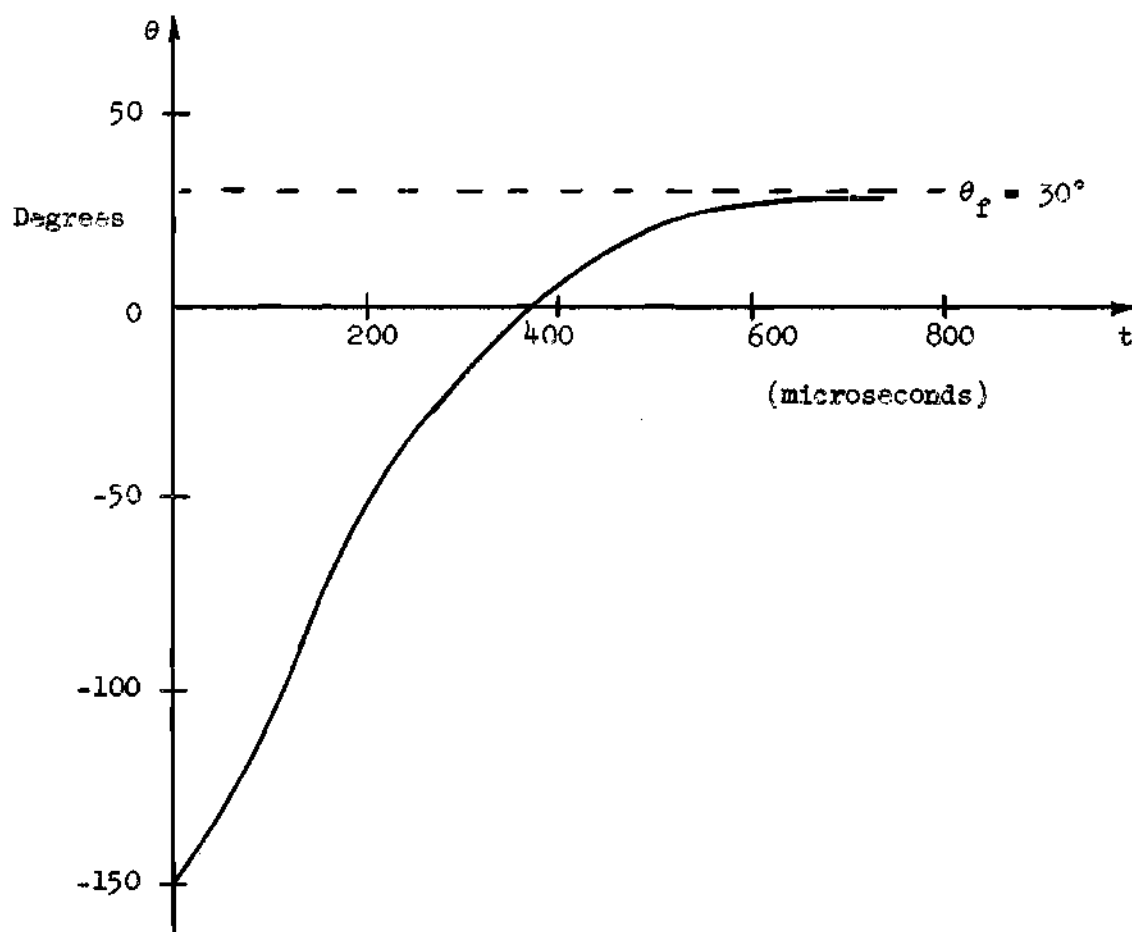


Figure 13. Instantaneous Phase Angle as a Function of Time for $\omega_s = 2\pi(500)$, $\omega_c = 2\pi(1000)$, and $\theta_o = -150^\circ$.

$$\begin{aligned} \frac{d\theta}{dBt} &= \frac{2 \frac{d}{dt} \left[k + \frac{1 - k^2}{k \pm e^{Bt}} \right]}{1 + \left[k + \frac{1 - k^2}{k \pm e^{Bt}} \right]^2} \\ &= \frac{\pm (k^2 - 1)}{(k^2 + 1) \cosh Bt \pm 2k} \end{aligned} \quad (61)$$

Finally

$$\frac{d\theta}{dt} = B \frac{d\theta}{dBt} \quad (62)$$

and

$$\frac{d\theta}{dt} = \frac{\pm B(k^2 - 1)}{(k^2 + 1) \cosh Bt \pm 2k} \quad (63)$$

Equation (63) can be combined with equation (38) to obtain

$$\omega = \omega_1 - d\theta/dt = \omega_1 + \left[\frac{\pm B(1 - k^2)}{(k^2 + 1) \cosh Bt \pm 2k} \right] \quad (64)$$

which is the equation for instantaneous frequency as a function of time.

IMPORTANT: For equations (61), (63), and (64),

use + sign for $\theta_f < \theta_o < \pi - \theta_f$ and

use - sign for $-\pi - \theta_f < \theta_o < \theta_f$.

Consider an example to illustrate the use of equation (64). Let $\omega_s = 2\pi (500)$ and $\omega_c = 2\pi (1000)$ which establishes $\sin \theta_f = \omega_s/\omega_c = 0.5$, $k = \tan 15^\circ = 0.268$, and $B = 2\pi (866)$. When these parameters are substituted in equation (64), the equation becomes

$$\omega = \omega_1 + \left[\frac{\pm 2\pi 866(0.928)}{(1.072) \cosh 2\pi 866t \pm 0.536} \right] \quad (65)$$

This equation is plotted in Figure 14(a). Figure 14(a) now shows all possible frequency transients that can occur as the oscillator is synchronized under the conditions of this example. To complete the picture, the effect of the initial phase angle between the synchronizing signal voltage and the oscillator voltage must be considered. Figure 14(b), obtained from Figure 12, is a plot of instantaneous phase angle versus time with the same constants that were used in Figure 14(a). If the curve of Figure 14(b) is entered at the value of the initial phase angle,

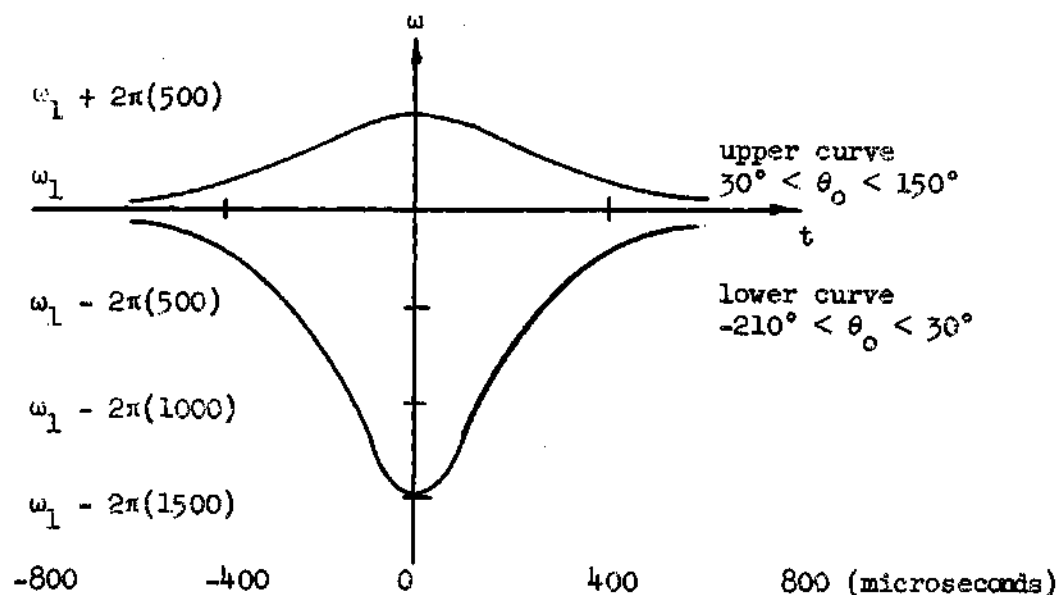


Figure 14(a). Instantaneous Frequency as a Function of Time for $\omega_s = 2\pi(500)$, $\omega_c = 2\pi(1000)$ and $\theta_f = 30^\circ$.

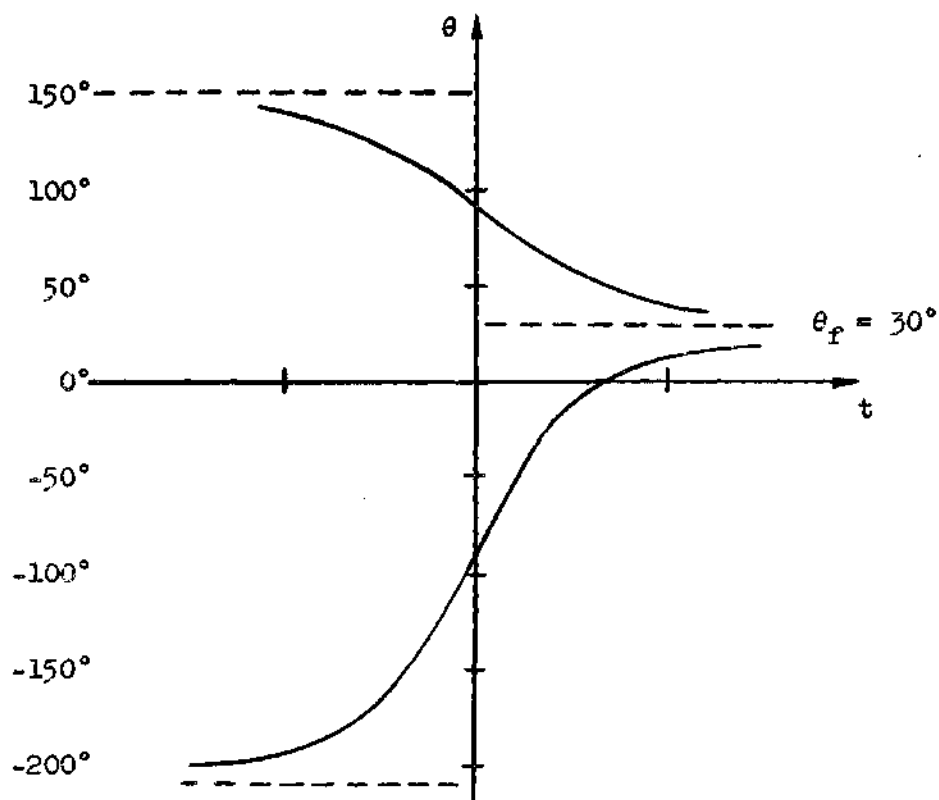


Figure 14(b). Instantaneous Phase Angle as a Function of Time for $\omega_s = 2\pi(500)$, $\omega_c = 2\pi(1000)$, and $\theta_f = 30^\circ$.

a certain time, which may be projected directly up to the curve of Figure 14(a), is read. This time is now taken as the reference $t = 0$ for the starting of the transient which then runs its course along the curve as t goes to infinity. Note that the θ curve with negative slope projects to the instantaneous angular velocity curve above ω_1 while the θ curve with positive slope projects to the instantaneous angular velocity curve below ω_1 . Note also that Figure 14 will hold with appropriate scale changes for any set of frequency values such that $\sin \theta_f = 0.5$. If the frequency values should double, the time of the transient would be cut to one half the original time and the amplitude of the transient would be twice the amplitude of the original transient, etc.

Figure 15 illustrates the transient that occurs when the initial phase angle is -200° , $\omega_s = 2\pi (200)$, $\omega_c = 2\pi (400)$, and $\sin \theta_f = 0.5$. Figure 15 is obtained from Figure 14 in the following manner. First the time scales of Figures 14(a) and 14(b) are multiplied by 2.5. Second the amplitude scale of Figure 14(a) is divided by 2.5. Third Figure 14(b) is entered at $\theta = -200^\circ$ where the time, $t = -1.5$ milliseconds on the new scale is read and projected upward to the lower frequency curve of Figure 14(a). Finally the transient is sketched by jumping from ω_0 to the lower curve at the projected point, now considered as $t = 0$, and by following the curve as t goes from zero to infinity. As a matter of interest some points measured experimentally are shown on the graph.

Figure 16 shows a family of transients obtained from Figure 14 by assuming different initial phase angles. This family is for the conditions $\sin \theta_f = 0.5$, $\omega_s = 2\pi (200)$, and $\omega_c = 2\pi (400)$. For comparison purposes an experimentally measured family can be seen in Figure 17. The same conditions apply.

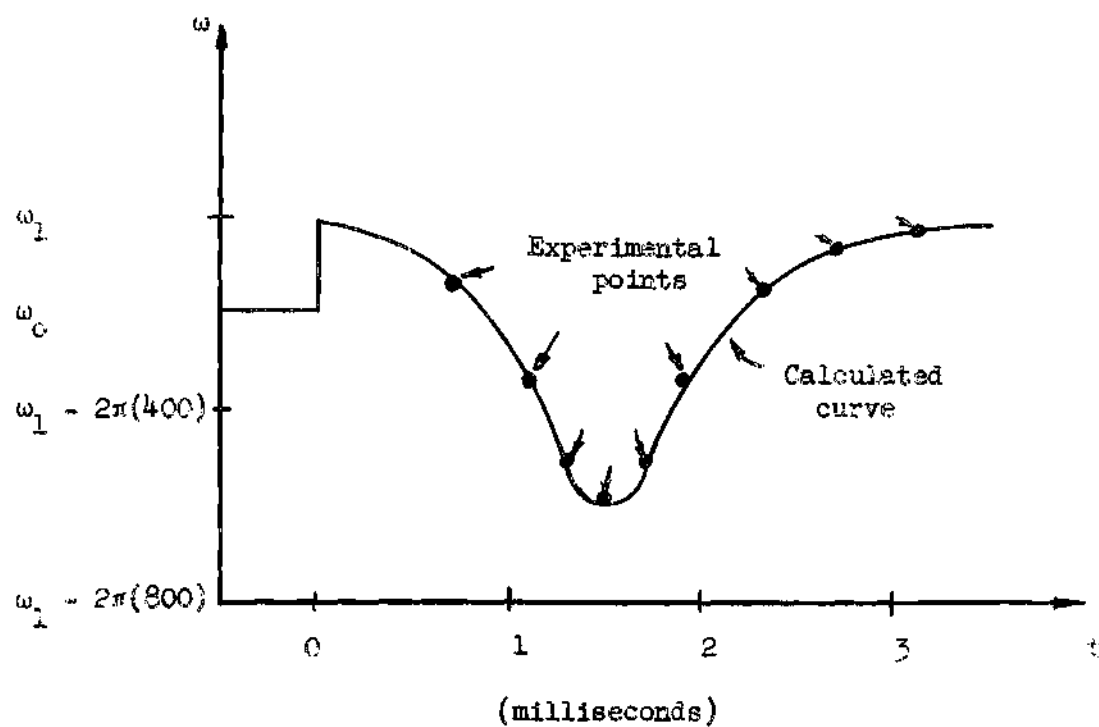


Figure 15. Instantaneous Frequency as a Function of Time for $\omega_s = 2\pi(200)$, $\omega_c = 2\pi(400)$, $\theta_f = 30^\circ$, and $\theta_c = -200^\circ$.

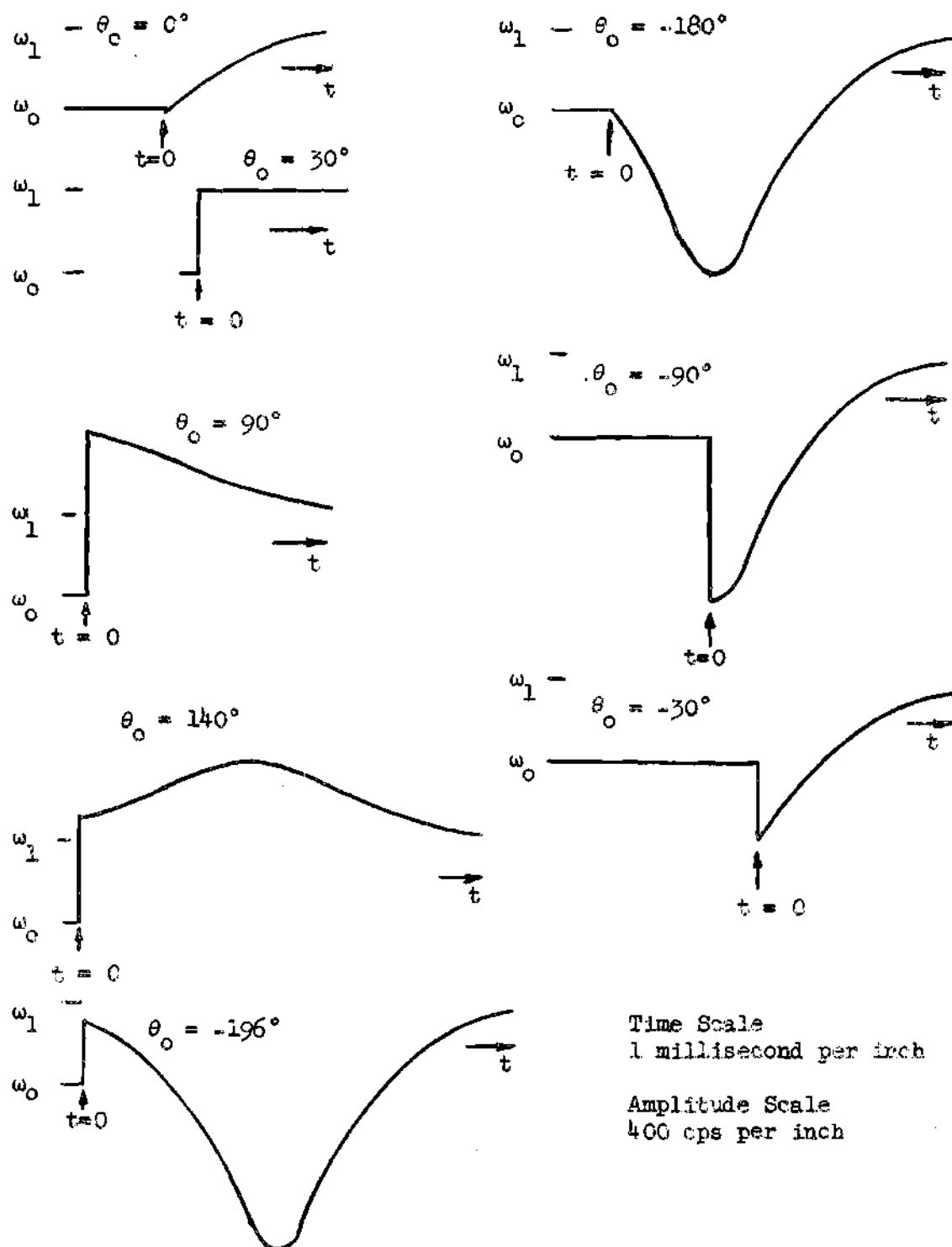
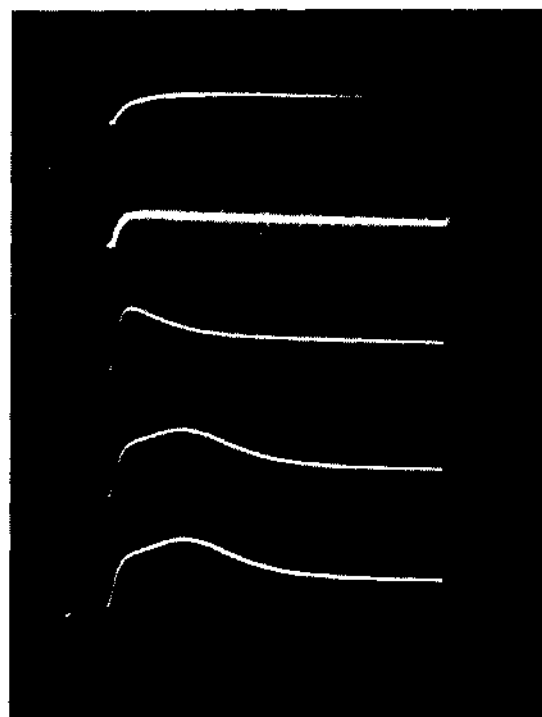


Figure 16. Theoretical Family of Frequency Transients for $\omega_s = 2\pi(200)$, $\omega_c = 2\pi(400)$, and $\theta_f = 30^\circ$.



$$\theta_0 = 20^\circ$$

$$\theta_0 = + 30^\circ$$

$$\theta_0 = + 90^\circ$$

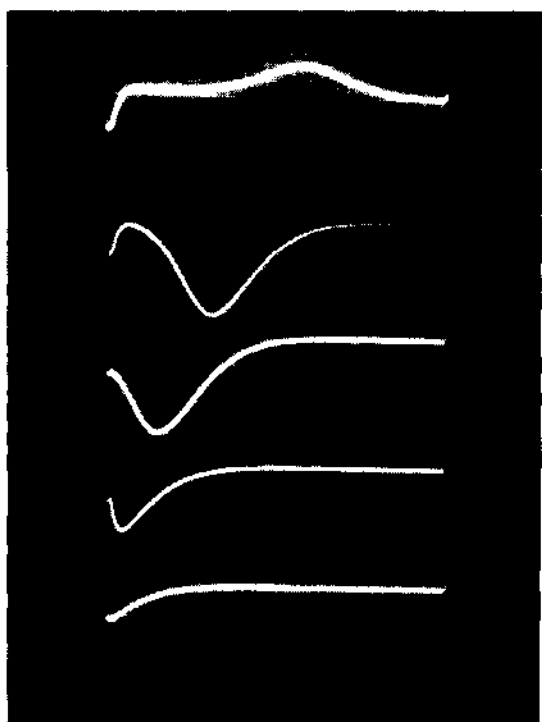
$$\theta_0 = + 125^\circ$$

$$\theta_0 = + 130^\circ$$

$$\omega_s = 2\pi(200)$$

$$\omega_c = 2\pi(400)$$

$$\theta_f = 30^\circ$$



$$\theta_0 = 150^\circ$$

$$\theta_0 = - 200^\circ$$

$$\theta_0 = - 180^\circ$$

$$\theta_0 = - 50^\circ$$

$$\theta_0 = 0^\circ$$

Time Scale: 0.4 millisec./cm.
Amplitude Scale: 200 cps/cm.

Figure 17. Experimental Family of Frequency Transients.

A complete treatment of all possible transients occurring in all the other cases (i.e., for all the other θ_f values) can be developed in expanded form in exactly the same manner as this case for $\sin \theta_f = 0.5$ was developed. The treatment starts with equation (64) which gives all possible frequency transients. Since ω_1 and B are known constants in a given case, it is convenient to plot the variable part of equation (64) rewritten as

$$-\frac{d\theta}{dBt} = \frac{\pm (1 - k^2)}{(1 + k^2) \cosh Bt \pm 2k} \quad (66)$$

Use + sign for $\theta_f < \theta_0 < \pi - \theta_f$.

Use - sign for $\pi - \theta_f < \theta_0 < \theta_f$.

This equation is plotted for several values of θ_f in Figure 18(a). Figure 18(b) is Figure 12 repeated for convenient reference in establishing the initial conditions.

Equation (66) or, in graphical form, Figure 18(a) represents the normalized difference between the oscillator angular velocity ω and the synchronizing signal angular velocity ω_1 . Since ω_1 is constant, the curves of Figure 18(a), properly scaled, show the actual angular frequency transients which can occur. An initial phase angle, θ_0 , can be taken into account by referring to Figure 18(b) and reading the Bt value at $\theta = \theta_0$. This Bt value establishes the $Bt = 0$ point (reference) for the frequency transient curve of Figure 18(a).

The entire development up to now has been based on the solution of the differential equation (33). The quantity ω_s has been defined as $\omega_1 - \omega_0$ which implies that the synchronizing frequency is above the

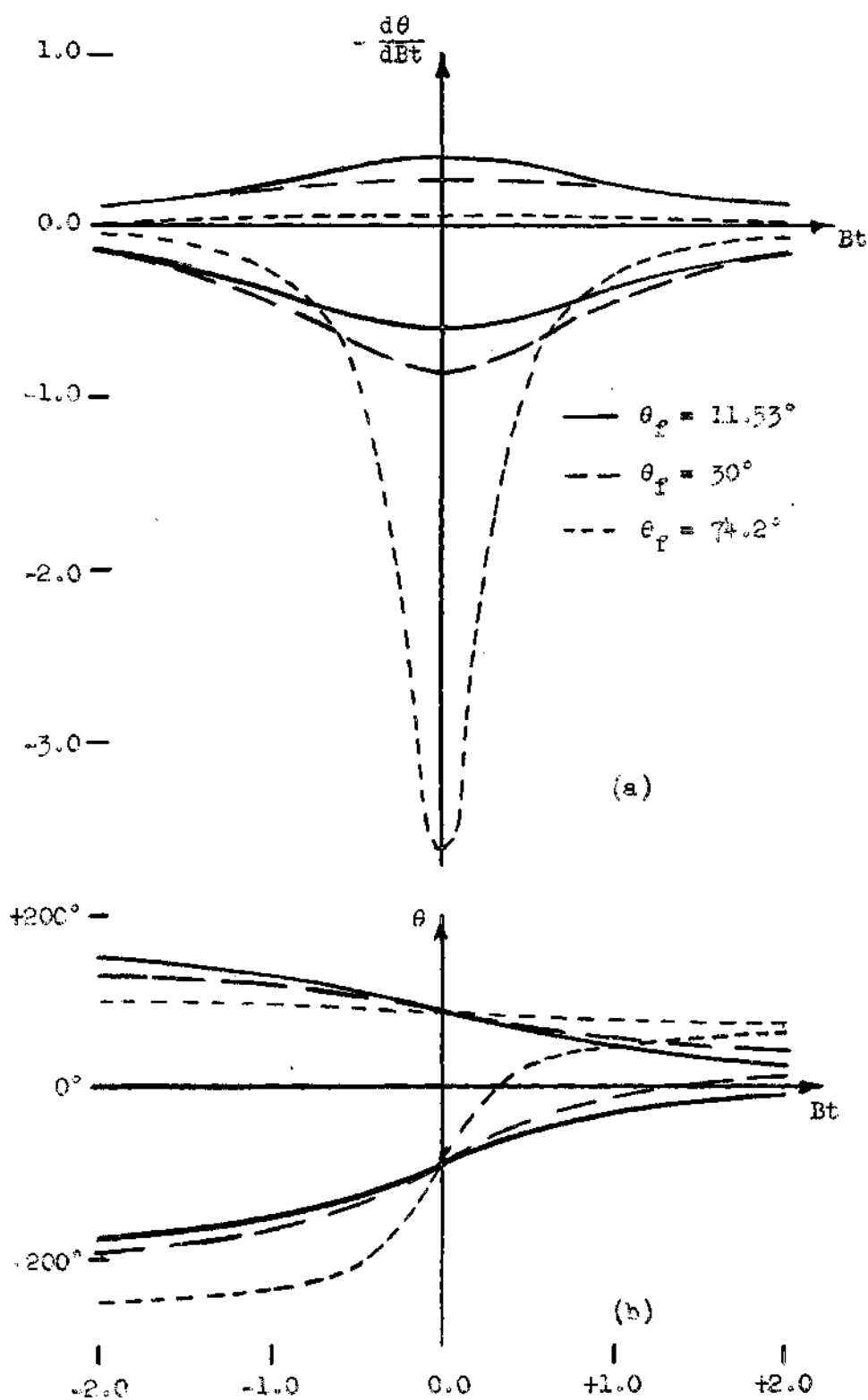


Figure 18. Family of Instantaneous Phase Angle and Frequency Curves for $\theta_f = 11.53^\circ$, $\theta_f = 30^\circ$, and $\theta_f = 74.2^\circ$.

oscillator frequency. There is no reason why ω_s cannot be negative which would be the case for the synchronizing frequency below the oscillator frequency. With the modifications listed below, which will hold for cases II and III as well, the solution to the problem when ω_s is negative is readily available.

1. The sign of the phase angle, θ , changes. In case I this amounts to an inversion of Figure 12.
2. The sign of $-d\theta/dt$ changes. In case I this amounts to an inversion of Figure 18(a).
3. The actual transients are inverted and the signs of the initial phase angles are changed. In case I this means that Figures 16 and 17 are inverted and the signs of the initial phase angles are changed.

The photograph of Figure 19 shows an experimental comparison of synchronization transients with the synchronizing signal above and below the oscillator frequency. Conditions in this photograph are the same as for Figure 17 except that ω_s takes on both signs.

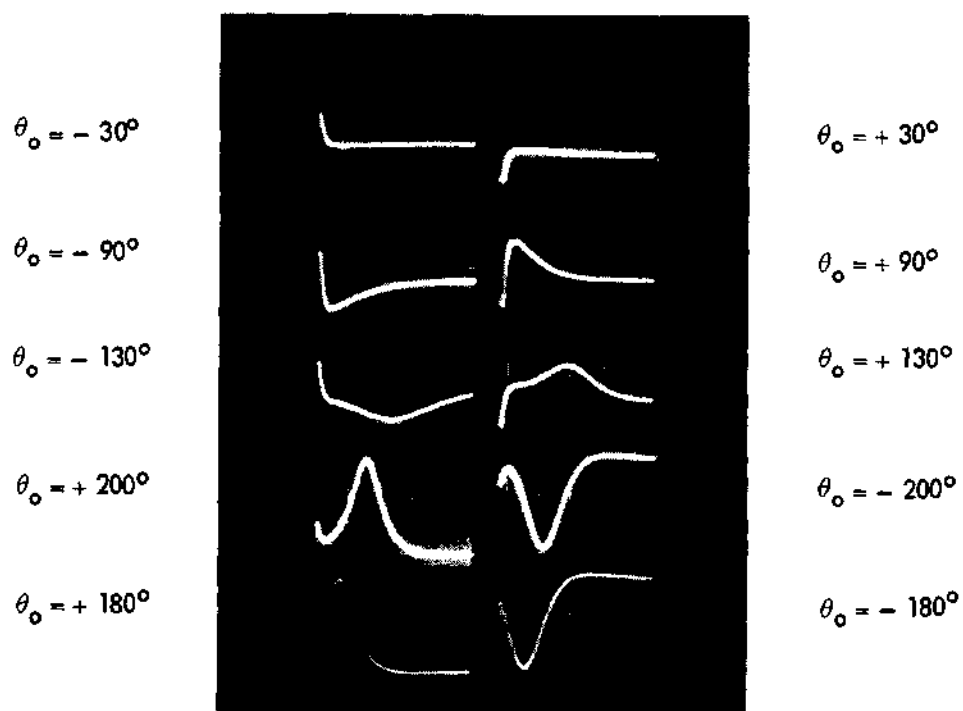
Development of Case II, $\omega_s > \omega_c$

Development of case II proceeds in the same way as the development of case I. A solution of equation (37) with $\omega_s > \omega_c$

$$\frac{d\theta}{dt} = \omega_s - \omega_c \sin \theta \neq 0 \quad (37)$$

yields θ as a function of time. $d\theta/dt$ is then obtained and used in the equation

$$\omega = \omega_1 - \frac{d\theta}{dt} \quad (38)$$



$$\omega_c = 2\pi(400)$$

$$\omega_c = 2\pi(400)$$

$$\omega_s = -2\pi(200)$$

$$\omega_s = +2\pi(200)$$

$$\theta_f = -30^\circ$$

$$\theta_f = +30^\circ$$

Time Scale: 0.8 milliseconds per centimeter.

Amplitude Scale: 200 cps per centimeter.

Figure 19. Family of Experimentally Observed Frequency Transients.

to establish the instantaneous angular frequency as a function of time. The only difference is that the condition of case II must apply. The effect of an initial phase angle, θ_0 , is handled by matching a time determined by θ_0 in the θ solution to a corresponding time in the $\omega(t)$ solution. This matched value on the curves amounts to a shift along the time axis which establishes a new $t = 0$ axis.

A plot of equation (37), shown in Figure 20, for the condition $\omega_s > \omega_c$ reveals that $d\theta/dt$ is never equal to zero. Since $d\theta/dt$ is never zero, ω never becomes equal to ω_1 and synchronization never occurs.

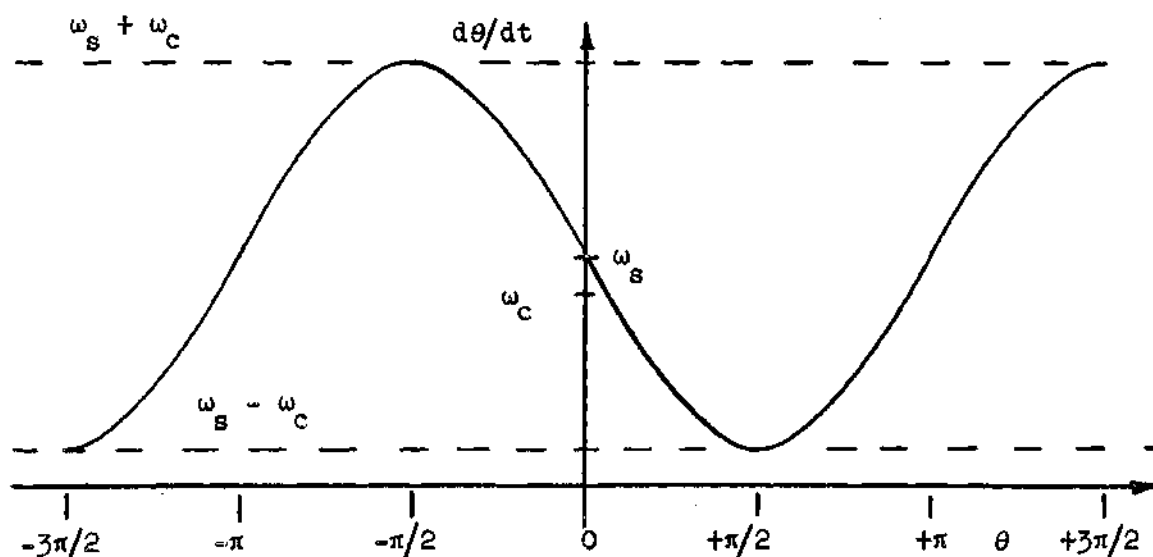


Figure 20. Plot of $d\theta/dt = \omega_s - \omega_c \sin \theta$ for $\omega_s > \omega_c$.

This case is not of primary importance in this work because interest is centered on the frequency transients during synchronization; however, it will be pursued further to add completeness to the general treatment.

Equation (37) can be written in the form

$$\frac{d\theta}{\omega_s - \omega_c \sin \theta} = dt \quad \omega_s > \omega_c \quad (67)$$

Equation 436.00 in Dwight's Table of Integrals (10) can be used to integrate equation (67) to give equation

$$\frac{2}{\sqrt{\omega_s^2 - \omega_c^2}} \tan^{-1} \frac{\omega_s \tan \theta/2 - \omega_c}{\sqrt{\omega_s^2 - \omega_c^2}} = t + t_0 \quad (68)$$

where t_0 is a constant of integration. Solve equation (68) for

$$\tan \theta/2 = \frac{\sqrt{\omega_s^2 - \omega_c^2}}{\omega_s} \tan \left[\frac{\sqrt{\omega_s^2 - \omega_c^2}}{2} (t + t_0) \right] + \frac{\omega_c}{\omega_s} \quad (69)$$

or

$$\theta = 2 \tan^{-1} \left[\frac{\omega_c}{\omega_s} + \frac{\sqrt{\omega_s^2 - \omega_c^2}}{\omega_s} \tan \frac{\sqrt{\omega_s^2 - \omega_c^2}}{2} (t + t_0) \right] \quad (70)$$

Use the trigonometric identity for the tangent of an angle to write equation (70) as

$$\theta = 2 \tan^{-1} \left\{ \frac{\omega_c}{\omega_s} + \frac{\sqrt{\omega_s^2 - \omega_c^2}}{\omega_s} \frac{\sin \left[\frac{\sqrt{\omega_s^2 - \omega_c^2}}{2} (t + t_0) \right]}{\cos \left[\frac{\sqrt{\omega_s^2 - \omega_c^2}}{2} (t + t_0) \right]} \right\} \quad (71)$$

or

$$\theta = 2 \tan^{-1} \frac{1}{\omega_s} \left\{ \frac{\omega_c \cos \left[\frac{\sqrt{\omega_s^2 - \omega_c^2}}{2} (t + t_0) \right] + \sqrt{\omega_s^2 - \omega_c^2} \sin \left[\frac{\sqrt{\omega_s^2 - \omega_c^2}}{2} (t + t_0) \right]}{\cos \left[\frac{\sqrt{\omega_s^2 - \omega_c^2}}{2} (t + t_0) \right]} \right\} \quad (72)$$

Define

$$\phi = \tan^{-1} \frac{\omega_c}{\sqrt{\omega_s^2 - \omega_c^2}} \quad (73)$$

and equation (72) becomes

$$\theta = 2 \tan^{-1} \frac{\sin \left[\frac{\sqrt{\omega_s^2 - \omega_c^2} (t + t_0)}{2} + \phi \right]}{\cos \left[\frac{\sqrt{\omega_s^2 - \omega_c^2} (t + t_0)}{2} \right]}. \quad (74)$$

No loss of generality occurs if

$$x = \sqrt{\omega_s^2 - \omega_c^2} \left(\frac{t + t_0}{2} \right) \quad (75)$$

is used; equation (74) can then be written

$$\theta = 2 \tan^{-1} \frac{\sin(x + \phi)}{\cos x}. \quad (76)$$

Equation (76) is the general solution for instantaneous phase angle as a function of time in case II. The general solution is sketched in Figure 21(a).

Since instantaneous frequency is of more interest than the instantaneous phase angle, equation (76) can be differentiated and combined with equation (38) for the desired result. Differentiating equation (76) with respect to x gives

$$\begin{aligned} \frac{d\theta}{dx} &= \frac{2 \frac{d}{dx} \frac{\sin(x + \phi)}{\cos x}}{1 + \frac{\sin^2(x + \phi)}{\cos^2 x}} \\ &= \frac{2 \cos \phi}{1 + \sin(2x + \phi) \sin \phi}. \end{aligned} \quad (77)$$

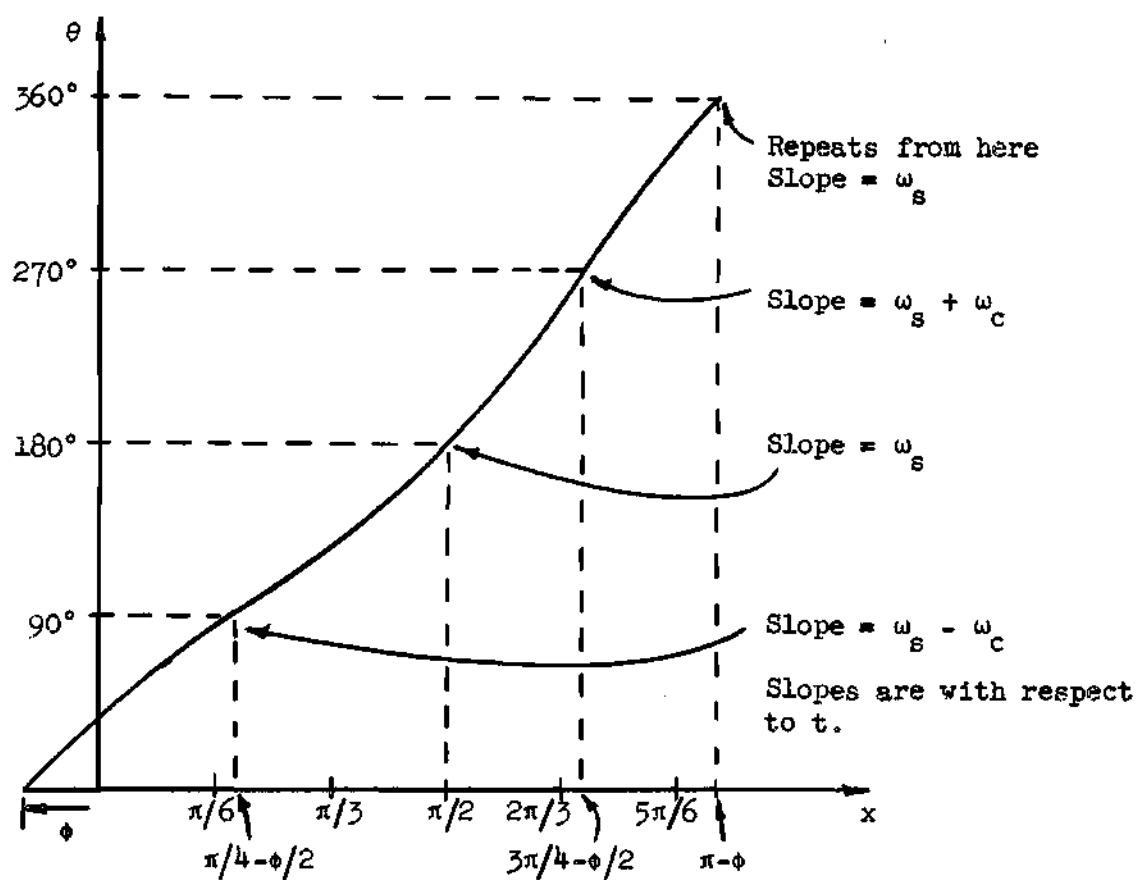


Figure 21(a). Instantaneous Phase Angle for $\omega_s > \omega_c$.

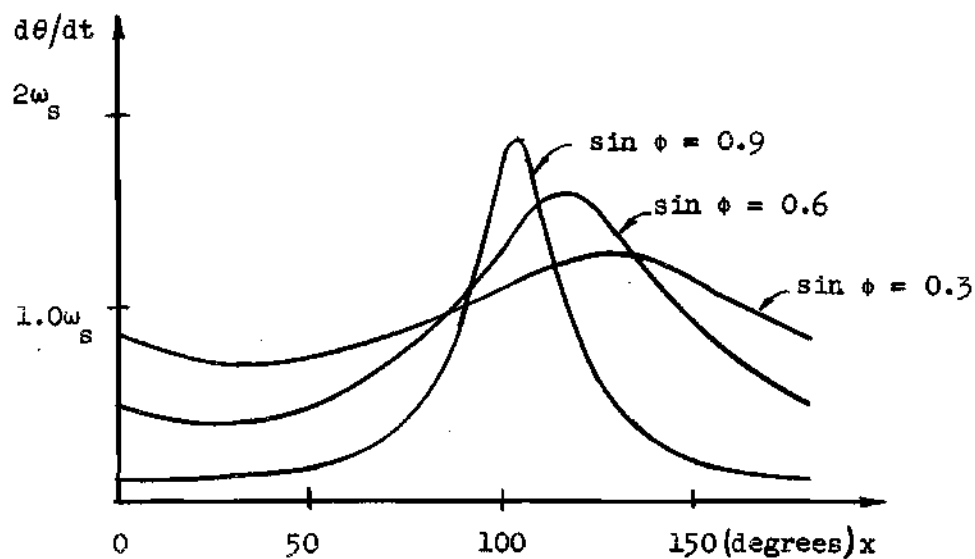


Figure 21(b). Instantaneous Frequency for $\omega_s > \omega_c$.

Since

$$\frac{d\theta}{dt} = \frac{d\theta}{dx} \frac{dx}{dt} = \frac{d\theta}{dx} \frac{\sqrt{\omega_s^2 - \omega_c^2}}{2} = \frac{d\theta}{dx} \frac{\omega_s \cos \phi}{2} \quad (78)$$

use equation (77) in equation (78) to obtain

$$\frac{d\theta}{dt} = \frac{\omega_s \cos^2 \phi}{1 + \sin(2x + \phi) \sin \phi} \quad (79)$$

and then use equation (79) in equation (38) to obtain

$$\omega = \omega_1 - d\theta/dt = \omega_1 - \frac{\omega_s \cos^2 \phi}{1 + \sin(2x + \phi) \sin \phi} \quad (80)$$

Since ω_1 is a constant in a given situation, the instantaneous frequency is determined by the variation of equation (79) which is plotted in Figure 21(b) for several values of ϕ .

Figure 21(b) is misleading because it seems to indicate that for different values of ϕ the range over which ω varies is different. Equation (79) can be written in the form

$$\frac{d\theta}{dt} = \frac{\omega_c \cos^2 \phi}{\sin \phi (1 + \sin(2x + \phi) \sin \phi)} \quad (81)$$

Figure 22 is a sketch of equation (81) and it shows the frequency variation in correct proportion. Note that the maximum value of equation (81) is $\omega_c(1 + \operatorname{cosec} \phi)$ and the minimum value of equation (81) is $\omega_c(\operatorname{cosec} \phi - 1)$. The difference between the maximum and minimum values of equation (81) is independent of ϕ and is always equal to $2\omega_c$.

Consider as an example a case where $\omega_s = 2\pi(1000)$ and $\omega_c = 2\pi(900)$.

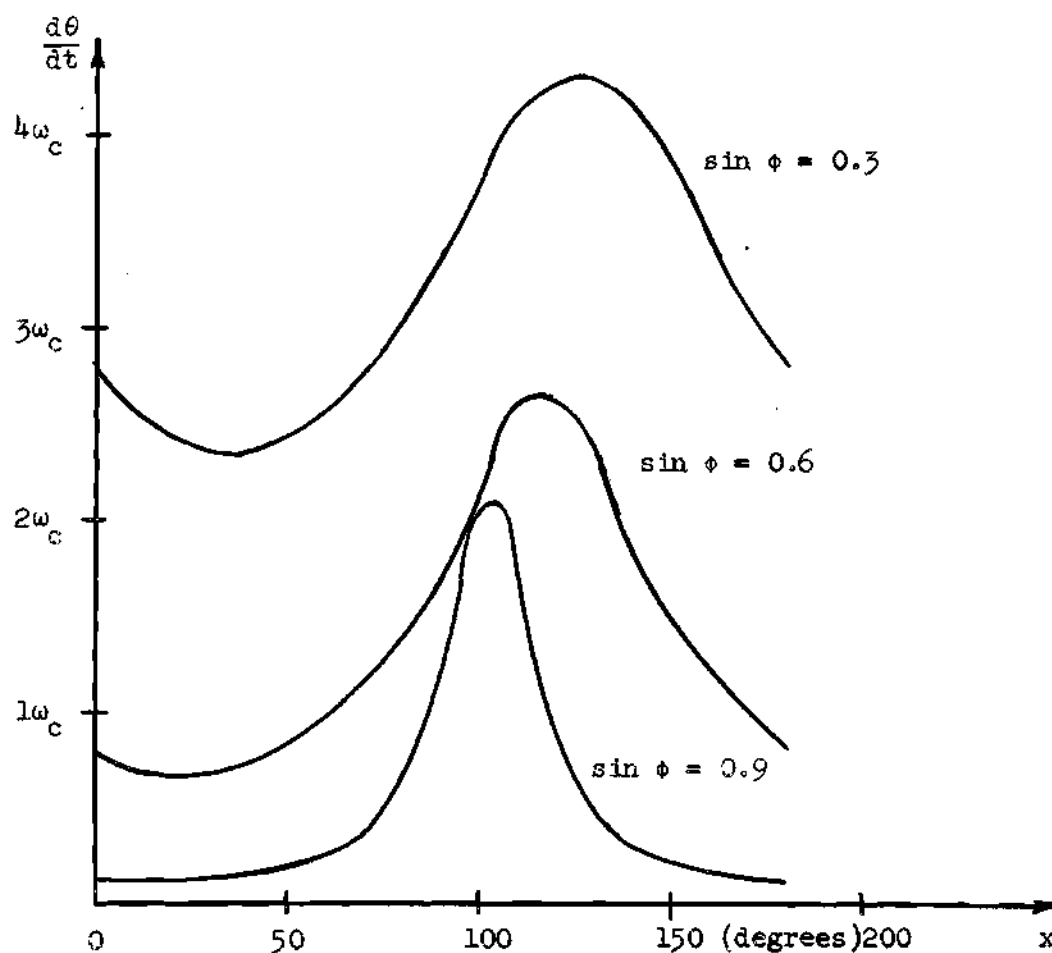


Figure 22. Instantaneous Frequency for $\omega_s > \omega_c$.

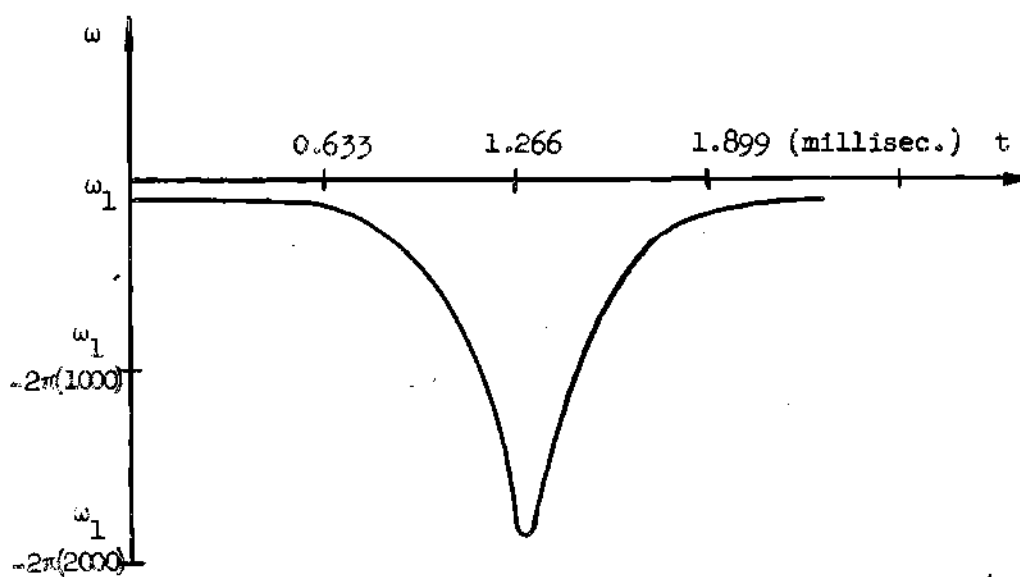


Figure 23. Oscillator Frequency Behavior for $\omega_s = 2\pi(1000)$, $\omega_c = 2\pi(900)$.

This determines $\sin \phi$ as 0.9 and the time scale factor as $2\pi(220)$. The properly modified curve of Figure 21(b) is subtracted from ω_1 to give ω , the instantaneous angular velocity, as a function of time. The resultant curve is sketched in Figure 23.

An initial phase angle can be taken into account in the following manner. First a curve like that of Figure 21(a) must be plotted for the proper value of $\phi = \sin^{-1} \omega_c / \omega_s$. A given θ_0 will, when used with this curve, determine an x value. This x value is then used in Figure 21(b) with the proper $\sin \phi$ curve to establish the $x = 0$ or $t = 0$ reference. Since synchronization is never attained, the instantaneous frequency curve is periodic and an initial θ value simply determines the starting point of the curve.

Development of Case III $\omega_s = \omega_c$

As in the previous two cases development proceeds by solving equation (37)

$$d\theta/dt = \omega_s - \omega_c \sin \theta \neq 0 \quad (37)$$

for $\theta(t)$ but with the condition $\omega_s = \omega_c$ in this case. $d\theta/dt$ is then obtained and used in the equation

$$\omega = \omega_1 - d\theta/dt \quad (38)$$

to establish $\omega(t)$. The initial phase angle is accounted for by matching proper time axis values of the $\theta(t)$ and $\omega(t)$ solutions.

Figure 24, a plot of equation (37) for the condition $\omega_s = \omega_c$, reveals that $d\theta/dt$ is equal to zero for only one value of θ , $\theta = \pi/2$.

Synchronization, therefore, occurs for only one value of θ , $\theta = \pi/2$,

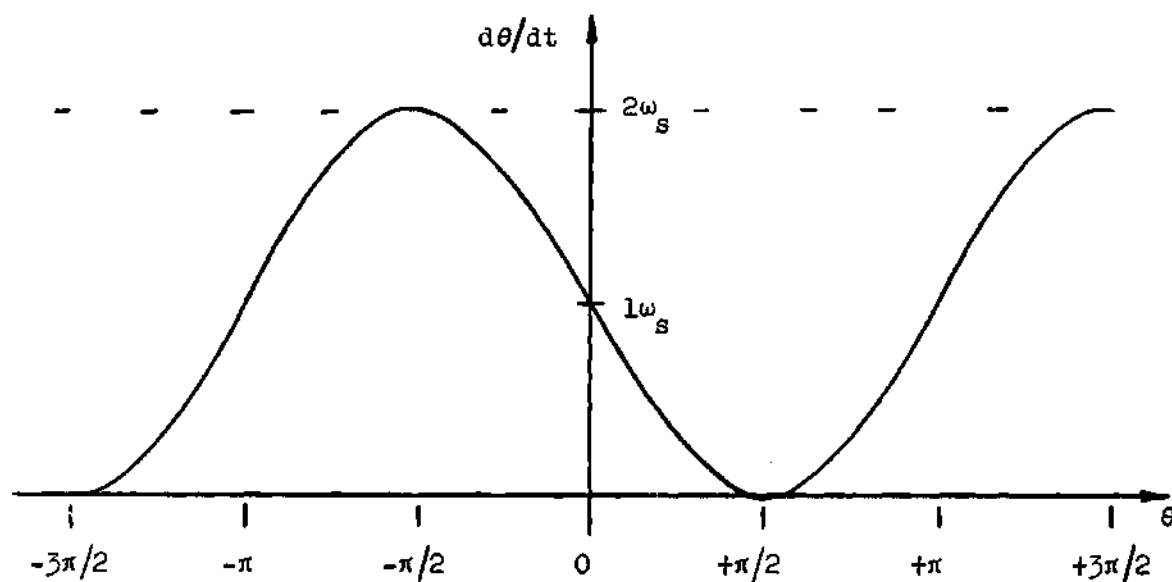


Figure 24. Plot of $d\theta/dt = \omega_s - \omega_c \sin \theta$ for $\omega_s = \omega_c$.

This case is the boundary between cases I and II and is a case of zero probability. Consider equation (37) rewritten as

$$\frac{d\theta}{\omega_s(1 - \sin \theta)} = dt, \quad \omega_s = \omega_c \quad (82)$$

Equation 433.02 of Dwight's Table of Integrals (10) gives for the solution of equation (82)

$$\tan(\pi/4 + \theta/2) = \omega_s(t + t_0) \quad (83)$$

where t_0 is a constant of integration. Solving equation (83) for θ gives

$$\theta = 2 \tan^{-1} \omega_s(t + t_0) - \pi/2 \quad (84)$$

No loss of generality occurs if $\omega_s t_0$ is arbitrarily set equal to zero.

This amounts to choosing $\theta = \pi/2$ at $t = 0$. Equation (84) becomes

$$\theta = 2 \tan^{-1} (\omega_s t) - \pi/2 \quad (85)$$

Equation (85) gives instantaneous phase angle as a function of $\omega_s t$ (or t upon division of the $\omega_s t$ scale by ω_s). Equation (85) is plotted in Figure 25(a).

Differentiating equation (85) with respect to $\omega_s t$ yields

$$\frac{d\theta}{d\omega_s t} = \frac{2}{1 + (\omega_s t)^2} \quad (86)$$

and since

$$\frac{d\theta}{dt} = \omega_s \frac{d\theta}{d\omega_s t}$$

the result

$$-\frac{d\theta}{dt} = -\frac{2\omega_s}{1 + (\omega_s t)^2} \quad (87)$$

is available. Finally, the instantaneous angular velocity is given by

$$\omega = \omega_1 - d\theta/dt = \omega_1 - \frac{2\omega_s}{1 + (\omega_s t)^2} \quad (88)$$

Equation (87) is plotted in Figure 25(b). Use of equation (88) with the curves of Figure 25 will allow calculation and plotting of any frequency transient with arbitrary initial phase conditions for the case $\omega_s = \omega_c$. Note that the curves of Figure 25 are similar to the curves of Figure 18.

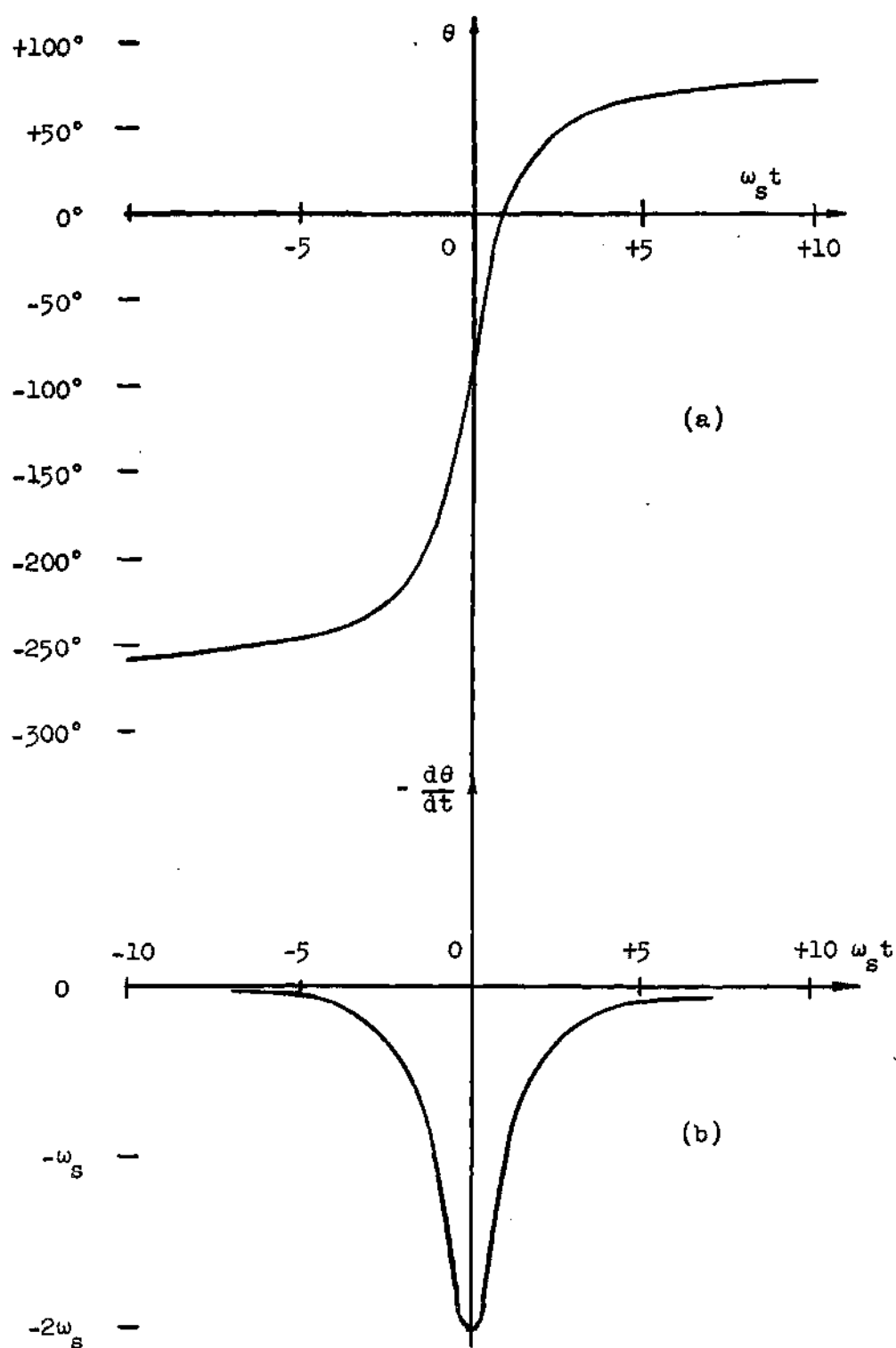


Figure 25. Plot of Instantaneous Phase Angle and Oscillator Frequency for $\theta_f = 90^\circ$.

Equation (88) can be developed as a limiting case of

$$\omega = \omega_1 + \frac{\pm B (1 - k^2)}{(k^2 + 1) \cosh Bt \pm 2k} \quad (64)$$

from which the curves of Figure 18(a) are sketched.

An example illustrates the use of Figure 25. Let $\omega_c = \omega_s = 2\pi(300)$ and let the initial phase angle be -200 degrees. Enter Figure 25(a) at $\theta = -200$ degrees and project down to the same $\omega_s t$ value, $\omega_s t = -1.45$, on Figure 25(b). This $\omega_s t$ value corresponds to $t = 0$ and the time scale is set up by dividing the $\omega_s t$ scale values by $\omega_s = 2\pi(300)$. Add ω_1 to all ordinate values, properly scaled, and the transient is sketched. Figure 26(a) shows this example and Figure 26(b) and 26(c) show the effects of two other initial angles. Figures 27 and 28 show experimental curves for several initial angles and several bandwidths. These experimental curves are actually for the case ω_s slightly less than ω_c .

Development of Universal Curves

The results of cases I and III can be modified and combined in one set of curves which can be used to solve any synchronization transient problem. Consider again the results of case I

$$\theta = 2 \tan^{-1} \left[k + \frac{1 - k^2}{k \pm e^{Bt}} \right] \quad (60)$$

and

$$\omega = \omega_1 - d\theta/dt = \omega_1 + \left[\frac{\pm B (1 - k^2)}{(k^2 + 1) \cosh Bt \pm 2k} \right] \quad (64)$$

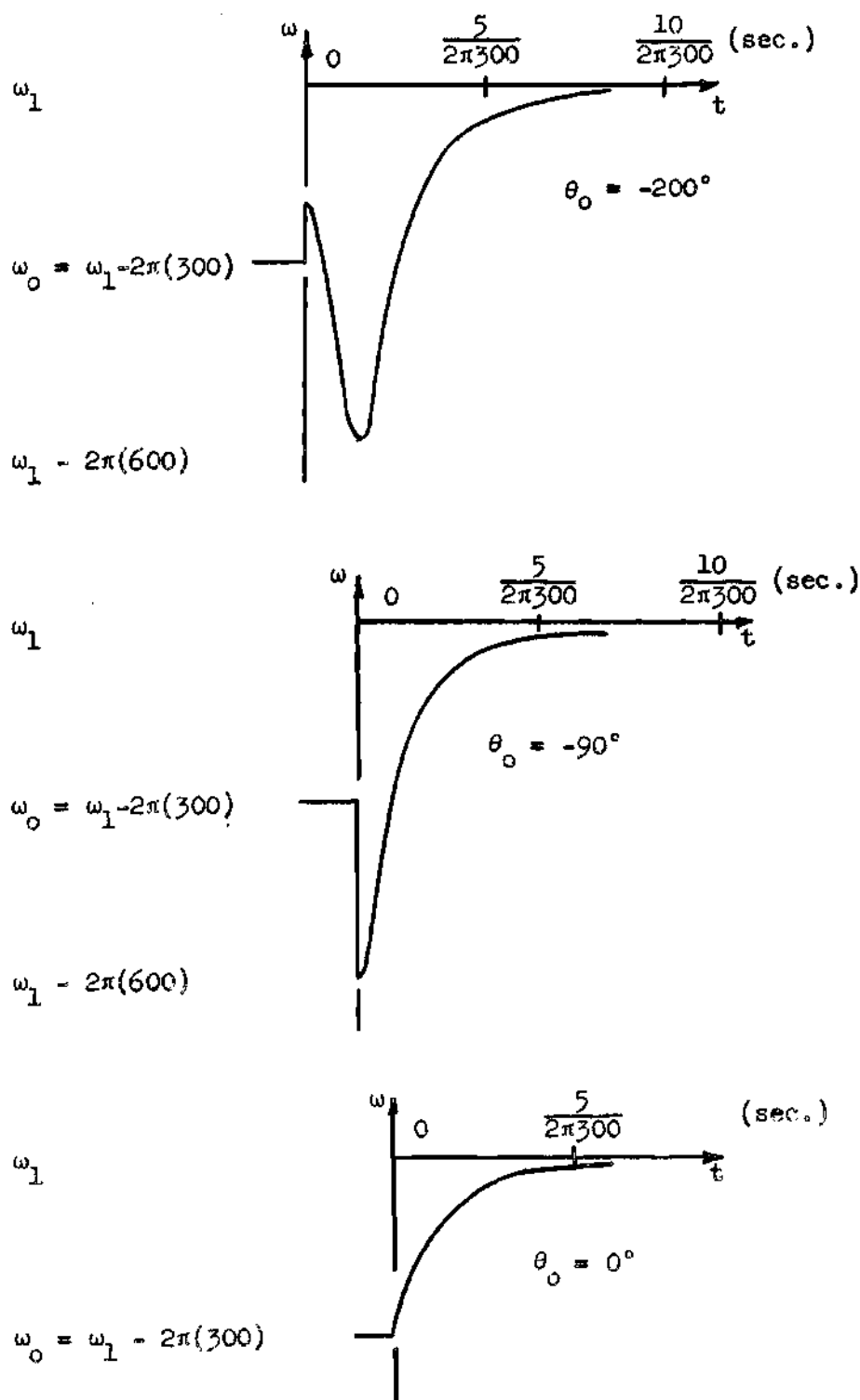
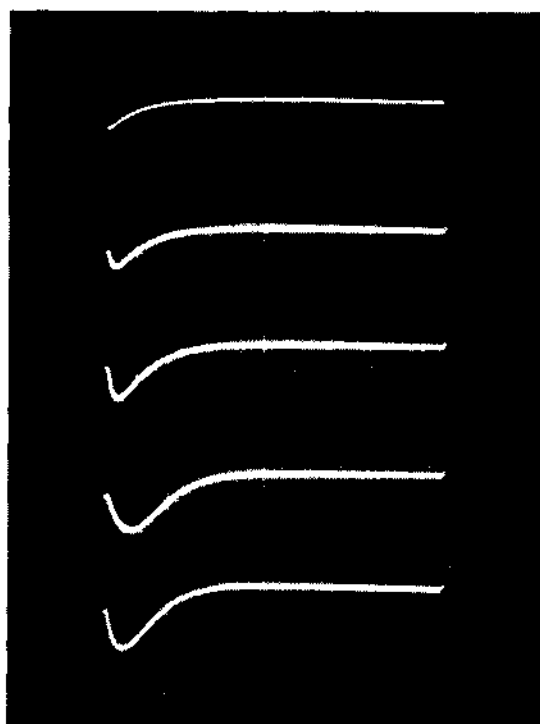


Figure 26. Several Oscillator Frequency Transients for $\omega_s = \omega_0 = 2\pi(300)$ and $\theta_f = 90^\circ$.



$$\theta_o = +10^\circ$$

$$\theta_o = -30^\circ$$

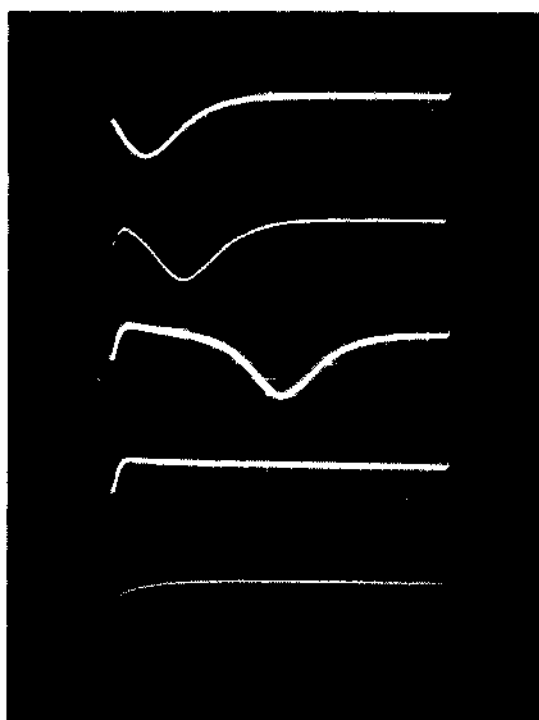
$$\theta_o = -70^\circ$$

$$\theta_o = -140^\circ$$

$$\theta_o = -110^\circ$$

Time Scale: 0.6 millise./cm.

Amplitude Scale: 200 cps/cm.



$$\theta_o = -170^\circ$$

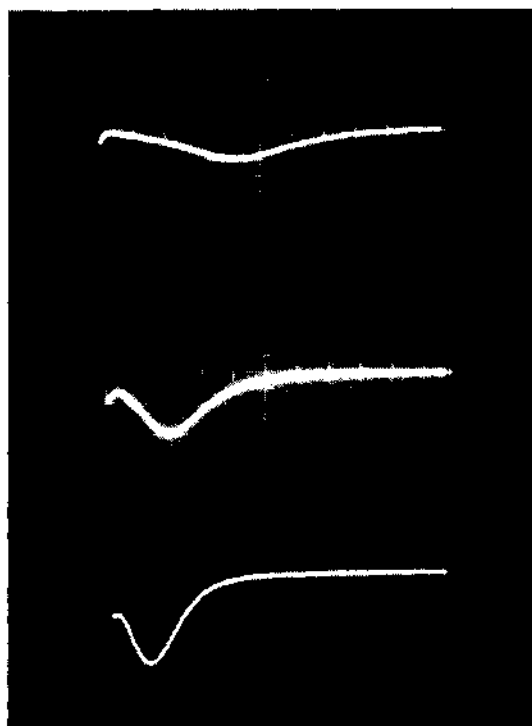
$$\theta_o = -210^\circ$$

$$\theta_o = -250^\circ$$

$$\theta_o = +80^\circ$$

$$\theta_o = +40^\circ$$

Figure 27. Family of Frequency Transients for $\omega_s = \omega_c = 2\pi(200)$.



Amplitude Scale: 200 cps/cm.

$$\omega_s = \omega_c = 2\pi(100)$$

Time Scale: 0.6 millise./cm.

$$\omega_s = \omega_c = 2\pi(200)$$

Time Scale: 0.6 millise./cm.

$$\omega_s = \omega_c = 2\pi(300)$$

Time Scale: 0.6 millise./cm.

Figure 28. Family of Experimentally Observed Frequency Transients. The effect of bandwidth on the transient amplitude and the transient duration is clearly shown.

where $k = \tan \theta_f/2$, $\sin \theta_f = \omega_s/\omega_c$, and $B = \sqrt{\omega_c^2 - \omega_s^2} = \omega_c \sqrt{1 - \sin^2 \theta_f} = \omega_c \cos \theta_f$. Use + sign for $\theta_f < \theta_0 < \pi - \theta_f$ and use - sign for $-\pi - \theta_f < \theta_0 < \theta_f$.

The results of case III are

$$\theta = 2 \tan^{-1} \omega_s t - \pi/2 \quad (85)$$

and

$$\omega = \omega_1 - d\theta/dt = \omega_1 - \left[\frac{2\omega_s}{1 + (\omega_s t)^2} \right] \quad (88)$$

where $\omega_s = \omega_c$.

Equations (60) and (85) are plotted in Figure 29(a) with the time scale of equation (60) adjusted by the relationship $B = \omega_c \cos \theta_f$ so that the abscissa is $\omega_c t$ rather than Bt . The time scale is already correct for equation (85). Note that all curves are adjusted so that $\theta = \pm \pi/2$ at $t = 0$.

The bracketed term of equation (64) has maximum values of

$$-\frac{d\theta}{dt}_{\max} = +B \left[\frac{1-k}{1+k} \right] = \omega_c (1 - \sin \theta_f) \quad (89)$$

and

$$-\frac{d\theta}{dt}_{\max} = -B \left[\frac{1+k}{1-k} \right] = -\omega_c (1 + \sin \theta_f). \quad (90)$$

If the bracketed term of equation (64) is normalized by dividing by the proper magnitude of equation (89) or equation (90) the result is

$$-\frac{d\theta}{dt}_n = \frac{(1+k)^2}{(1+k^2)\cosh Bt + 2k} \quad (91)$$

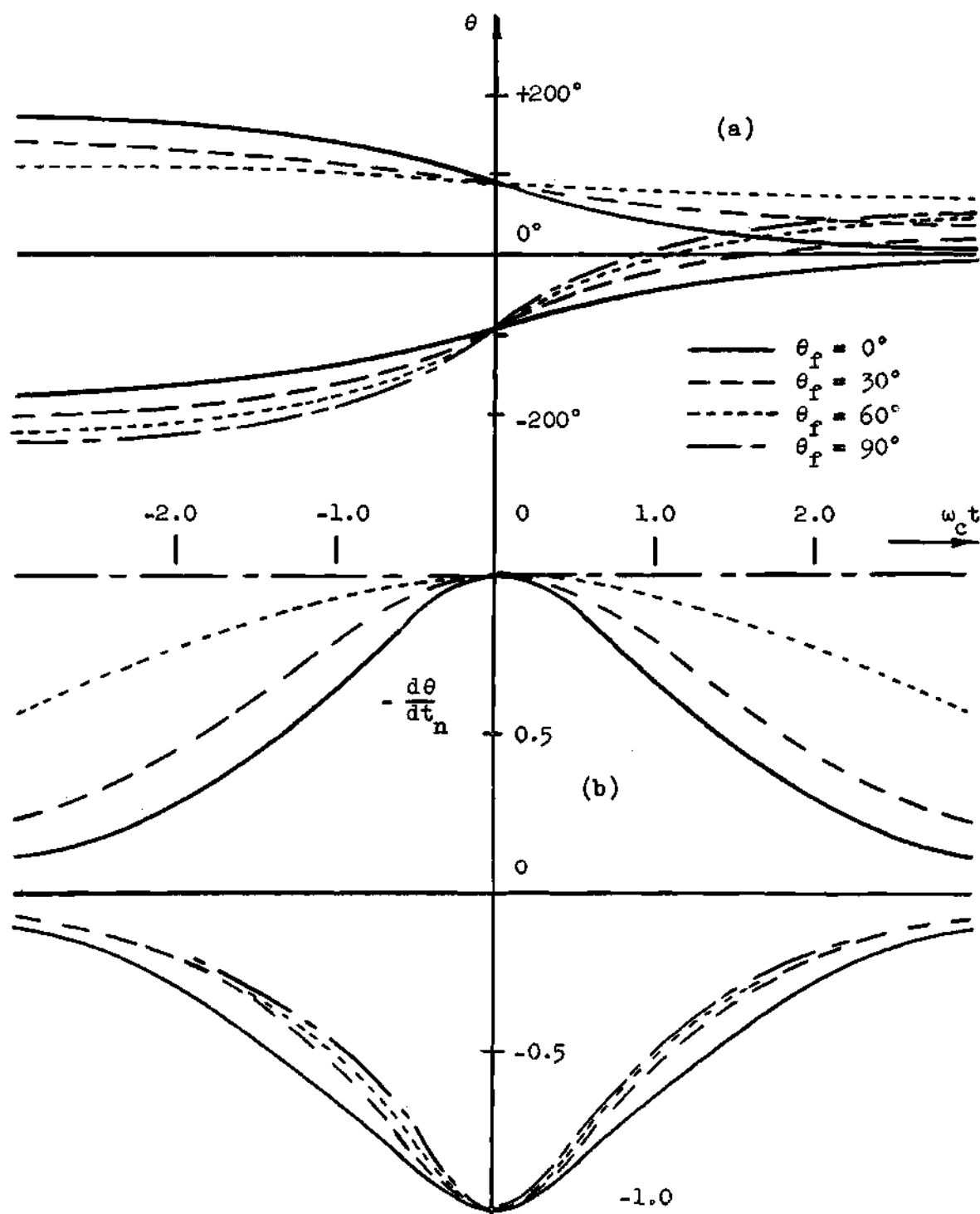


Figure 29. (a) Family of Instantaneous Phase Angle Curves.
 (b) Family of Normalized Instantaneous Frequency Curves.

for $\theta_f < \theta_o < \pi - \theta_f$ and

$$-\frac{d\theta}{dt_n} = \frac{-(1-k)^2}{(1+k^2)\cosh Bt - 2k} \quad (92)$$

for $-\pi - \theta_f < \theta_o < \theta_f$.

The bracketed term of equation (88) is normalized by dividing by $2\omega_c = 2\omega_s$ which is the maximum value of the term. The term becomes

$$-\frac{d\theta}{dt_n} = -\frac{1}{1 + (\omega_c t)^2} \quad (93)$$

Equations (91), (92), and (93) are plotted in Figure 29(b) for the corresponding θ_f values of Figure 29(a).

Figure 29 gives the solution for any synchronization frequency transient which can occur regardless of the initial phase relationship between the synchronizing source voltage and the voltage of the oscillator to be synchronized. The solution is effected in the following manner with known quantities being ω_c , ω_s , ω_o , and ω_l . $\sin \theta_f = \omega_s/\omega_c$ determines the proper curves of Figure 29 to use.

1. Enter Figure 29(a) on the curve determined by θ_f and read the $\omega_c t$ value corresponding to the initial phase angle.
2. The $\omega_c t$ value read in step 1 determines the starting point ($t = 0$) on the particular transient curve of Figure 29(b) corresponding to the θ_f value.
3. The abscissa scale of Figure 29(b) is divided by ω_c to give the time scale in seconds.
4. The ordinate scale of Figure 29(b) is multiplied by $\omega_c(1-\sin\theta_f)$

if the upper curve is used, and by $\omega_c(1 + \sin \theta_f)$ if the lower curve is used.

5. ω_1 is added to all the ordinate values corrected as in step 4.
6. The complete instantaneous angular velocity curve is given by following $\omega = \omega_0$ to the $\omega_c t$ value corresponding to $t = 0$. At this point the instantaneous angular velocity changes stepwise to the curve of part 5 and follows this curve as t goes to infinity where ω equals ω_1 .

The normalized curves of Figure 29(b) tend to disguise the fact that the actual frequency transients above and below the $\omega_c t$ axis differ in amplitude. An alternate set of curves is given in Figure 30. Figure 30(a) is the same as Figure 29(a) but Figure 30(b) differs from Figure 29(b) in the fact that the ordinate of Figure 30(b) is $-d\theta/d\omega_c t$ and the curves are not normalized. Multiplying the ordinate scale of Figure 30(b) by ω_c gives $-d\theta/dt$. These curves show the relative amplitudes of the transients. The same six steps for using the curves of Figure 29 apply for using the curves of Figure 30 with the exception that the step 4 multiplying factor for Figure 30 is ω_c for all the instantaneous frequency curves. The appendix gives several individual curves for different values of θ_f . These curves are more accurate and are easier to read.

The fact that ω_s is negative for $\omega_1 < \omega_0$ offers no difficulty in the use of the general curves of Figures 29 and 30. The curves are used by changing the sign of θ in Figures 29(a) and 30(a) and by changing the sign of $-d\theta/dt$ in Figures 29(b) and 30(b). This amounts to an inversion of the curves. As an illustration consider $\theta_0 = 150^\circ$ with $\omega_1 < \omega_0$. Figure 29(a) is used as though $+150^\circ$ is below the time axis and the time

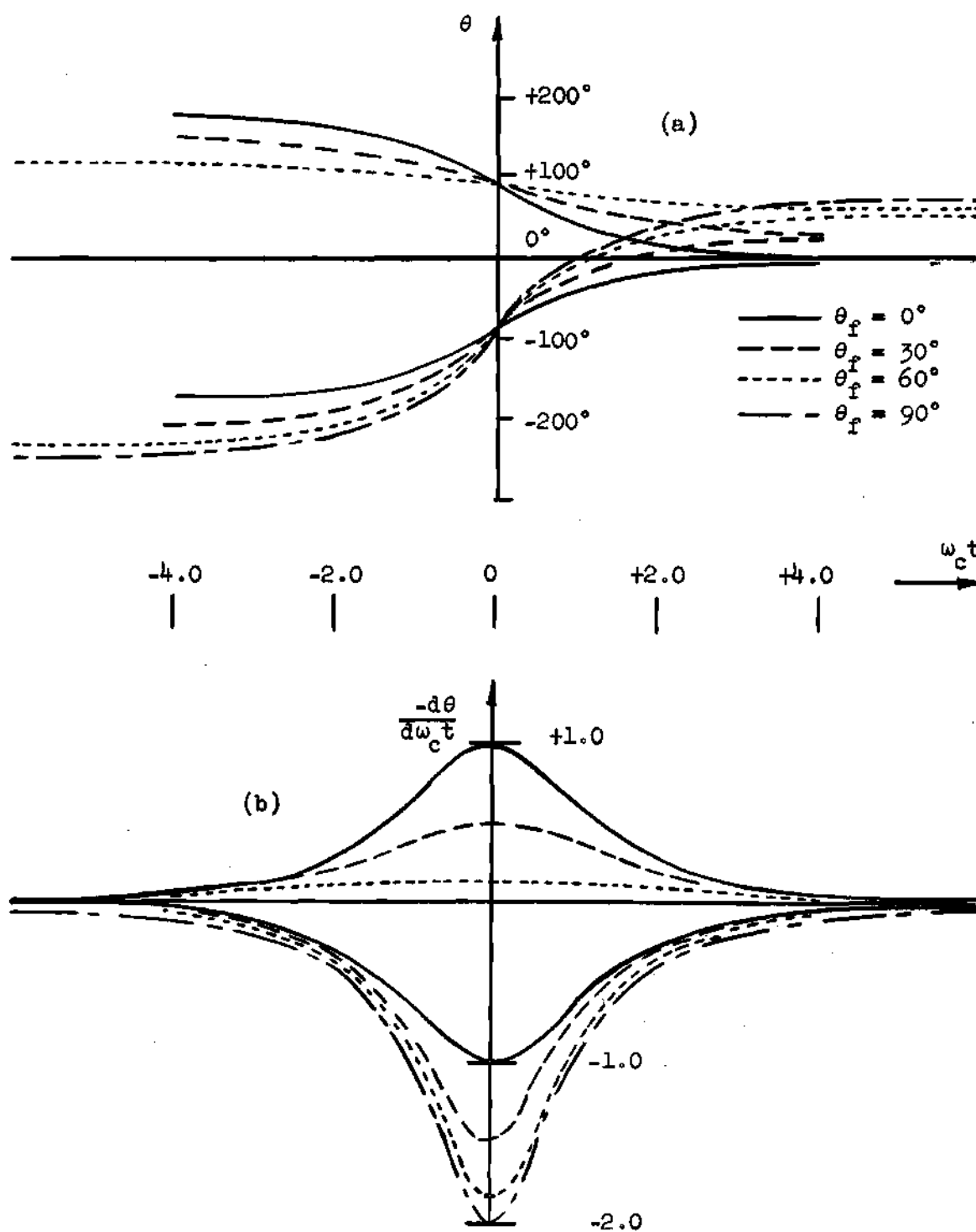


Figure 30. (a) Instantaneous Phase Angle as a Function of Time.
 (b) Instantaneous Frequency as a Function of Time.

value read on the proper θ_f curve is used to establish the reference $t = 0$ on Figure 29(b). The lower curve, for the proper θ_f value, of Figure 29(b) is inverted to yield the desired transient.

CHAPTER V

MEASUREMENT OF SYNCHRONIZATION FREQUENCY TRANSIENTS

The object of the experimental work is to observe the frequency transients that occur when the frequency of the oscillator to be synchronized is pulled from its free-running value to its final value. This pulling is effected by an instantaneously injected synchronization frequency of arbitrary but controllable initial phase. The final frequency of the oscillator is the same as the frequency of the synchronizing source. These experimental observations are compared with the theoretical transients predicted by the results of Chapter IV.

The experimental set-up for the observation of synchronization frequency transients offers the following features:

1. A control circuit to inject the synchronizing signal when the proper phase relationship exists between the oscillator and source voltages;
2. A circuit for measuring and controlling the phase angle between the oscillator and source voltages;
3. A circuit for observing and measuring the actual frequency transients;
4. A delay circuit for ensuring that one transient has completely died out after observation and that the oscillator has returned to the normal free-running condition before the synchronizing signal is injected again; and

5. A circuit for careful measurement of the reference frequencies involved, namely ω_0 and ω_1 .

Experimental verification of the predicted transients of Chapter IV requires measuring equipment some of which must meet rather critical specifications. This chapter considers, first, the general nature of the experiment from a block diagram viewpoint and, second, some details of using and calibrating the equipment. Finally, the chapter describes the more important pieces of equipment in sufficient detail that the measurement could be duplicated.

General Description of the Equipment

A block diagram of the equipment devised for observing the frequency transients that occur when a synchronizing signal of arbitrary and controllable phase is injected into an oscillator is shown in Figure 31. To simplify the discussion, let the equipment be classified according to its function as subject, control, and measurement equipment.

The subject equipment consists of the oscillator to be synchronized and the synchronizing source. As the word subject implies, the entire experiment concentrates on the behavior of this equipment, in particular the effect of the source frequency on the oscillator frequency is desired.

The control equipment consists of mixer number one, the counter, the monostable multivibrator, the phase shifter, and the gate circuit. The function of the control equipment is to inject the synchronizing source signal voltage into the free-running oscillator at the time that the desired phase relationship exists between the voltages of the free-

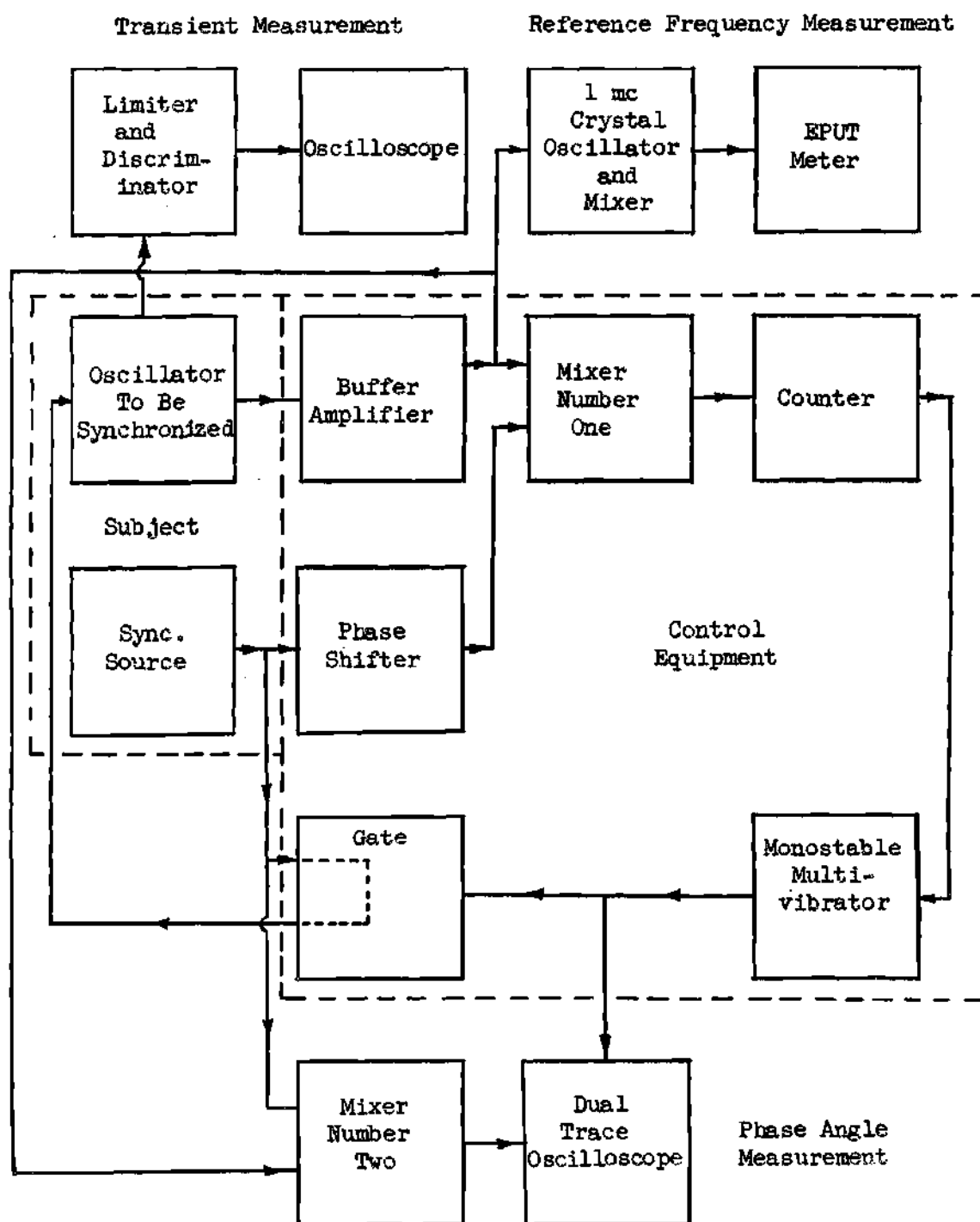


Figure 31. Block Diagram of Experimental Equipment for Observing Oscillator Synchronization Frequency Transients.

running oscillator and the synchronizing source. The control equipment allows enough time for the transient to completely run its course and it then removes the synchronizing signal. After the signal has been removed, the control equipment introduces enough delay for the oscillator to return to normal before the cycle is repeated.

Signals from the synchronizing source and the oscillator to be synchronized are fed continuously to mixer number one. When the oscillator is synchronized, the mixer output through a low-pass filter is zero and when the oscillator is not synchronized, the mixer output through the low-pass filter is at the difference frequency, $\omega_1 - \omega_0$. The instantaneous amplitude of the difference-frequency voltage is uniquely related to the instantaneous phase difference between the oscillator voltage and the synchronizing source voltage. Because of this relationship, the phase shifter between the synchronizing source and mixer number one can control, with respect to time, the zero-crossing points of the difference-frequency voltage appearing at the output of the mixer. The counter, actuated by the positive-going zero-crossing points of the difference-frequency voltage, counts cycles of the difference frequency any time the oscillator is not synchronized. After a set number of counts the counter delivers a pulse to the monostable multivibrator. The monostable multivibrator immediately operates the gate circuit which allows the synchronizing source to synchronize the oscillator. Since the control of the gate circuit comes from the output pulse of the counter and this pulse depends on the zero-crossing time, controlled by the phase shifter, of the difference-frequency voltage, the synchronizing signal voltage

can be introduced with a predetermined phase relationship relative to the oscillator voltage. When the synchronizing signal is introduced, a transient occurs; the duration of the gate pulse, determined by the period of the monostable multivibrator, must be long enough for the transient to be seen. When the multivibrator switches back to normal, the gate is closed, synchronization is lost, a difference frequency again appears at the output of the mixer, another count is started and the cycle is repeated. The counter simply creates a time delay, controllable by varying the number of counts before an output pulse appears, to ensure that the oscillator has returned to its normal free-running condition before the next synchronization cycle.

The measurement equipment consists of three basic units. The unit formed by the one-megacycle crystal oscillator and mixer combined with the Events Per Unit Time Meter, abbreviated EPUT meter, measures, with respect to the frequency of the one-megacycle crystal, the frequency $f_0 = (\omega_0/2\pi)$ of the free-running oscillator and the frequency $f_1 = (\omega_1/2\pi)$ of the synchronizing source. The second basic measurement unit consists of the limiter and discriminator followed by an oscilloscope. This unit presents a trace on the oscilloscope screen which is proportional to the instantaneous frequency, $\omega(t)$, of the oscillator. The third basic unit consists of mixer number two and the dual trace oscilloscope. This unit displays simultaneously on the face of the oscilloscope screen a difference-frequency voltage, resulting from mixing the oscillator and the synchronizing source outputs, and the gate control voltage. The relative time position of these two voltages provides the value of the relative phase angle between the oscillator voltage and the synchronizing

source voltage at the time the gate is actuated.

The transient-measuring unit is described in more detail in another section of this chapter, but a brief discussion of its operation is necessary here. The limiter keeps amplitude variations of the oscillator from affecting the discriminator and it contributes nothing to the measurement itself. The discriminator is a ratio detector to minimize even more the amplitude effects of the oscillator. The actual frequency measurement is made by the discriminator and the oscilloscope. The oscillator is being synchronized when the gate is open and it loses synchronization when the gate is closed. The output of the discriminator thus jumps back and forth between the values ω_0 and ω_1 and this output appears as a near rectangular wave form on the oscilloscope screen. The actual frequency transient appears each time as the ω_1 value is approached as Figure 32 illustrates. The transient is available in more detail when the oscilloscope sweep circuit with an expanded scale is triggered by the gate control voltage each time the gate is operated.

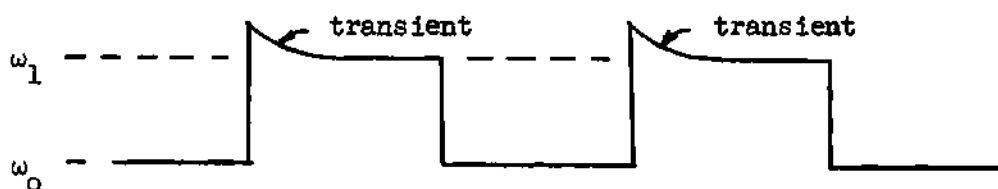


Figure 32. Oscilloscope Trace Showing Discriminator Output.

Measurement of the instantaneous phase angle between the oscillator voltage and the synchronizing voltage involves the output voltage of mixer number two and the control voltage for the gate circuit. These two signals appear simultaneously on the dual trace oscilloscope in a form

similar to Figure 33. When the gate opens, the synchronizing signal is applied to the free-running oscillator. The mixer output voltage immediately changes wave shape, indicating that a transient is occurring as the oscillator is pulled into synchronization. The transient is indicated by the dashed portion of Figure 33. At the time of the gate opening the

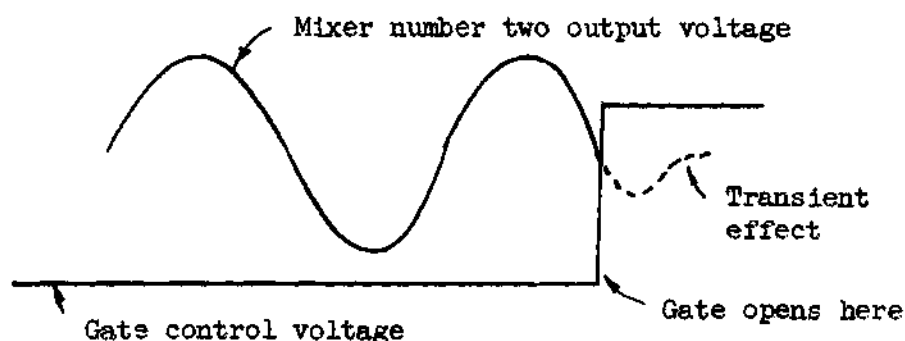


Figure 33. Typical Trace on Dual Trace Oscilloscope.

relative phase angle between the free-running oscillator voltage and the synchronizing source voltage is measured by the intersection of the gate control voltage step with the mixer output voltage curve. For instance, an intersection at the zero-crossing of the mixer output voltage curve, as indicated in Figure 33, would indicate a phase difference of ninety degrees if all phase shifts in the measuring equipment could be ignored. More detail is given in another section of this chapter.

Use of the Equipment and Calibration Procedures

This section describes the complete experimental procedure. In addition, as the need for each measurement arises, the calibration procedure for that measurement is clarified.

An experimental run shows the instantaneous frequency, ω , of the

oscillator as a function of time. Four parameters, constants for a given run, determine the actual instantaneous frequency behavior of the oscillator. These parameters, which must be measured and set to their desired values before each run, are:

1. The free-running frequency, ω_o , of the oscillator to be synchronized;
2. The frequency, ω_1 , of the synchronizing source;
3. The half synchronization bandwidth, ω_c , of the oscillator; and
4. The initial phase angle, θ_o , between the oscillator voltage and the synchronizing voltage.

Other constants, ω_s , θ_f , and k , are established from the above four constants by the relationships of Chapter IV.

A general discussion of the necessary measurements is now presented. Included with the discussion is an example using $\theta_o = 150^\circ$, $\omega_s = 2\pi(200)$ rps, $\omega_c = 2\pi(400)$ rps, and $f_o = (10^6 + 7550)$ cps.

The free-running frequency of the oscillator is measured by comparing it with the frequency of the one-megacycle crystal oscillator. The two different signal frequencies present at the inputs of the mixer cause the mixer to deliver a difference frequency signal to the EPUT meter. The EPUT meter counts this difference frequency, $(f_o - 10^6)$ cps. The difference frequency for the example is 7550 cps.

The frequency of the synchronizing source is now compared with the crystal oscillator frequency and the synchronizing source frequency is varied until the desired ω_1 , or ω_s , value is indicated by the EPUT meter. For the example, ω_s is $2\pi(200)$ rps so the EPUT meter counts 7750 cps.

The synchronization bandwidth of the oscillator is a linear function of the amplitude of the synchronizing signal voltage, V_1 . In the experimental equipment V_1 is related to the output voltage of the synchronizing source by a constant, since a voltage divider and a linear amplifier are between the synchronizing source and the injection point at the oscillator. It is more convenient to read the output voltage of the synchronizing source than to read the actual value of V_1 injected into the oscillator, so the synchronization bandwidth calibration curve in Figure 34 is plotted as a function of the actual source voltage, $k_1 V_1$,

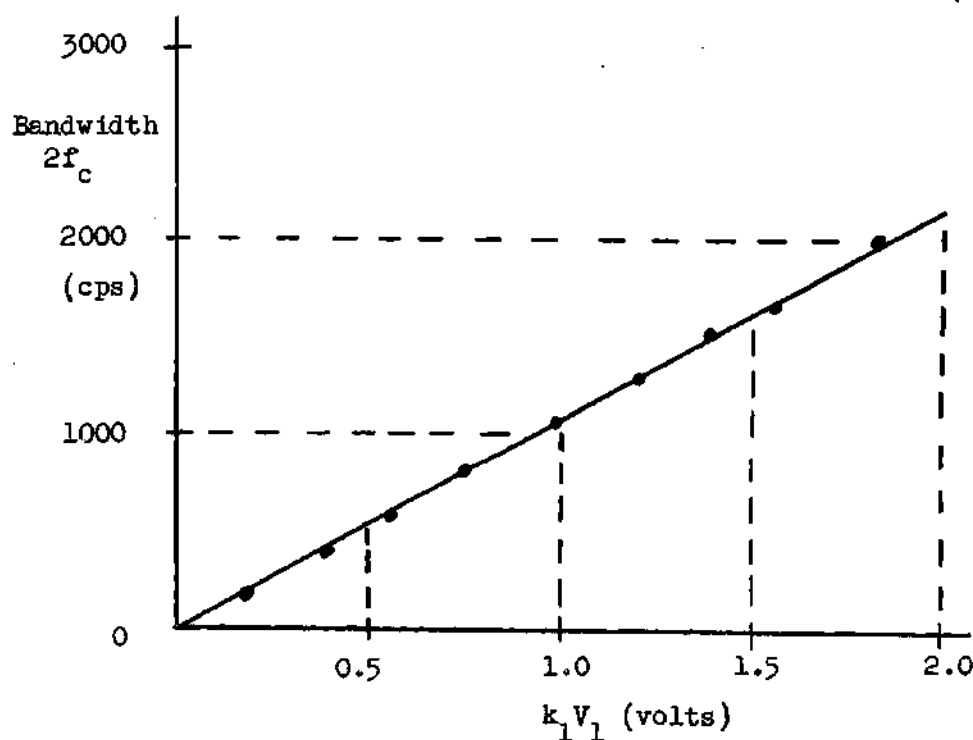


Figure 34. Synchronization Bandwidth as a Function of Signal Source Voltage.

rather than as a function of the injected signal voltage, V_1 . Note that the calibration curve is linear. In the example, adjusting the source voltage to $k_1 V_1 = 0.72$ volts sets the ω_c value to $2\pi(400)$ rps.

The initial phase angle, θ_0 , between the synchronizing signal voltage and the free-running oscillator voltage is controlled by the time appearance of the gate step. The phase shifter moves the gate step voltage in a manner discussed previously until the gate step voltage curve intersects the output voltage curve of mixer number two at the point corresponding to the desired θ_0 . This measurement is made on the screen of the dual trace oscilloscope.

Before the actual calibration curves used in the experiment are given, a general discussion of mixer operation is helpful. Assume that one input is

$$v_g = V_{gm} \sin \omega_o t \quad (94)$$

and the other input is

$$v_1 = V_{1m} \sin (\omega_o t + \theta) \quad (95)$$

where θ is a function of time and

$$d\theta/dt = \omega_1 - \omega_o . \quad (96)$$

To a good approximation, the mixer output depends on the product of the two inputs and it can be written in the form

$$v_o = V_{om} \cos \theta(t) \quad (97)$$

after the high frequency terms are removed. The instantaneous phase angle between the two input voltages can be written

$$\theta(t) = (\omega_1 - \omega_o)t . \quad (98)$$

Note that ω_1 can be greater than or less than ω_0 . This means that $\theta(t)$ can increase positively or negatively with time according to equation (98). In either case the output of the mixer is given by equation (97). Since

$$\cos x = \cos (-x) , \quad (99)$$

the output of the mixer appears the same for both cases. The sign of the instantaneous phase angle is important in the study of synchronization transients, therefore, it is expedient to use two curves to relate the instantaneous amplitude of the mixer output to the instantaneous phase angle. The upper curve of Figure 35 is used when ω_1 is greater than ω_0 and the lower curve is used when ω_1 is less than ω_0 .

Several of the circuits used in the experiment introduce phase differences between their input and output voltages. These phase differences must be accounted for in the calibration procedure used in calibrating the instantaneous difference-frequency output voltage of mixer number two as a function of the actual instantaneous phase angle existing between the oscillator voltage and the injected synchronizing voltage. Phase shifts of 180° are introduced by the buffer amplifier, mixer number two, and the gate circuit. A piece of coaxial cable, used to carry the output of the buffer amplifier to mixer number two, causes a loading effect which makes the mixer number two input voltage from the buffer amplifier lag the oscillator output voltage by 30° . Stray effects within the gate circuit cause the actual voltage injected into the oscillator for the purpose of synchronization to lag the synchronizing source voltage input to mixer number two by 30° . Without considering the 180°

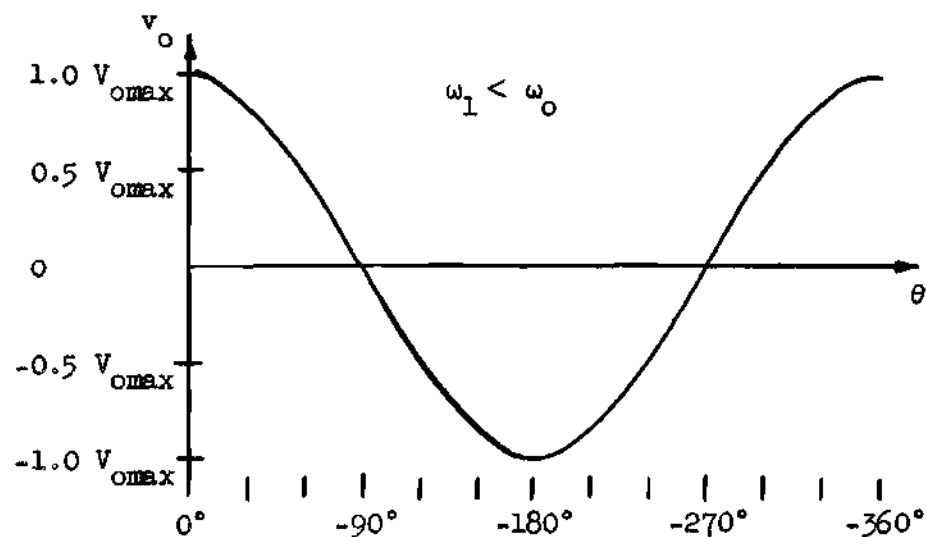
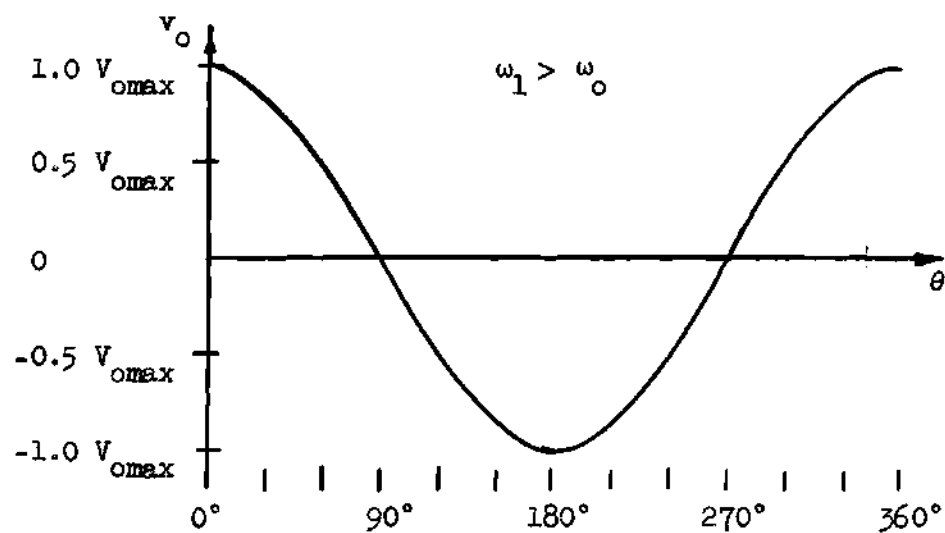


Figure 35. Calibration Curves Relating Instantaneous Output Voltage Amplitude to Instantaneous Phase Between Two Input Signals. The Curves are for the Ideal Case.

phase shifts, the actual calibration curve must differ from the ideal curve by this effective 60° lag. When the 180° phase shifts are considered, the actual calibration curve differs from the ideal curve, point by point, by 120° . Figures 36(a) and 36(b) give the actual calibration curves used in the experiment. To set $\theta_0 = 150^\circ$ in the example, use Figure 36(a) as a reference and set the intersection of the gate control voltage step and the difference-frequency voltage curve on the dual trace oscilloscope to the point where the instantaneous value of the difference-frequency voltage curve is 0.866 times the positive maximum value of the difference-frequency voltage on the negative-going side of the curve.

All required values are now introduced into the circuit. The performance of the oscillator during synchronization is cycled over and over at fixed intervals. The transient is available as a trace on the oscilloscope following the discriminator. Figure 37 shows that the discriminator response is linear over a range greater than the instantaneous frequency range of the transient. It is convenient to calibrate the oscilloscope by adjusting its input attenuator so that a fixed distance, say one cm., represents $\omega_1 - \omega_0$. Adjustment of the oscilloscope sweep time puts the near-rectangular output wave shape of the discriminator on the oscilloscope screen for this calibration procedure. After the calibration, the sweep time is chosen so the transient itself occupies most of the screen. The oscilloscope time scale calibration is used to determine the actual time values for the transient. Figure 38 shows several photographs of the same frequency transient. The amplitude scale is the same for each of these photographs but the time scales are different.

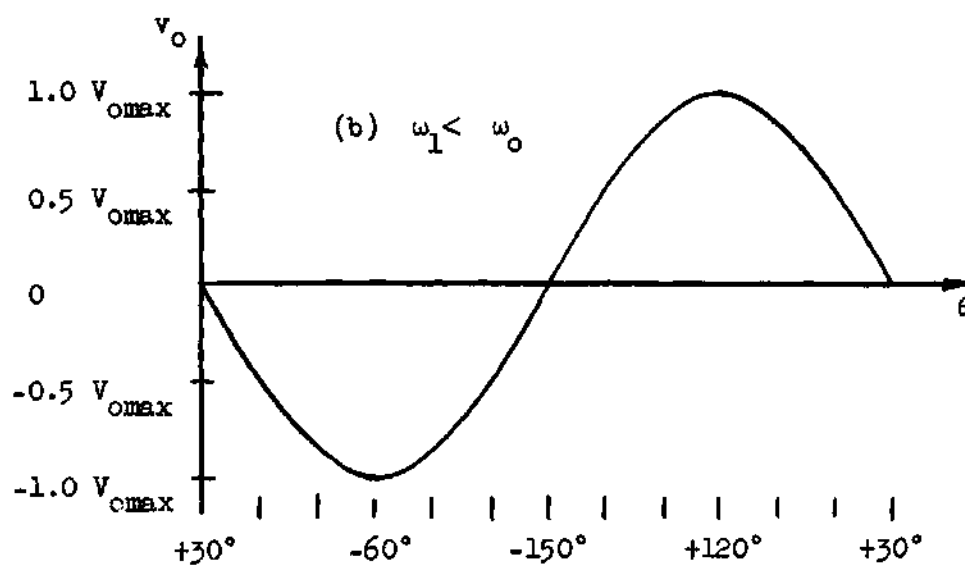
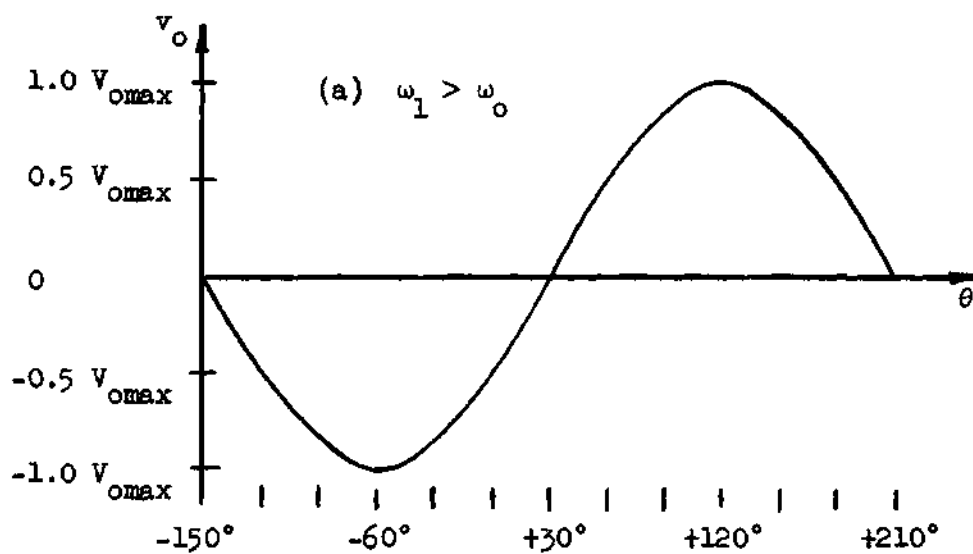


Figure 36. Calibration Curves Relating Mixer Instantaneous Output Voltage Amplitude to Instantaneous Phase Between Two Input Signals. These Curves Are the Actual Curves Used.

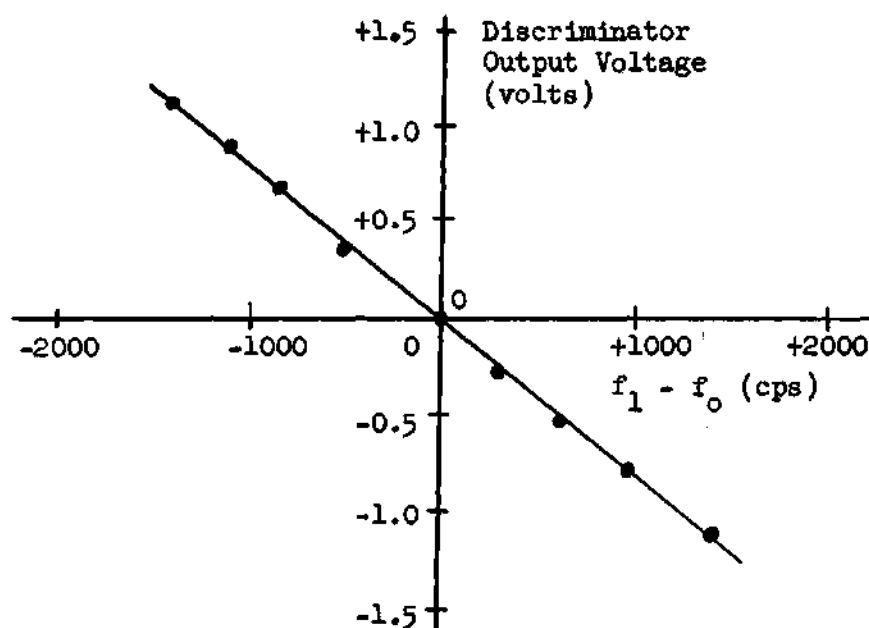
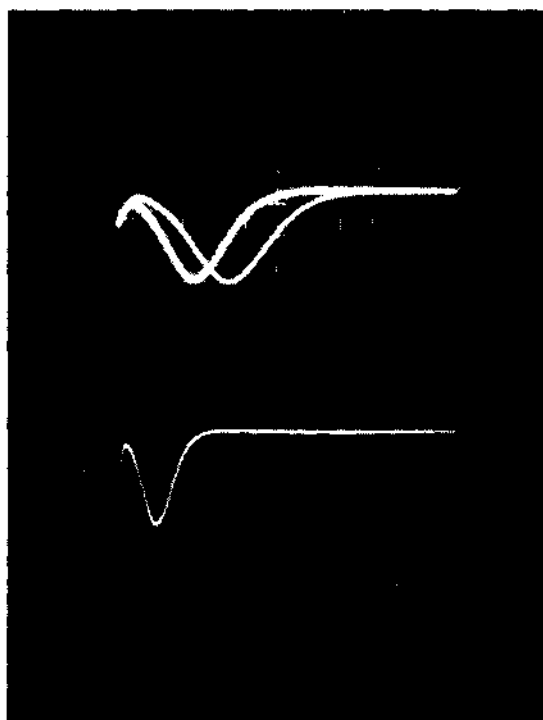


Figure 37. Linearity of Discriminator in Range of Instantaneous Observed Values.

Equipment Details

The oscillator to be synchronized is basically a tuned-plate oscillator. The oscillator circuit is shown in Figure 39. In all of the theoretical work presented in Chapter IV concerning the synchronization of the oscillator, the assumption is made that ω_c is the true half bandwidth of synchronization. This assumption is valid if the oscillator operates in a linear phase region. Any experimental departure from this condition causes non-symmetrical transients for the two cases, ω_1 greater than ω_c and ω_1 less than ω_c . Figure 39 differs slightly from an ordinary tuned-plate oscillator because of the addition of an R-C section between the secondary coil and the coupling capacitor. This network, with experimentally adjusted values, serves to adapt the oscillator for operation in the linear phase region so that ω_c is



Time Scales: 0.4 millise./cm.
0.5 millise./cm.

Time Scale: 1.0 millise./cm.

In all Three Cases

$$\omega_s = 2\pi(200)$$

$$\omega_c = 2\pi(400)$$

$$\theta_f = 30^\circ$$

$$\theta_o = -200^\circ$$

Amplitude Scale: 200 cps/cm.

Figure 38. Experimentally Observed Frequency Transient.

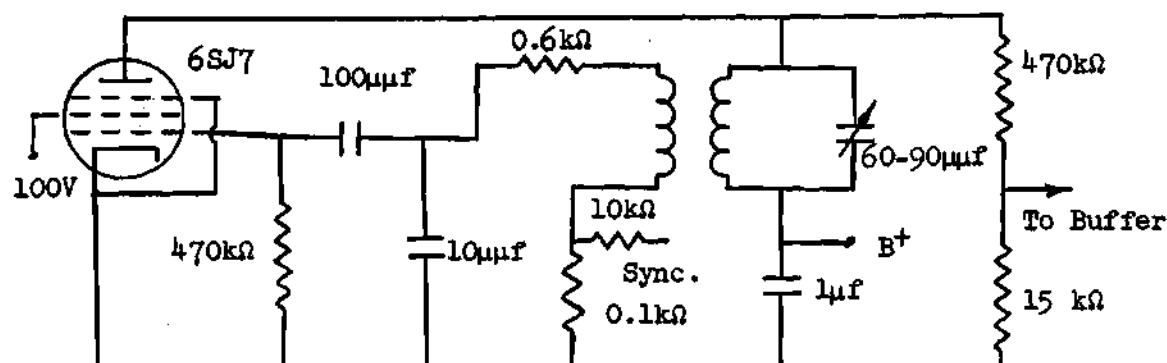
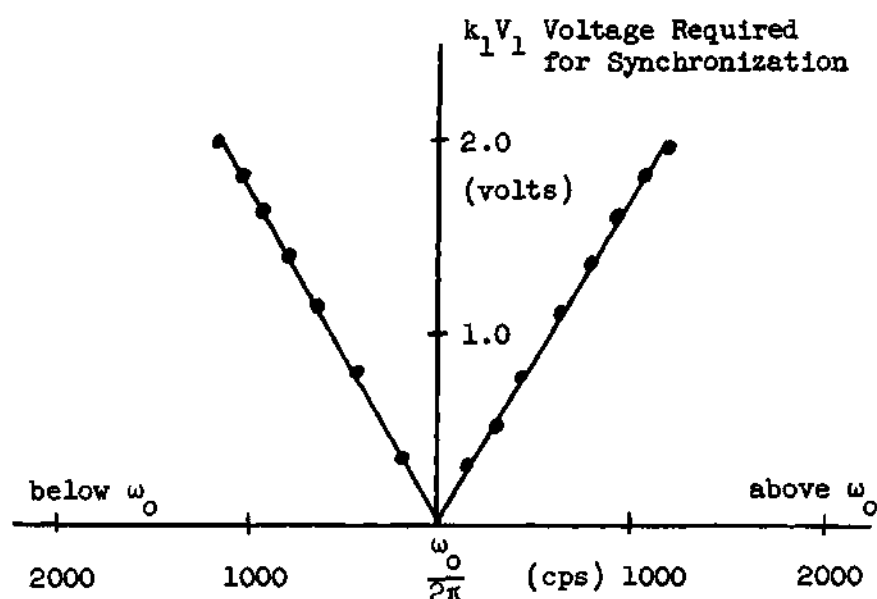


Figure 39. Test Oscillator.

established at the center of the synchronization band of the oscillator.

Figure 40 illustrates the symmetry achieved.

Figure 40. Symmetry of Synchronization Bandwidth about ω_0 .

The buffer amplifier following the oscillator under test is an ordinary R-C amplifier using one half of a 12AU7 vacuum tube.

The synchronizing source is a Measurements Corporation Standard Signal Generator, Model 65-B.

Mixer number one is a typical vacuum tube mixer using a 6SA7 pentagrid tube. The mixer output is delivered through a low-pass filter to the counter.

The counter is a six stage binary type counter using type 5963 vacuum tubes in the multivibrator units.

The monostable multivibrator circuit is shown in Figure 41; there are no special features of this circuit. It provides a variable "on time," roughly the order of ten times the transient duration, for the control of the gate circuit.

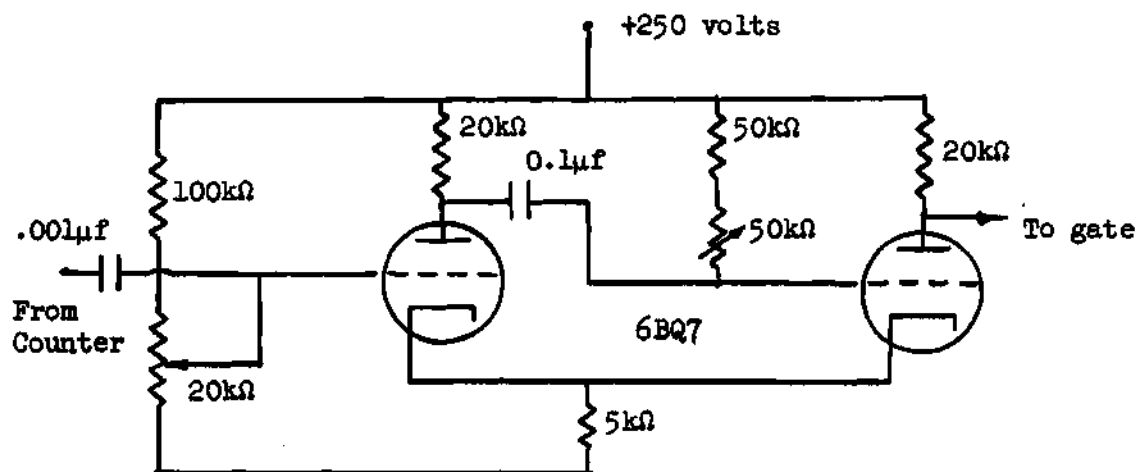


Figure 41. Monostable Multivibrator.

The gate circuit is shown in Figure 42. The large time constants in the different parts of the circuit are necessary to make sure the "on time" is sufficiently long for the transient to be seen. The diode is added to improve the rise time response of the gate so that the synchronizing signal can be switched in with a minimum delay in build-up of output signal amplitude. Actual rise time is less than five microseconds.

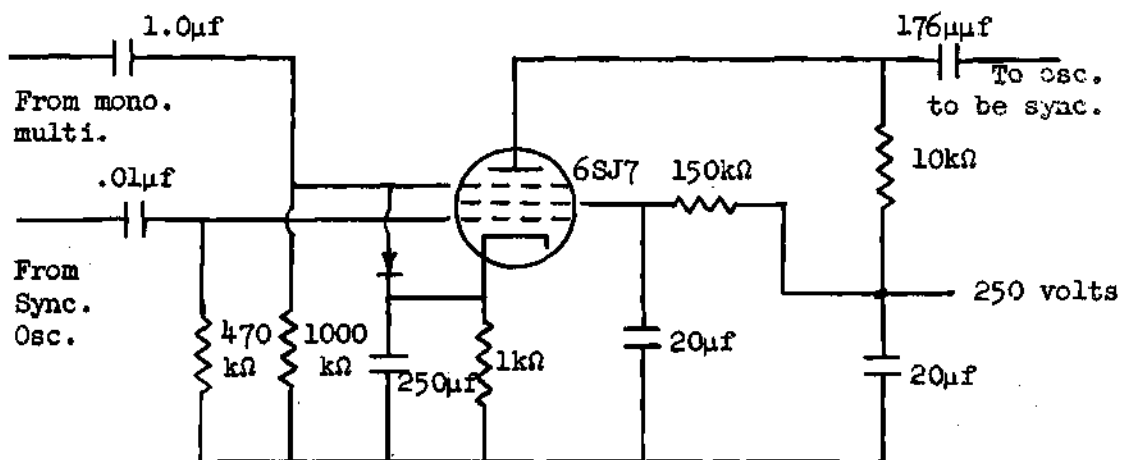


Figure 42. Gate Circuit.

The phase shifter, shown in Figure 43, is an R-C bridge followed by a difference amplifier. The amplifier is necessary to preserve the proper signal ground. The voltage divider from which the (b) output is taken is necessary to equalize the gains of the two halves of the amplifier.

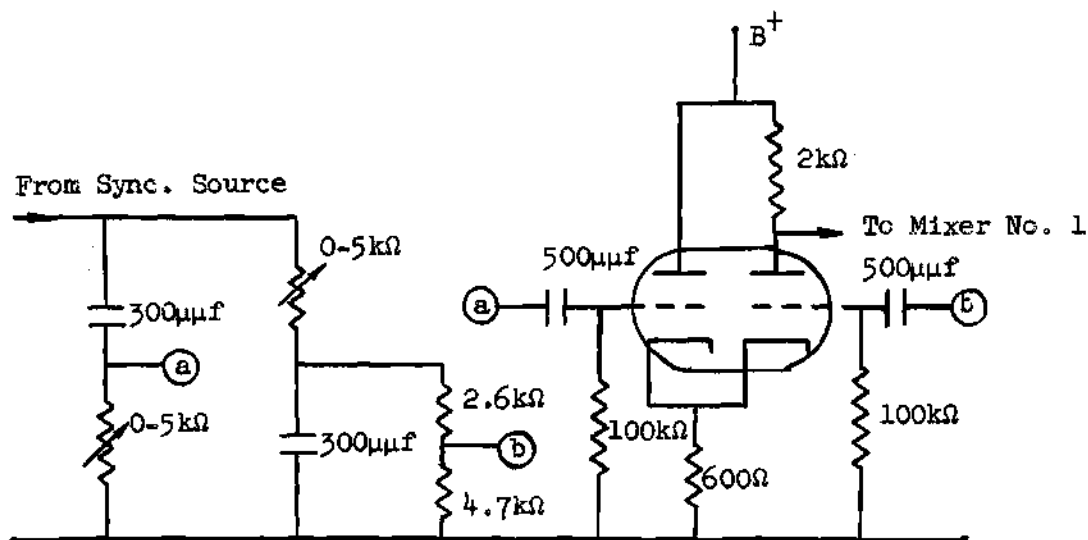


Figure 43. Phase Shifter and Amplifier.

The one-megacycle crystal oscillator and mixer are an integral unit obtained by modifying a U. S. Army Signal Corps BC 221-C Frequency Meter. The local oscillator is disabled and only the crystal oscillator is running. This crystal oscillator is used with the internal mixer and a signal of unknown frequency to produce an audio output difference-frequency. The output filter is broadened in response bandwidth to accommodate expected audio frequencies, up to 20 kc.

As the results of Chapter IV show, the maximum duration of a synchronization frequency transient is of the order of $t = 10/\omega_c$ seconds. The transient response of the discriminator, used to measure the synchronization transient, must be fast enough not to interfere with the measurement. In the experiment most of the measurements were made with $\omega_c = 2\pi(400)$ rps which gives a maximum synchronization transient duration of 4.0 milliseconds. The discriminator used in the experiment has a rise time of less than 0.2 milliseconds. (This includes the effect of the output filter.) This rise time is short enough that only a few of the measurements were appreciably affected by it.

This discriminator, shown in Figure 44, contains hand wound coils.

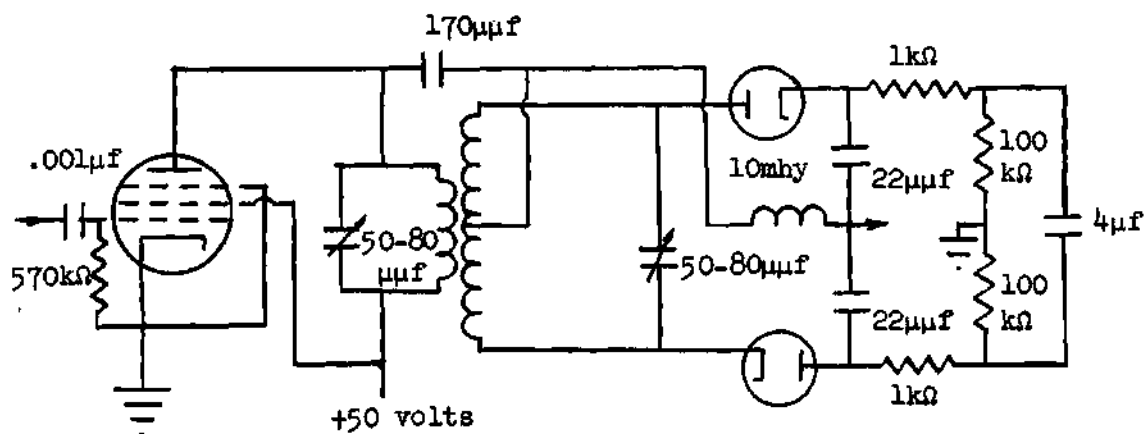


Figure 44. Limiter and Discriminator.

These coils have unloaded Q's approximately equal to 50 and their loaded Q's are approximately equal to 25. An estimate of the linear bandwidth of the discriminator is given by $f_o/2Q$ as 20 kc. Figure 45 shows the actual amplitude versus frequency curve for the unit. The smaller more linear portion in which operation actually occurs is shown in Figure 37.

The output of the discriminator is fed through a low-pass filter to eliminate as much high frequency interference as possible. The filter output is observed on the screen of a Tektronix 514AD cathode ray oscilloscope.

Mixer number two is a typical vacuum tube mixer using a 6L7 pentagrid vacuum tube. The mixer has a low-pass filter in its output circuit. The filter output is observed on a dual-trace Hewlett-Packard Model 122A cathode ray oscilloscope.

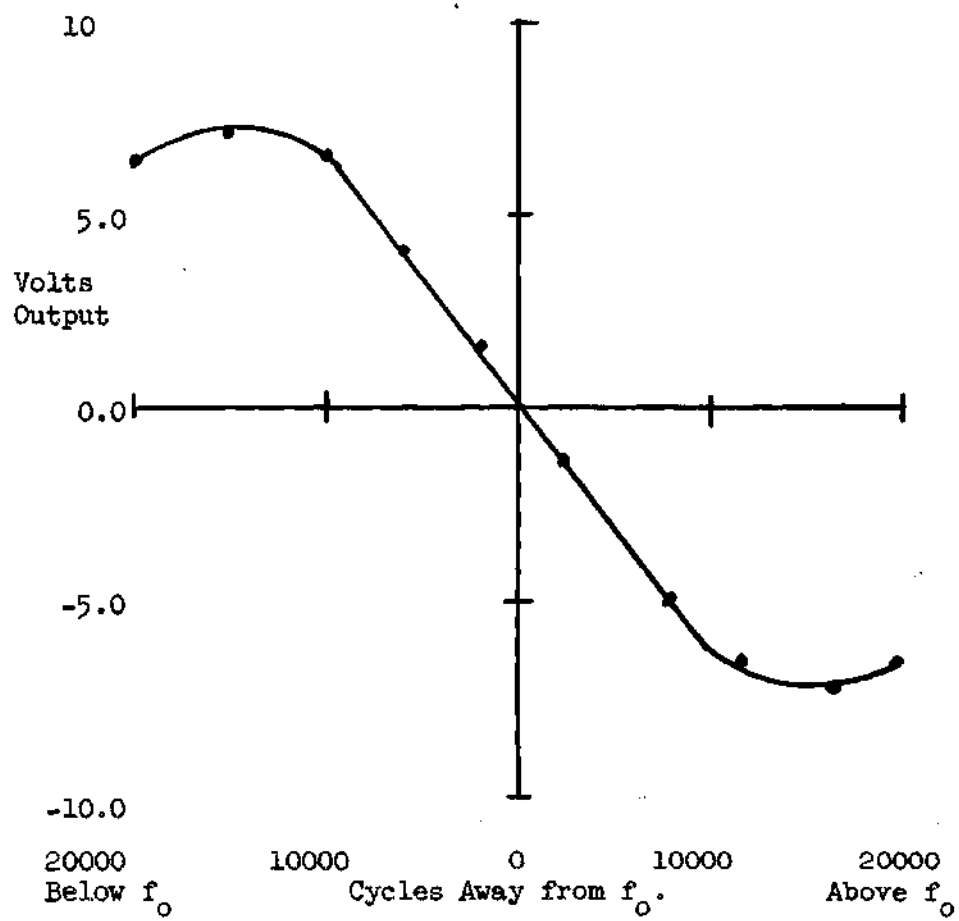


Figure 45. Discriminator Characteristic

CHAPTER VI

APPLICATIONS

Interrupted Synchronizing Signals

Fraser (8) analyzed a synchronization problem involving the use of a gated synchronizing signal of the form of Figure 46. The synchronizing signal of frequency ω_1 is applied to the oscillator to be synchronized for KT seconds out of the period T seconds of the rectangular modulating (gating) signal. Synchronization is a function of ω_1 , the

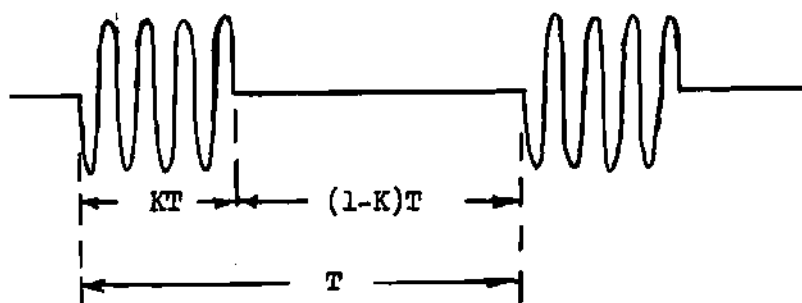


Figure 46. Synchronizing Signal Used by Fraser.

frequency of the synchronizing source, T , the period of the gating function, and K , the duty cycle of the gating source. Synchronization is attained when the average frequency of the oscillator to be synchronized is equal to the frequency of the synchronizing signal. Fraser's analysis is complete but an alternate approach to his problem using the method developed in Chapter IV is given below.

If synchronization is to be maintained by a synchronizing signal

of the form of Figure 46, the change of phase angle θ during the "on time," KT , must be balanced by a negative change of the same amount during the "off time," $(1 - K)T$. This can be explained in terms of Figure 47 where V_1 is the phasor representing the synchronizing signal

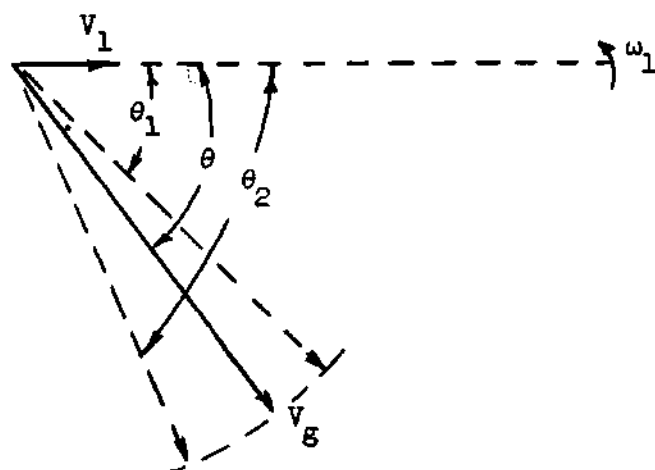


Figure 47. Illustration of Change of Phase Angle During One Period of Gate Signal.

voltage of angular velocity, ω_1 , and V_g is the phasor representing the oscillator active element voltage of angular velocity, ω . During the "on time," θ changes from θ_2 to θ_1 nonlinearly according to equation (60) in Chapter IV and during the "off time," θ changes from θ_1 to θ_2 linearly according to the relationship

$$\theta = \omega_s t = (\omega_1 - \omega_o)t. \quad (100)$$

Since V_g was taken as the reference in the development of Chapter IV, θ_1 and θ_2 must be taken as positive quantities in Figure 47.

Note that two solution curves are given by equation (60). One curve approaches θ_f from above for $\theta_f < \theta_o < \pi - \theta_f$ and the other curve approaches θ_f from below for $-\pi - \theta_f < \theta_o < \theta_f$. If synchronization is

effected the θ variation is given by the upper curve. This is evident because the $-d\theta/dt$ curve, which is the companion to the lower θ curve, gives a negative frequency deviation. This frequency deviation combined with ω_1 makes $\omega < \omega_1$ during the "on time." Since $\omega_0 < \omega_1$, ω is less than ω_1 during the "off time," also. The average frequency, therefore, cannot equal ω_1 for θ variation along the lower curve.

A graphical procedure based on the discussion in the preceding paragraph and the results of Chapter IV solves a particular example of Fraser's problem. In a later development a general graphical procedure will be outlined for the solution of the general case of Fraser's problem. Consider for the example that $\omega_c = 2\pi(400)$, $\omega_s = 2\pi(80)$, $K = 0.5$, and $T = 1.59$ milliseconds. These values establish $\sin \theta_f = 0.2$, $\theta_f = 11.55^\circ$, $KT = 0.795$ milliseconds, and $(1 - KT) = 0.795$ milliseconds. The synchronizing signal is on for 0.795 milliseconds and off for 0.795 milliseconds. During the "on time" the oscillator phase angle, θ , follows the nonlinear θ curve of Figure 12 corresponding to $\theta_f = 11.55^\circ$. During the "off time" θ changes linearly according to equation (100). In this example the slope given by equation (100) is $6.28 (0.08) 57.3 = 28.8$ degrees per millisecond or for 0.795 milliseconds the change in θ is 23° . The graphical solution is illustrated in Figure 48. The nonlinear θ curve is repeated after a time corresponding to T so the complete cycle can be constructed with the linear variation linking the nonlinear variations. The cycle is constructed by sliding the linear portion of slope 28.8 degrees per millisecond over the two nonlinear curves until a fit is achieved with the change in θ of $+23^\circ$ in 0.795 milliseconds of "on time" offset by a change in θ of -23° in 0.795 milliseconds of "off time."

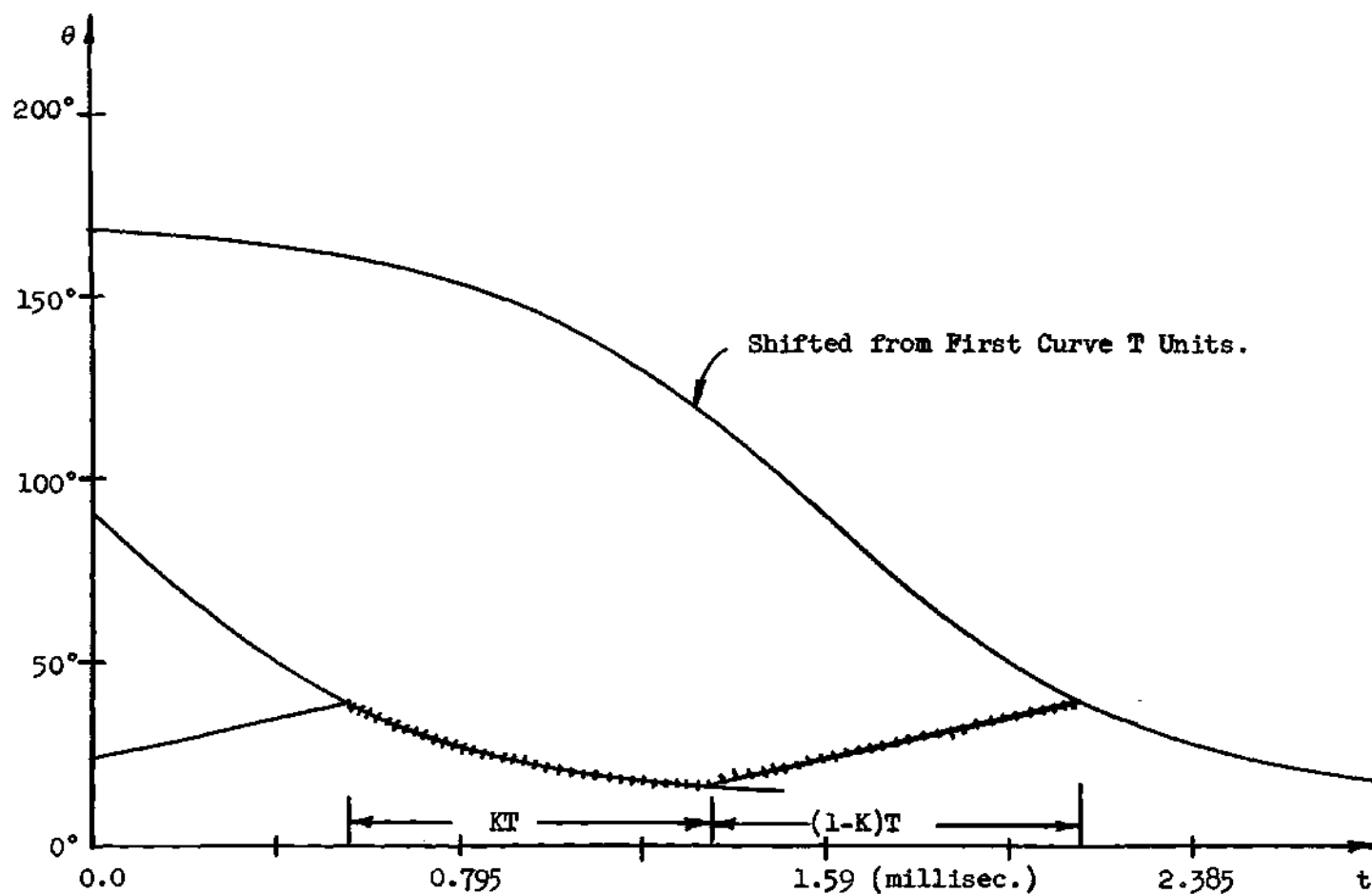


Figure 48. Change in Oscillator Phase Angle During One Period of Gating Function When Oscillator is Synchronized by Interrupted Synchronizing Signal for $\omega_s = 2\pi(80)$, $\omega_c = 2\pi(400)$, $T = 1.59$, $K = 0.5$, and $\theta_f = 11.53^\circ$.

Although the construction just discussed gives a true time representation of the θ cycle, it is awkward to develop and use. An alternate construction method is much easier to use. If synchronization is achieved, θ forms a closed cycle in the sense that a change of θ in one direction during the "off time" is cancelled by a change of θ in the other direction during the "on time." This closed cycle is easily constructed if the linear change of θ is plotted in the reverse direction along the time axis during the "off time." Although the linear θ curve must still be moved across the nonlinear θ curve to establish a fit, this construction makes matching conditions easy to read. Figure 49 shows the same example with the alternate construction.

As a second example consider the case where $\omega_c = 2\pi(400)$ and $\omega_s = 2\pi(200)$ which establishes $\sin \theta_p = 0.5$ and $\theta_p = 30^\circ$. Let the duty cycle be 0.75 which means the synchronizing signal is on three times as long as it is off. Finally, let the frequency of the gating signal be 675 cps with a corresponding period of 1.48 milliseconds. The "on time" is, therefore, 1.11 milliseconds and the "off time" is 0.37 milliseconds. Figure 50 gives the proper θ curve for use with this example. The value of $\omega_s = 2\pi(0.200) 57.3 = 72$ degrees per millisecond establishes the slope of the change of θ during the "off time" but a modification of the time scale must be used to take the duty cycle into account. Since the nonlinear θ curve applies for $0.75T$ and the linear portion applies for $0.25T$, the time scale in Figure 50 used with the nonlinear curve must be divided by three for use with the linear 72 degrees per millisecond curve. This allows a closed loop to describe the full cycle of θ . The cycle is located by sliding the linear curve over the nonlinear curve until the time, measured on the original time scale, between the points of intersection

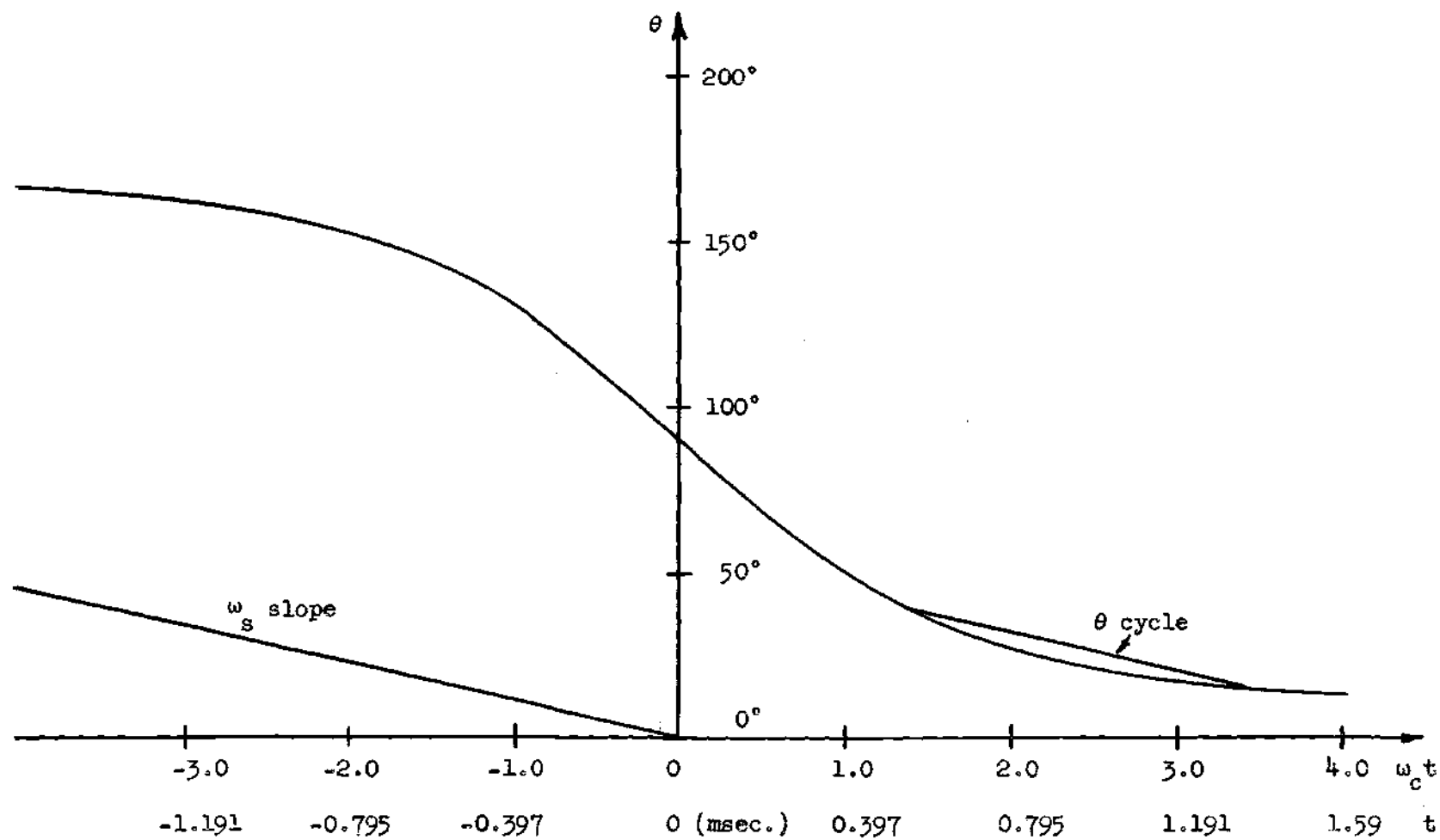


Figure 49. Alternate Solution to First Example of Synchronization by Interrupted Signal.

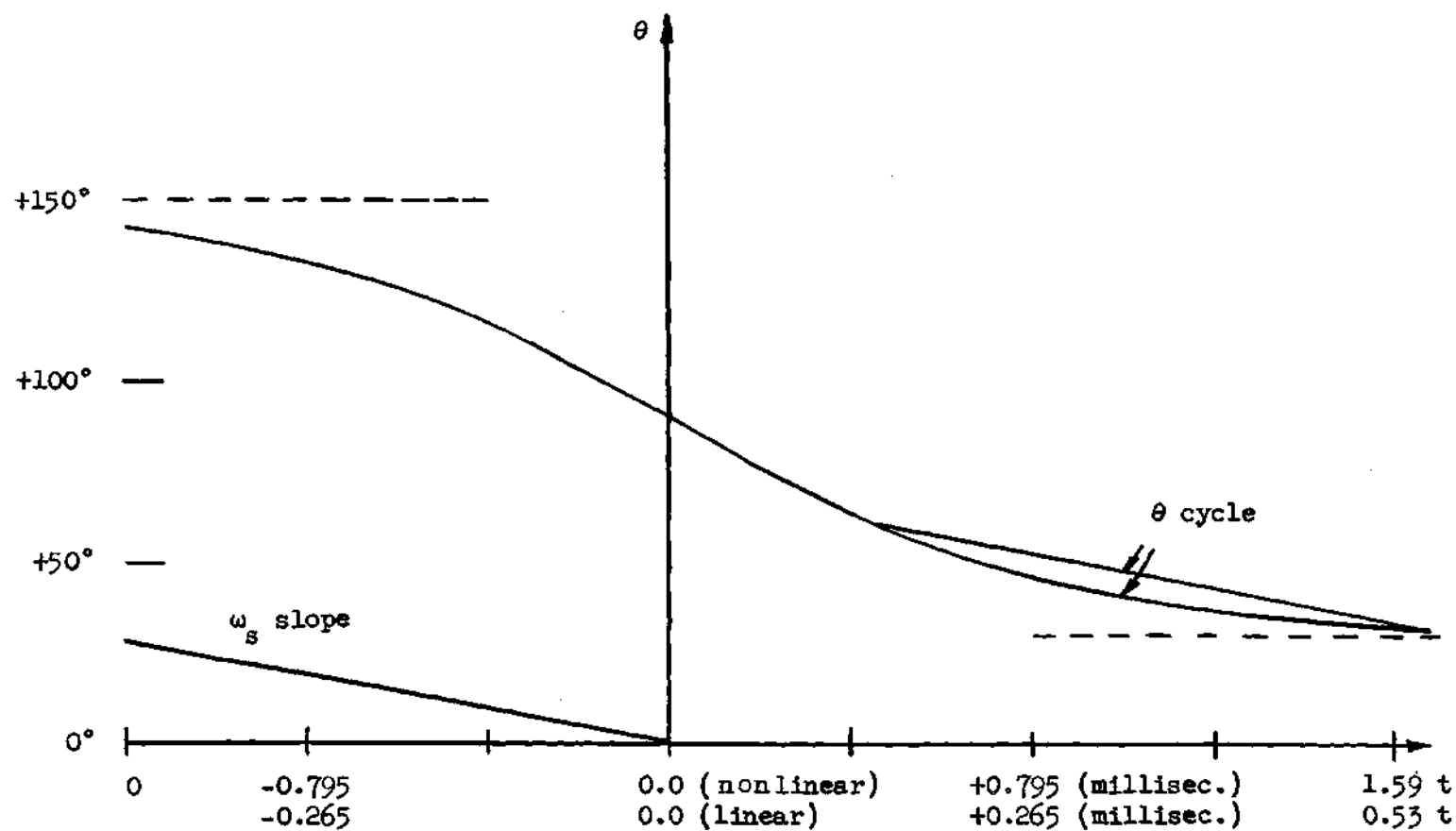


Figure 50. Synchronization by an Interrupted Synchronizing Signal for $\omega_s = 2\pi(200)$, $\omega_c = 2\pi(400)$, $\omega_m = 2\pi(675)$, $K = 0.75$, and $\theta_f = 30^\circ$.

is 1.11 milliseconds. The resultant cycle is labeled on Figure 50.

As a matter of interest, Figure 51 shows one cycle of the θ variation for example two as it actually occurs in time. Underneath the θ curve an instantaneous frequency curve shows the behavior of the oscillator frequency. Note that the average frequency, as predicted by Fraser, is truly f_1 . The nonlinear portion of the instantaneous frequency curve is a result of scaling the proper curve of Figure 29 in Chapter IV.

A general procedure is now developed to allow the solution of many problems associated with Fraser's study. Some results obtained from the graphical procedure are compared with Fraser's theoretical and measured results.

Figure 52 gives two typical curves from the results of Chapter IV. One curve shows instantaneous phase angle as a function of time and the other curve shows instantaneous frequency deviation from ω_1 as a function of time. Only one of the possible θ curves is shown because a change of θ beyond the $\pi - \theta_f$ value cannot be recovered during the "on time" of the synchronizing signal. The proof of this statement lies in the fact that instantaneous frequencies associated with the omitted curve are less than ω_1 and, since ω_0 is less than ω_1 , the average frequency during a cycle consisting of the omitted curve and the linear curve must be less than ω_1 . The given curve, therefore, shows all possible "on time" values of θ if synchronization is effected. During the "off time" the angle θ changes linearly according to a slope $d\theta/dt = +\omega_s$. A complete cycle of θ follows the θ curve toward θ_f until the synchronizing signal is removed at $\theta = \theta_1$ whereupon θ increases linearly to $\theta = \theta_2$.

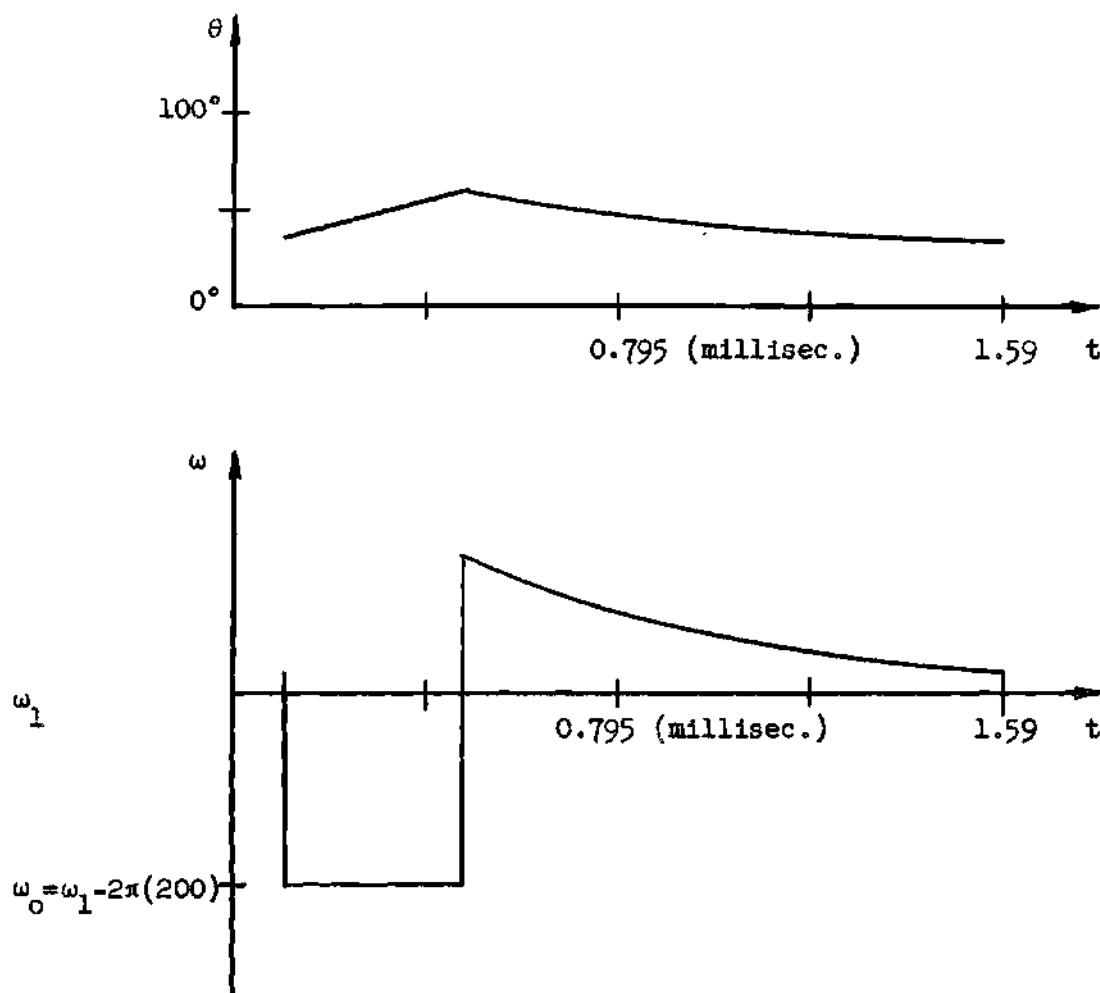


Figure 51. Instantaneous Oscillator Phase Angle and Frequency for $\omega_s = 2\pi(200)$, $\omega_c = 2\pi(400)$, $\theta_f = 30^\circ$, $\omega_m = 2\pi(675)$, and $K = 0.75$.

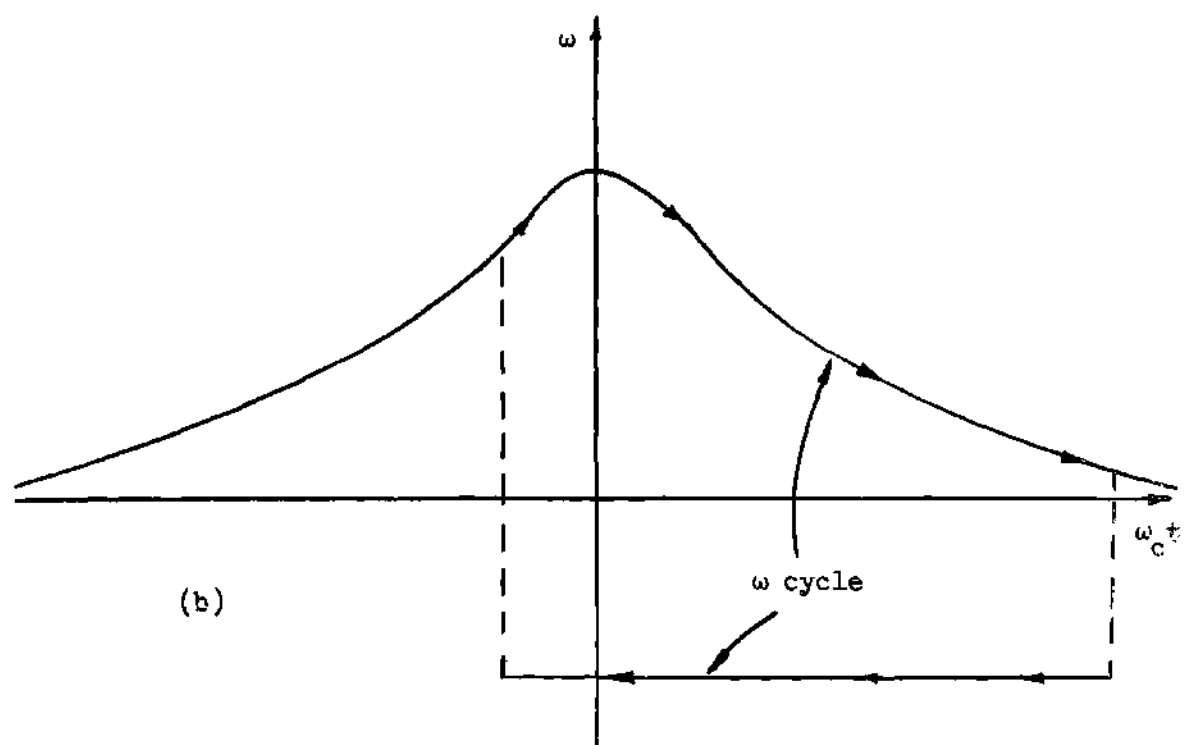
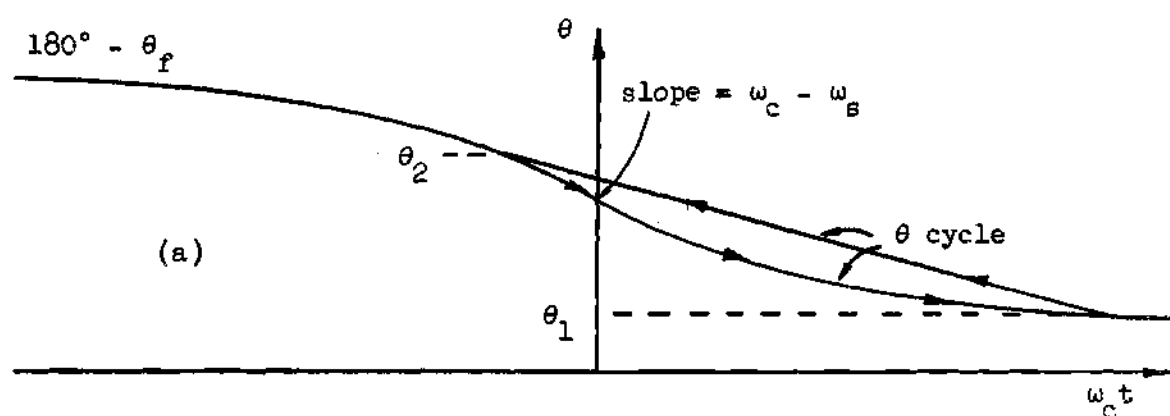


Figure 52. Synchronization by a Synchronizing Signal Interrupted by a Rectangular Gating Function.

Note that the abscissa is labeled $\omega_c t$. The actual time scale for the nonlinear θ curve is obtained by dividing the $\omega_c t$ scale by ω_c . The time scale of the linear θ curve is modified, to account for the duty cycle of the gate signal, by dividing the $\omega_c t$ scale by $K\omega_c/(1-K)$. The ω_s slope of the linear portion is plotted with respect to this modified scale. Refer to Figure 47 for the notation and to Figure 52(a) for a complete typical θ cycle.

A complete frequency cycle is shown in Figure 52(b). During the "on time," KT seconds, the nonlinear curve applies. The abscissa time scale for this portion of the cycle is obtained by dividing the $\omega_c t$ scale by ω_c . During the "off time," $T(1-K)$ seconds, the oscillator is free-running at ω_0 radians per second. The time scale for this portion of the cycle is obtained by dividing the $\omega_c t$ scale by $\omega_c K/(1-K)$. The frequency cycle in Figure 52(b) is drawn for $K = 0.5$ to show that the average frequency during the cycle is equal to ω_1 , the synchronizing frequency.

The nonlinear θ curve of Figure 52(a) has a maximum slope, $d\theta/dt_{\max}$, of $\omega_c - \omega_s$ radians per second. Inspection of the Figure shows that the straight line portion of the cycle must have a slope equal to or less than this maximum slope if synchronization is to be effected. The straight line has an effective slope, because of the modified abscissa scale, of $(1-K)\omega_s/K = \frac{(1-K)}{K} \omega_c \sin \theta_f$. Equating the equivalent slope of the straight line to the maximum slope of the nonlinear portion determines the limiting value of the duty cycle.

$$\frac{1-K}{K} \omega_c \sin \theta_f = \omega_c - \omega_s = \omega_c (1 - \sin \theta_f) \quad (101)$$

or

$$(1 - K) \omega_c \sin \theta_f = \omega_c K(1 - \sin \theta_f) . \quad (102)$$

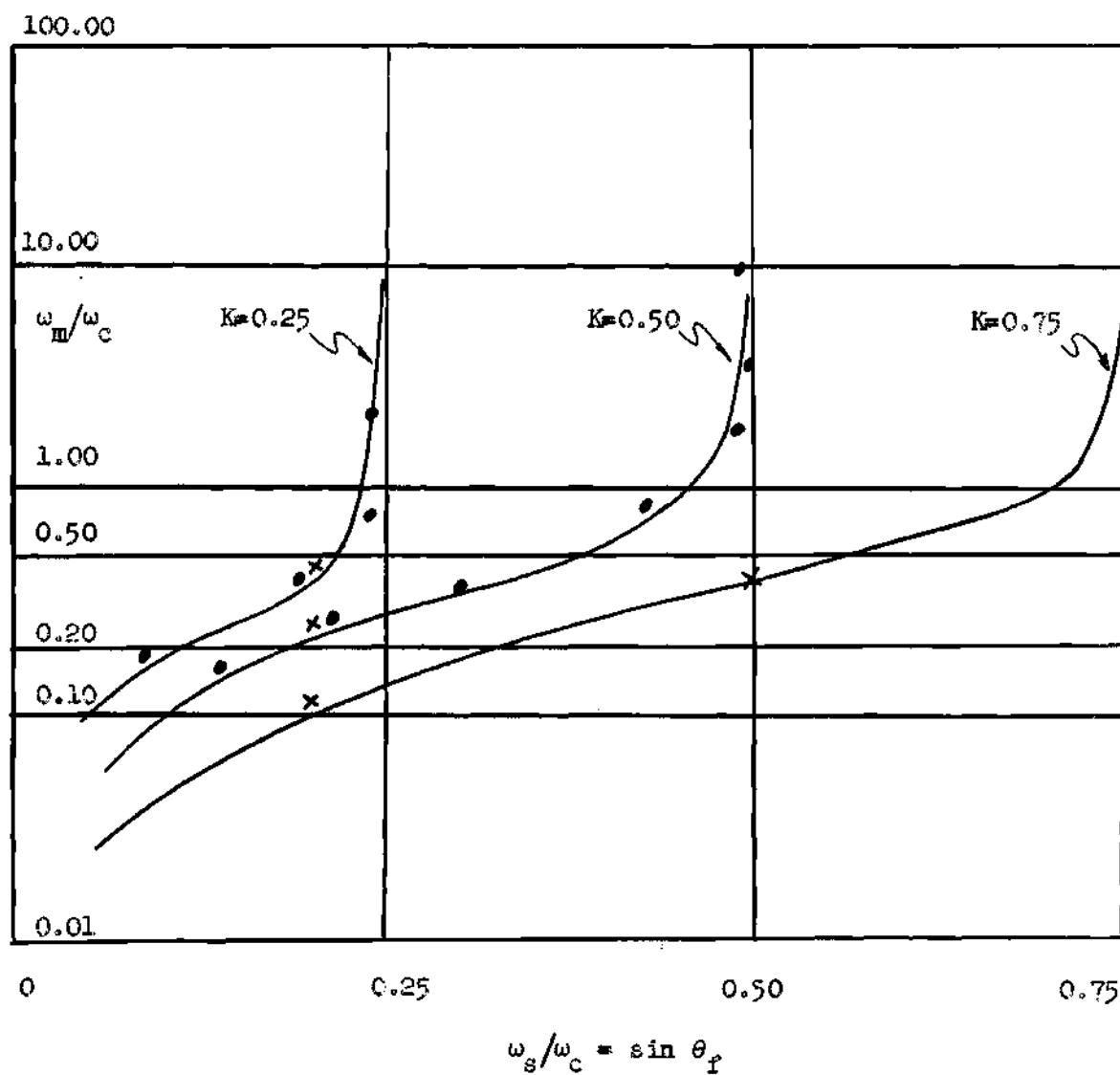
The solution of equation (102) determines the limiting value of K to be

$$K_{\text{limiting}} = \sin \theta_f . \quad (103)$$

This conclusion verifies Fraser's calculated and experimental results shown in graphical form in Figure 53.

These graphical procedures are useful in still another area of Fraser's study. Assume that a duty cycle has been established by choice. If the period of the gating function is too long, the change in θ during the "off time" is too much to be recovered during the "on time." The question of a minimum gate function frequency thus arises. The procedure for arriving at this value follows.

In a given case ω_s and ω_c are known quantities. This establishes $\theta_f = \sin^{-1} \omega_s / \omega_c$ and $\tan \theta_f / 2 = k$ which determines the proper θ curve, of the form of Figure 52(a), to use from the general set. The duty cycle is also known, which establishes K . The value of K determines the equivalent slope of the straight line portion of the θ cycle. The minimum value of the gate function frequency is obtained by moving the straight line until it becomes tangent to the nonlinear θ curve. With the line in this position, KT is read as the time between the tangent point of the two curves and the other intersection point of the two curves. Figure 54 shows a typical construction for obtaining the minimum frequency of the gating function. KT divided by K , of course, gives



Curves are theoretical - Fraser

Dots are experimental - Fraser

x's are graphical - Alternate Method

Figure 53. Modulation Frequencies Required for Synchronization.

the period of the gating function. Several limiting values of gating function frequency are calculated from the curves of Figures 49 and 50. These values are placed in Figure 53 on a family of curves calculated and verified experimentally by Fraser. Note that the graphically calculated values agree more nearly with Fraser's measured values than they agree with his theoretical values. The agreement is good, however, in both cases.

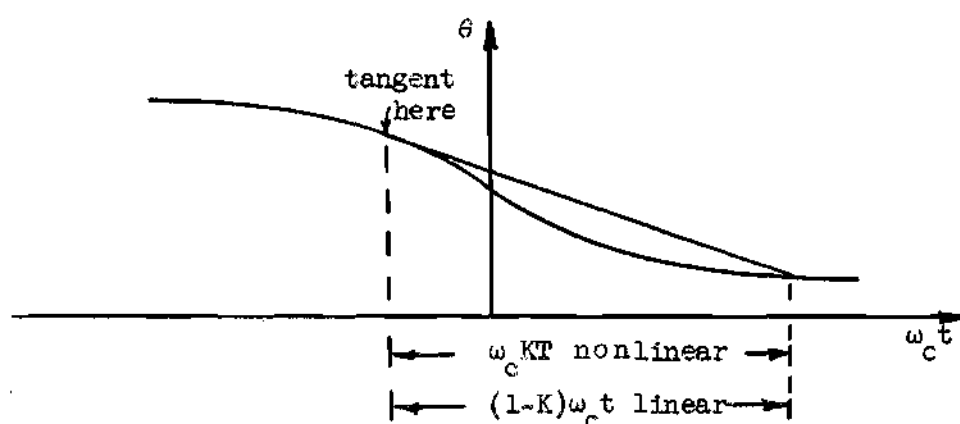


Figure 54. Determination of Minimum Gate Function Frequency.

Synchronization by Sidebands

Fraser discovered that synchronization to an average frequency, ω_1 , could be effected by a synchronizing signal of the form of Figure 46. He also discovered that synchronization by the same signal form to an average frequency, $\omega_1 \pm n\omega_m$, is possible. The quantity $n\omega_m$ is an integer times the frequency of the gating function and the frequencies $\omega_1 \pm n\omega_m$ are sideband frequencies. A general treatment of this subject is possible using the methods of the present development.

For example, let $\omega_c = 2\pi(400)$, $\omega_s = 2\pi(200)$, $\omega_m = 2\pi(263)$ and

$K = 0.417$. These values establish $\sin \theta_f = 0.5$, $\theta_f = 30^\circ$, $T = 3.81$ msec., $KT = 1.59$ msec., and $(1 - K)T = 2.22$ msec. Figure 55 shows θ and $-d\theta/dt$ curves applicable to the example. During the "off time" θ changes linearly according to a slope ω_s which is equivalent to 72 degrees per millisecond. Since the "off time" is 2.22 msec., the change in θ is 160° . For synchronization to be effected the total θ change per T period must be zero or integral multiples of 360° . The change in θ during the "off time" is 160° which is greater than the range of the upper θ curve of Figure 55(a), therefore, the lower θ curve must be used. Zero total change of θ during the T period is impossible in this case but a change of 200° during 1.59 milliseconds is available to make the total change during T equal to 360° . The resultant θ curve is sketched in Figure 55(a). Figure 55(b) shows the behavior of the oscillator frequency for one cycle. Note that the average frequency is $\omega_1 - \omega_m$ which corresponds to synchronization by the first lower sideband.

Minimizing the Frequency Transient

An oscillator to be synchronized must have a finite synchronization bandwidth. If this oscillator is synchronized, the initial phase angle between the synchronizing voltage and the oscillator voltage determines what kind of frequency transient occurs and the synchronization bandwidth of the oscillator determines the maximum frequency deviation and the maximum time duration of the transient. It is conceivable that for some applications a frequency transient is not desirable. An outgrowth of the experimental procedure used in the verification of the results of this study can be used to inject a synchronization signal at the proper time so that only a minimum

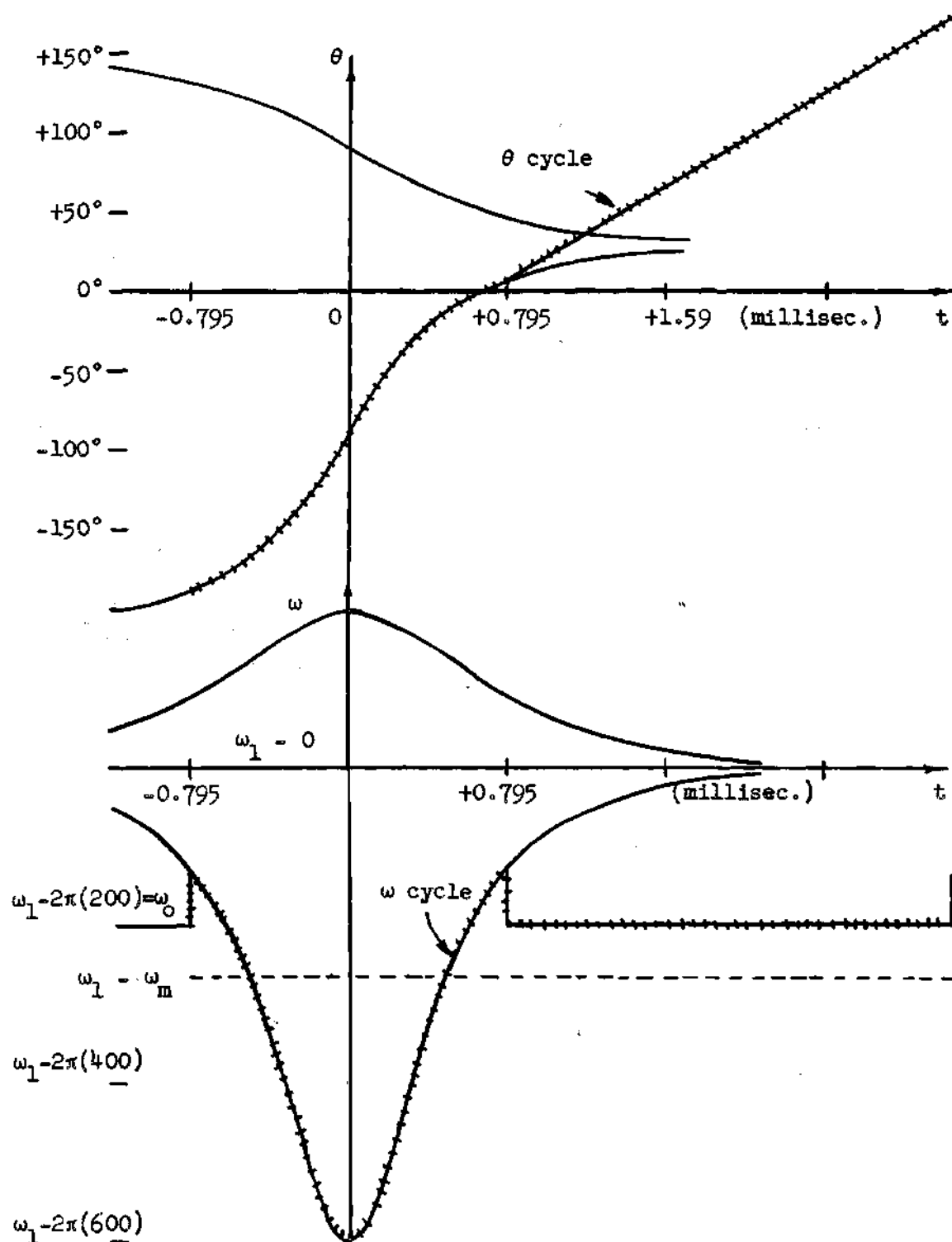


Figure 55. Synchronization by the First Lower Sideband for $\omega = 2\pi(200)$
 $\omega_c = 2\pi(400)$, $\omega_m = 2\pi(263)$, $K = 0.417$, and $\theta_f = 30^\circ$.

transient occurs. Figure 56 shows a system in block diagram form which automatically injects the synchronizing signal at the proper time to minimize the transient regardless of the values of ω_s , ω_c or θ_o .

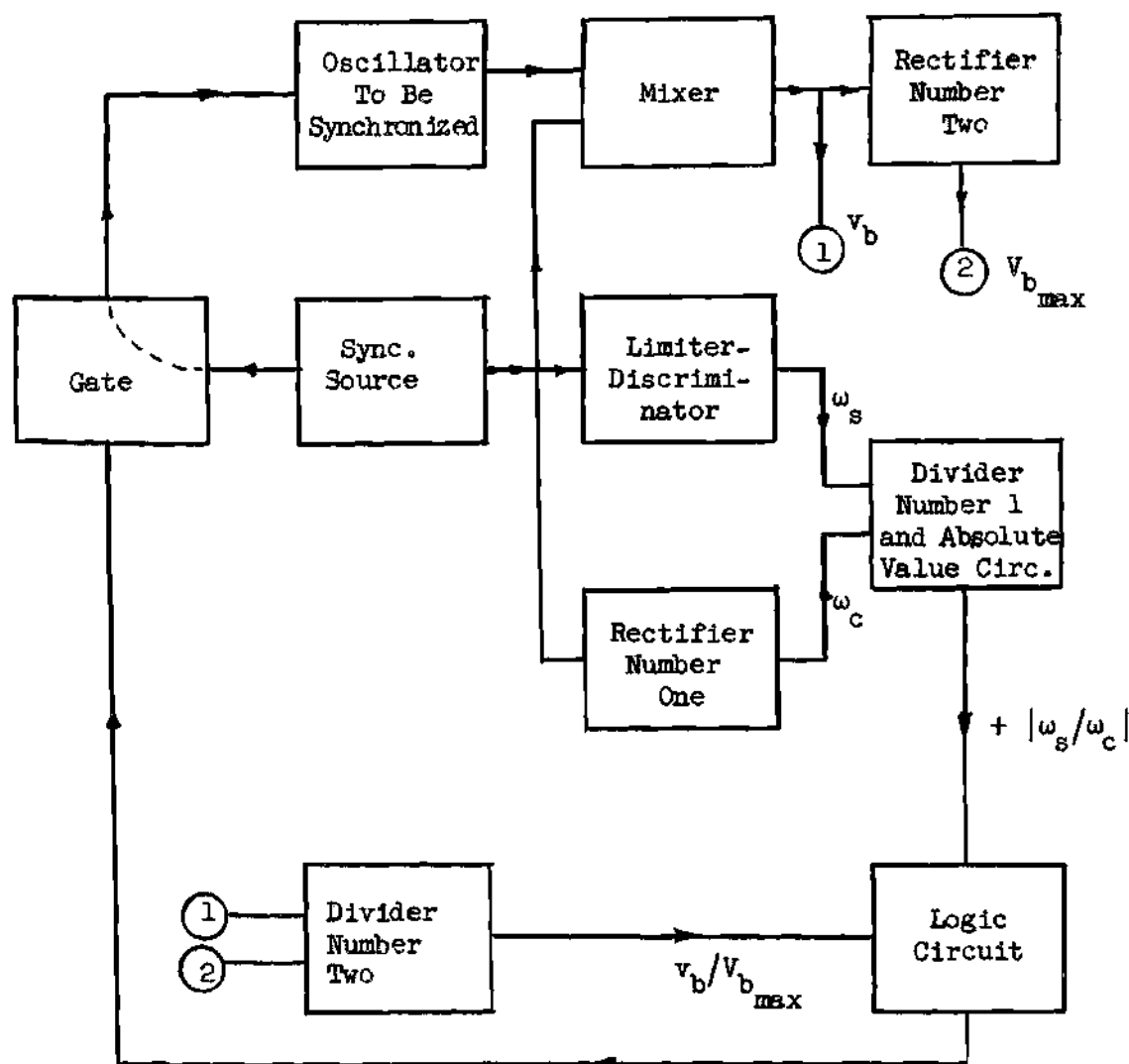


Figure 56. Block Diagram of Circuit for Minimizing Frequency Transient.

Operation of the circuit of Figure 56 proceeds in the following manner. The synchronizing source of frequency ω_1 delivers a signal to the limiter-discriminator which is tuned to the free-running frequency

of the oscillator to be synchronized. The discriminator is adjusted so that its output is zero for $\omega_1 = \omega_0$, positive for $\omega_1 > \omega_0$, and negative for $\omega_1 < \omega_0$. In effect the discriminator output is proportional to $\omega_1 - \omega_0$ which is ω_s . The amplitude of the synchronizing source voltage determines the synchronization bandwidth of the oscillator, therefore, the output of rectifier number one is a d-c output proportional to ω_c . The number one divider divides the output of the discriminator by the output of rectifier number one and the divider output is a d-c voltage proportional to $|\omega_s/\omega_c|$ which is the sine of the angle at which the synchronizing source voltage should be injected into the oscillator.

The output of the oscillator to be synchronized and the 90° shifted output of the synchronizing source are fed to the mixer whose low frequency output is at the instantaneous difference frequency $\omega_1 - \omega_0 = \omega_s$. The instantaneous amplitude of the difference frequency can be expressed in the form

$$v_b = V_{b_{\max}} \sin \omega_s t \quad (104)$$

and when

$$\omega_s t = \sin^{-1} \omega_s / \omega_c, \quad (105)$$

$$\omega_s / \omega_c = v_b / V_{b_{\max}}. \quad (106)$$

The voltage ratio of equation (106) is obtained by dividing the mixer output, which is v_b , by the output of rectifier number two. This rectifier output is proportional to $V_{b_{\max}}$. The ratio $v_b / V_{b_{\max}}$, which is the divider number two output, carries its sign.

Note that the final value of θ always lies between 0° and 90° . There are four times in the difference frequency cycle when equation (106) is satisfied in magnitude. At only one of these times does the desired θ value appear and that time corresponds to a coincident $v_b/V_{b_{\max}}$ ratio and a positive slope of the v_b curve. The logic circuit which could consist of two comparators, a differentiator, and a coincidence circuit, compares $v_b/V_{b_{\max}}$ and $|\omega_s/\omega_c|$. There is an output from the logic circuit only when the conditions, described above, are correct for the desired θ value. The output of the logic circuit actuates the gate. The equipment could be designed for repetitive use or it could be designed with a hold circuit for one time injection only.

The system of Figure 56 needs to run for a few difference cycles to make sure the reference voltages have stabilized before synchronization is effected. Since the period of the difference frequency cycle is of the same order of magnitude as the duration of the frequency transient, this system would introduce a time delay of synchronization longer than the transient duration.

It is possible that a synchronization scheme could be devised for injecting the synchronizing signal at the first time the proper phase relationship arises. Such a system would allow a minimum transient and the delay in synchronization would be of the same order of magnitude as the transient duration.

CHAPTER VII

SUMMARY AND CONCLUSIONS

A sinusoidal oscillator synchronized by a small amplitude sinusoidal signal can be analyzed for frequency transients by the semi-graphical procedure developed from Adler's equation. The procedure gives the transient frequency as a function of time and it considers the effect of the phase angle existing between the synchronizing voltage and the oscillator voltage at the time the synchronizing voltage is injected into the oscillator. The family of curves necessary for such an analysis is given in Figure 57.

In a given case, the free-running oscillator frequency, ω_0 ; the synchronizing signal frequency, ω_1 ; the half synchronization bandwidth, ω_c ; and the initial phase angle, θ_0 , existing between the oscillator voltage and the signal voltage, are known quantities. The difference frequency, $\omega_1 - \omega_0$, gives ω_s which establishes $\theta_f = \sin^{-1} \omega_s / \omega_c$. The value of this angle fixes the choice of the curves to be used in Figure 57. The initial phase angle, θ_0 , determines the point of entry into the θ curve. The instantaneous variation of θ is given by this curve as θ progresses from the original $\theta = \theta_0$ value to the final $\theta = \theta_f$ value. The instantaneous variation of frequency is obtained by using the $\omega_c t$ value read of the θ curve at $\theta = \theta_0$ to establish the reference value of $\omega_c t$ on the $-d\theta/dt$ curve. The complete frequency picture is obtained by following ω_0 , located $\omega_s = \omega_c \sin \theta_f$ units below the $\omega_c t$ axis, to the reference $\omega_c t$ value at which point the instantaneous frequency of the oscillator

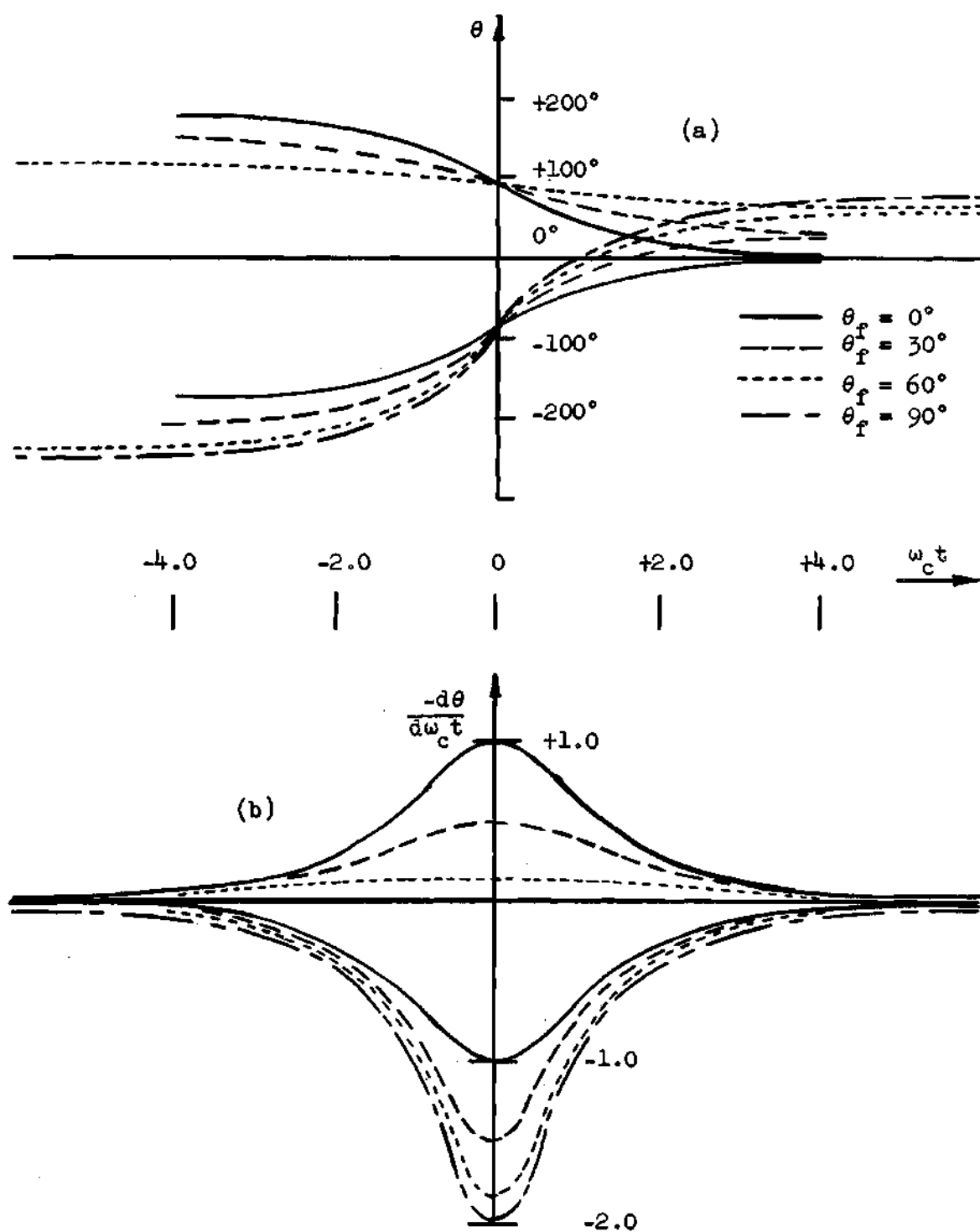


Figure 57. (a) Instantaneous Phase Angle as a Function of Time.
 (b) Instantaneous Frequency as a Function of Time.

changes step-wise to the $-d\theta/dt$ curve. The instantaneous value of the frequency is given by this curve as $\omega_c t$ goes to infinity. The final value of the oscillator frequency is ω_1 . Note that dividing the abscissa values by ω_c gives the time scale and multiplying the ordinate values by ω_c gives the frequency scale.

The conclusions to be drawn from the present study may be summarized as follows:

1. The possible frequency transients that can occur in a given oscillator being synchronized by a given source are determined by the two quantities ω_c and ω_s and the actual frequency transient that does occur is determined by the initial phase angle, θ_0 .

2. No matter what the value of ω_0 is, the maximum deviation of instantaneous frequency from ω_0 in either direction is equal to the value of ω_c .

3. The maximum theoretical duration of the frequency transient is infinite; practically, however, when ω approaches within a certain nearness to ω_1 , synchronization may be said to have occurred; if the nearness is defined by a frequency band $0.1 \omega_c$ wide on either side of ω_1 , the maximum transient duration is given by the approximate relationship $\omega_c t_{\max} = 10$.

4. If a frequency transient during synchronization is to be minimized, the synchronizing signal must be injected into the oscillator at such a time that the initial instantaneous phase angle, θ_0 , is equal to the final value of θ , θ_f , to be reached.

5. Oscillators with a large synchronization bandwidth, $2\omega_c$, have greater frequency fluctuations during synchronization but the

duration of the transient is shorter in proportion.

6. The frequency transients are independent of the actual values of ω_0 and ω_1 ; it is the difference between the two that affects the transient.

7. The analysis developed in Chapter IV holds for $\omega_1 < \omega_0$ and the same curves can be used if they are inverted.

8. The period of the difference frequency, ω_s , is always of the same order as or greater than the maximum duration of the frequency transient.

The conclusions listed above apply to many oscillator synchronization problems but it is important to note the limitations of the analysis. The analysis applies only if the time constants of the oscillator are short compared with one period of the difference frequency, if the oscillator and synchronizing source are sinusoidal, if the amplitude of the synchronizing signal is small so that amplitude modulation of the oscillator is negligible, and if the synchronization bandwidth of the oscillator is symmetrical about the free-running frequency of the oscillator.

A P P E N D I X

APPENDIX

The appendix consists of individual curves which can be used to solve frequency transient problems. These curves are of the same form as those given in Figure 57. Curves are given for $\theta_f = 0^\circ$, $\theta_f = 11.55^\circ$, $\theta_f = 30^\circ$, $\theta_f = 53.1^\circ$, $\theta_f = 60^\circ$, and $\theta_f = 90^\circ$.

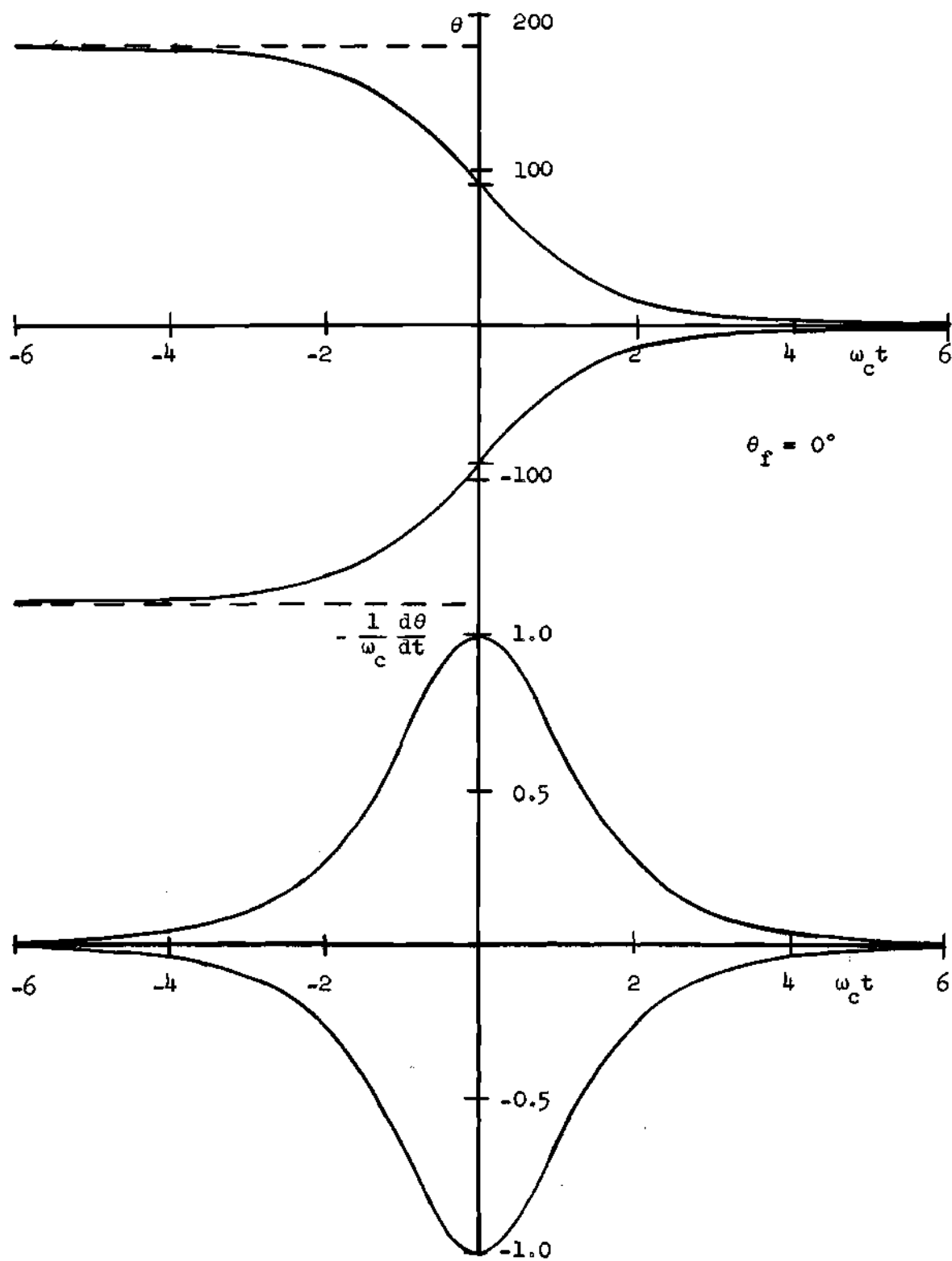


Figure 58. Instantaneous Phase Angle and Instantaneous Frequency Curves for $\theta_f = 0^\circ$.

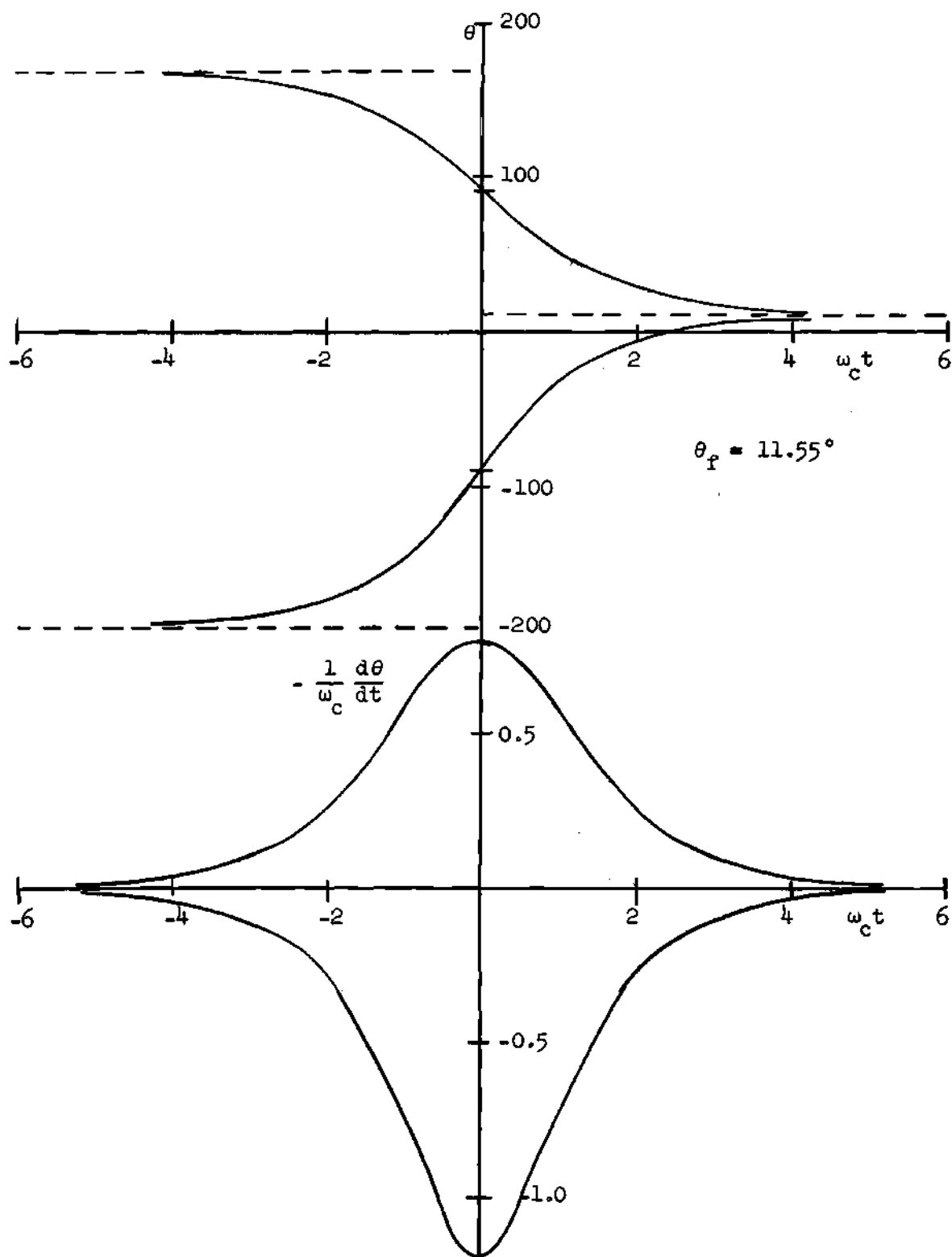


Figure 59. Instantaneous Phase Angle and Instantaneous Frequency Curves For $\theta_f = 11.55^\circ$.

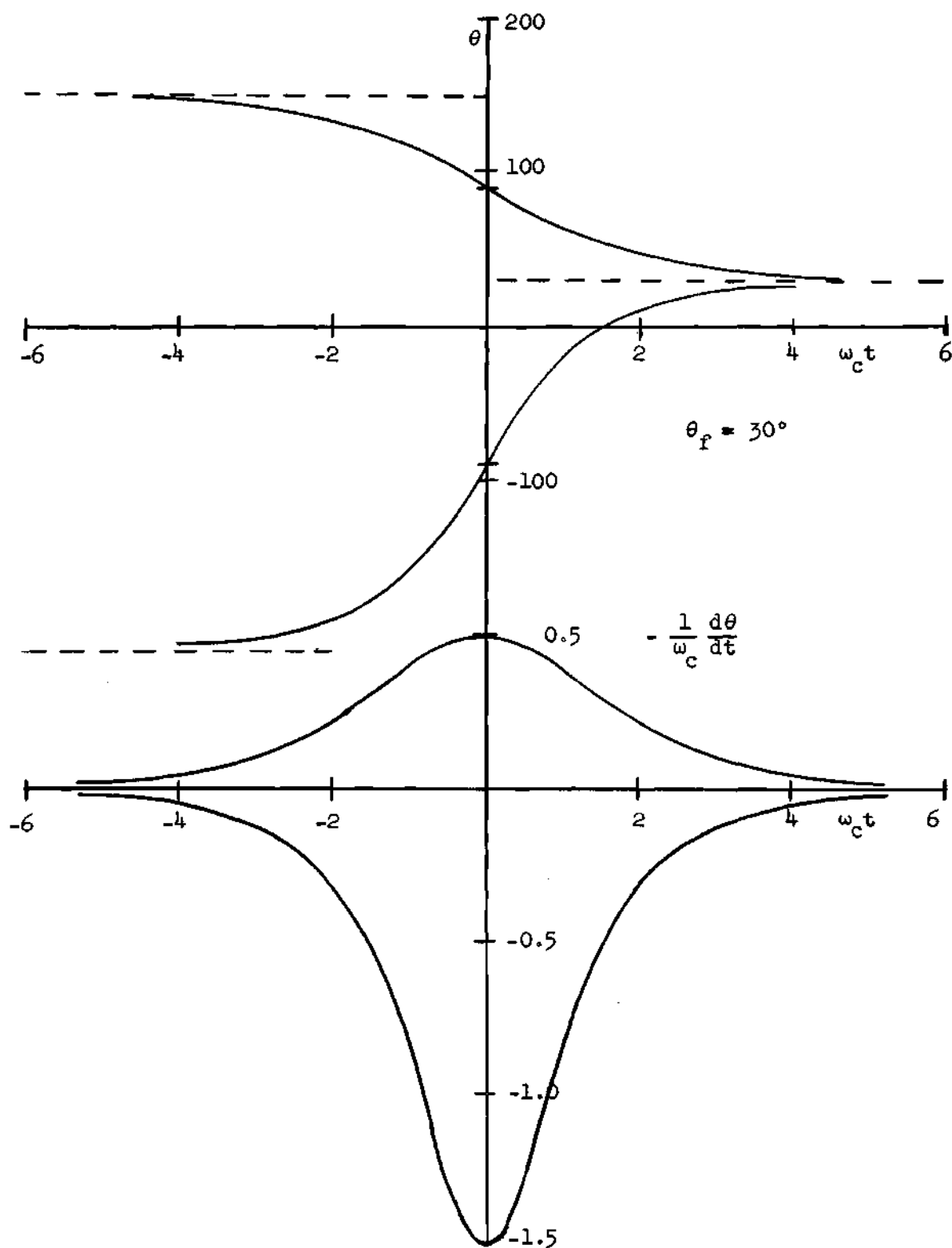


Figure 60. Instantaneous Phase Angle and Instantaneous Frequency Curves For $\theta_f = 30^\circ$.

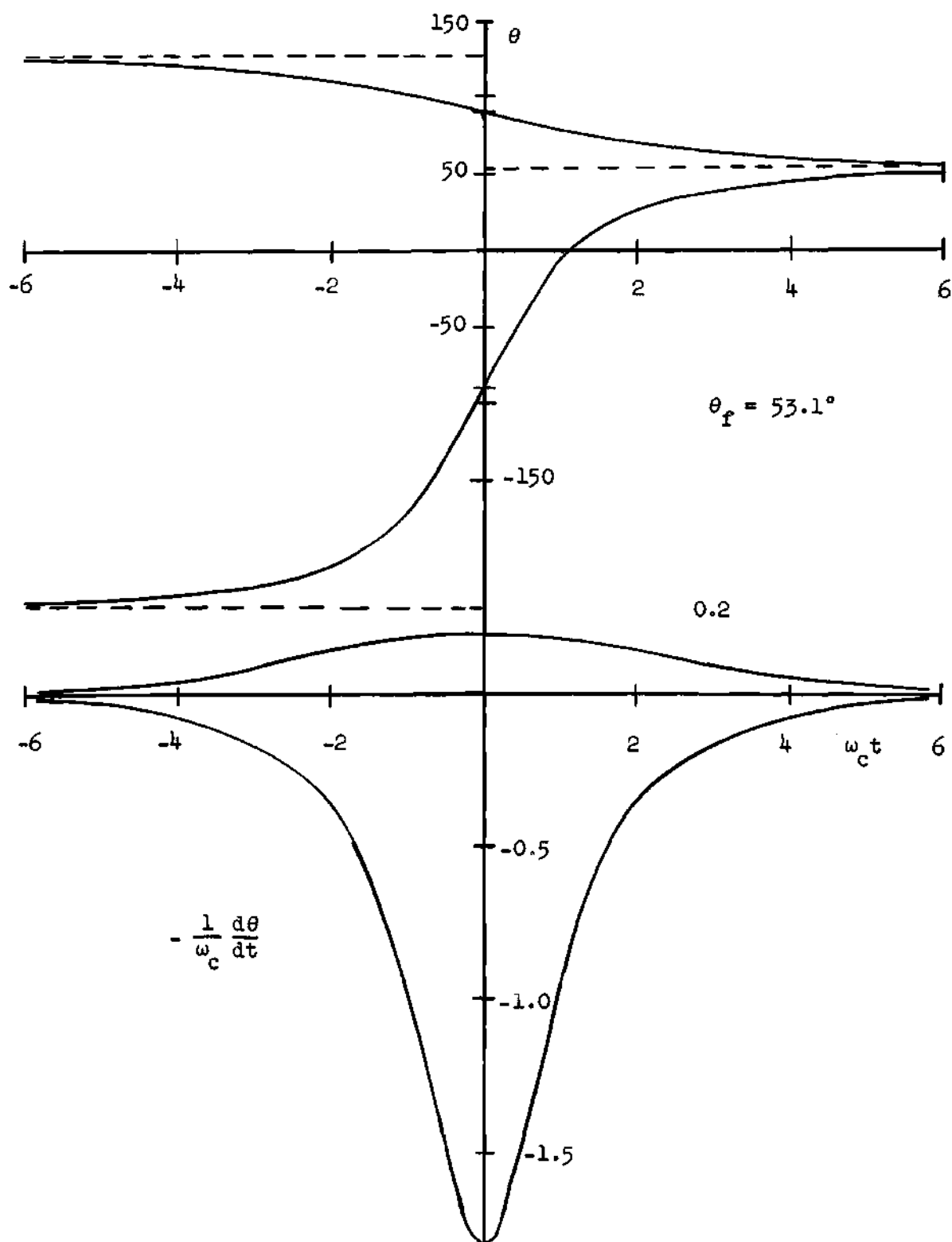


Figure 61. Instantaneous Phase Angle and Instantaneous Frequency Curves for $\theta_f = 53.1^\circ$.

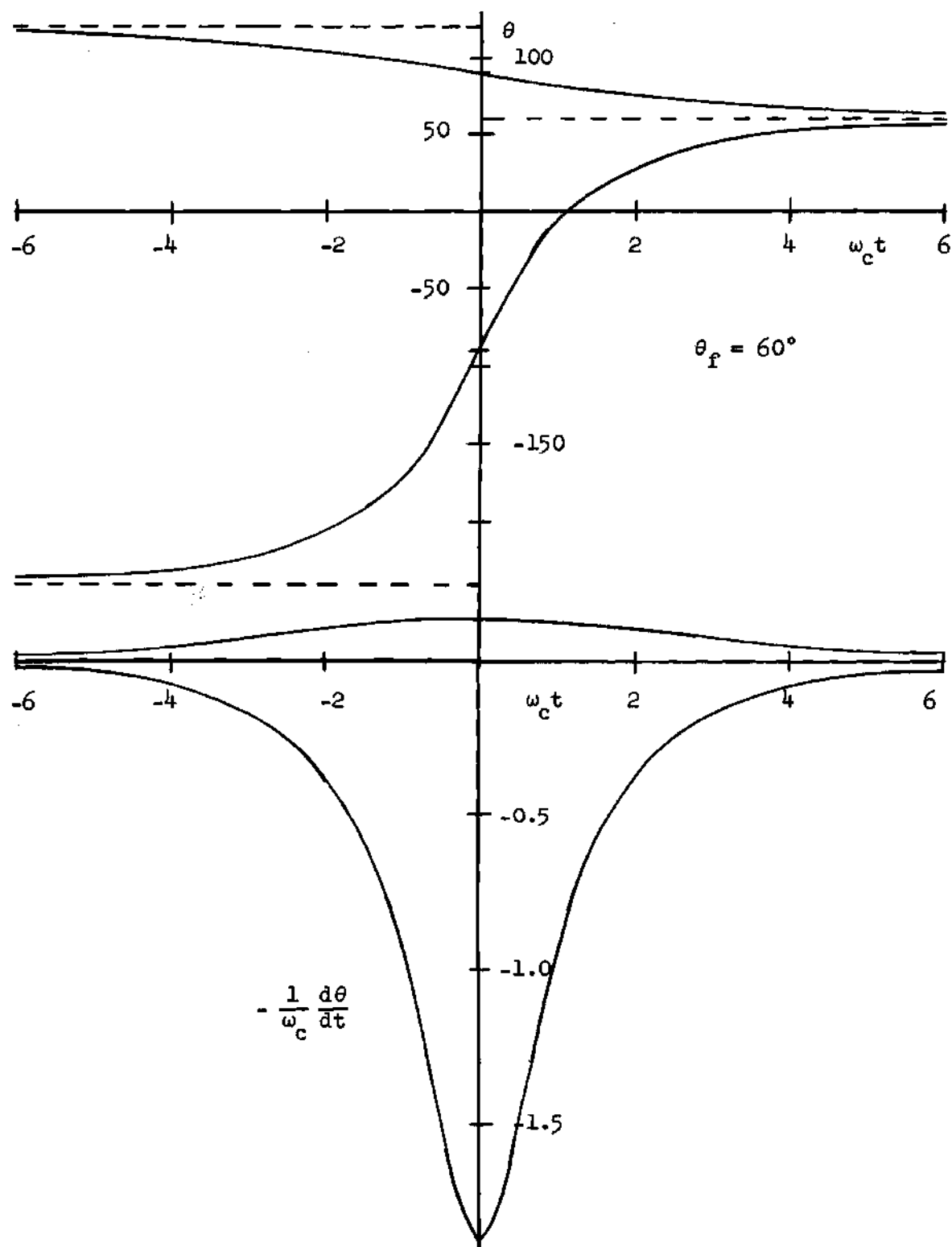


Figure 62. Instantaneous Phase Angle and Instantaneous Frequency Curves for $\theta_f = 60^\circ$.

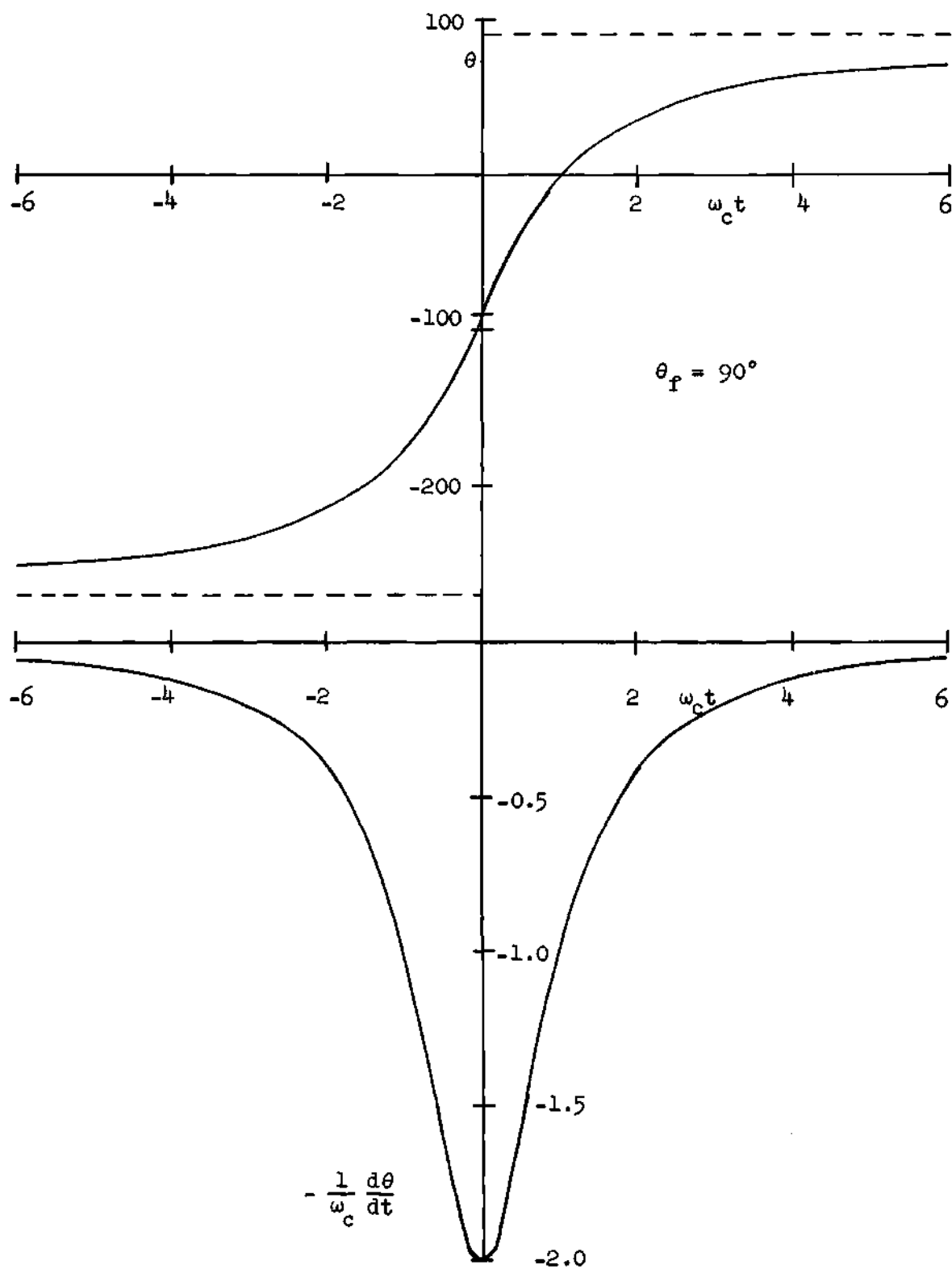


Figure 63. Instantaneous Phase Angle and Instantaneous Frequency Curves for $\theta_f = 90^\circ$.

BIBLIOGRAPHY

1. Edison, W. A., Vacuum-Tube Oscillators, New York, John Wiley and Sons, Inc., 1953.
2. Van der Pol, Balth, "The Nonlinear Theory of Electric Oscillations," Proceedings of the Institute of Radio Engineers, Vol. 22, Sept., 1934, p. 1051.
3. Gillies, A. W., "Electrical Oscillations, A Physical Approach to the Phenomena," Wireless Engineer, Vol. 30, 1953, p. 143.
4. Appleton, E. V., "The Automatic Synchronization of Triode Oscillators," Cambridge Philosophical Society Proceedings, Vol. 21, 1922-1923, p. 231.
5. Huntoon, R. D., and A. Weiss, "Synchronization of Oscillators," Proceedings of the Institute of Radio Engineers, Vol. 35, 1947, pp. 1415 - 1423.
6. Adler, R., "Locking Phenomena in Oscillators," Proceedings of the Institute of Radio Engineers, Vol. 34, 1946, pp. 351 - 357.
7. Labin, E., "Theory of Synchronization by Phase Control," Phillips Research Reports, Vol. 4, 1949, pp. 291 - 315.
8. Fraser, D. W., Synchronization of Oscillators by Interrupted Wave Trains, Ph. D. Thesis, Georgia Institute of Technology, Atlanta, Georgia, 1955.
9. Jones, W. B., Jr., Synchronized Oscillators with Frequency Modulated Synchronizing Signals, Ph. D. Thesis, Georgia Institute of Technology, Atlanta, Georgia, 1953.
10. Dwight, H. B., Tables of Integrals, Revised Edition, New York, Macmillan, 1947.

VITA

Thomas Mitchell White, Jr. was born on November 22, 1925 in Hawkinsville, Georgia. He is the son of Thomas M. White and Elema H. White. In 1948 he married the former Gloria Lee Smith and they are the parents of two children.

Mr. White attended the public schools of Cochran, Georgia, where he graduated from high school in 1942. He attended Middle Georgia College from 1942 to 1943, Georgia Institute of Technology from 1943 to 1944, and Texas Agricultural and Mechanical College from 1944 to 1945. In 1946 he returned to Georgia Institute of Technology where he received the Bachelor of Electrical Engineering in 1947 and the Master of Science in Electrical Engineering in 1948.

In 1945 he was an Instructor of Telephony at the Army Signal Corps School at Fort Monmouth, New Jersey. From 1948 through 1963 he has been on the staff of the Georgia Institute of Technology. He joined the staff as an Instructor and was promoted to Assistant Professor in 1955.